Folia Histochemica et Cytobiologica

Scientific quarterly devoted to problems of histochemistry, cytochemistry and cell & tissue biology

www.fhc.viamedica.pl

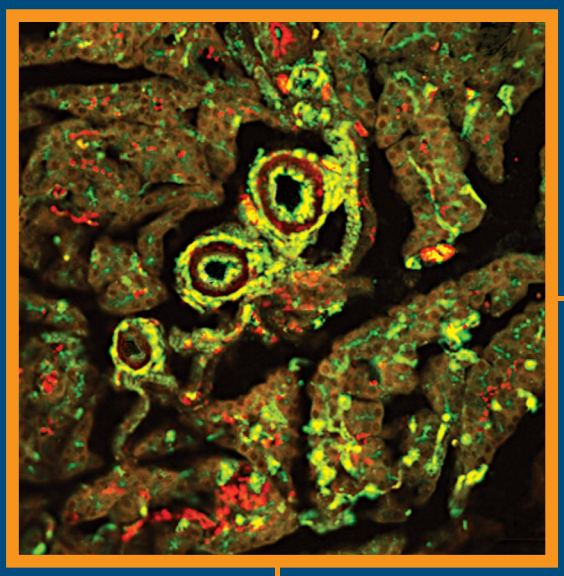

Vol. 58
No. 1
2020

ISSN 0239-8508

VIA MEDICA

Folia Histochemica et Cytobiologica

Scientific quarterly devoted to problems of histochemistry, cytochemistry and cell & tissue biology

www.journals.viamedica.pl/folia_histochemica_cytobiologica

Vol. 58
No. 1
2020

Official Journal of the Polish Society for Histochemistry and Cytochemistry

EDITORIAL OFFICE:
Department of Histology
Medical University of Gdansk
Debinki St. 1, 80–210 Gdansk, Poland
tel.: + 48 58 349 14 37
fax: + 48 58 349 14 19
e-mail: zkmiec@gumed.edu.pl
http://www.journals.viamedica.pl/folia_histochemica_cytobiologica

Folia Histochemica et Cytobiologica (pISSN 0239–8508, eISSN 1897–5631) is published quarterly, one volume a year, by the Polish Society for Histochemistry and Cytochemistry at VM Media sp. z.o.o VM Group sp.k., Gdansk.

Indexed in: Index Medicus/MEDLINE, Excerpta Medica/EMBASE, Chemical Abstracts/CAS, SCI Expanded, SciSearch, Biochemistry & Biophysics Citation Index, ISI Alerting Services, Biosis Previews Index Copernicus, Biological Abstracts, SCOPUS, Research Alert, ProQuest, EBSCO, DOAJ, Ulrich's Periodicals Directory.

POLISH SOCIETY FOR HISTOCHEMISTRY AND CYTOCHEMISTRY STATEMENT OF FOLIA HISTOCHEMICA ET CYTOBIOLOGICA EDITORIAL POLICY

Folia Histochemica et Cytobiologica is an international, English-language journal devoted to the rapidly developing fields of histochemistry, cytochemistry, cell and tissue biology.

The Folia Histochemica et Cytobiologica publishes papers that meet the needs and intellectual interests of medical professionals, basic scientists, college and university teachers and students. Prospective authors should read most recent issues of FHC to determine the appropriateness of a possible contribution. However, such an examination does not provide an infallible guide because editorial policy is always under review. Technical correctness is necessary, but it is not the only condition for acceptance. Clarity of exposition and potential interest of the readers are important considerations; it is the reader, not the author, who must receive the benefit of the doubt.

Folia Histochemica et Cytobiologica publishes review articles, original articles, short communications and proceedings of scientific congresses/symposia. Fields of particular interests include development and application of modern techniques in histochemistry and cell biology, cell biology and pathology, cell-microenvironment interactions, tissue organization and pathology.

Manuscripts announcing new theoretical or experimental results, or manuscripts questioning well-established and successful theories, are highly desirable and are a subject for evaluation by specialists. Manuscripts describing original research that clarifies past misunderstandings or allows a broader view of a subject are acceptable. Manuscripts that demonstrate new relations between apparently unrelated areas of fields of interests are appropriate. Manuscripts that show new ways of understanding, demonstrating, or deriving familiar results are also acceptable. Such manuscripts must provide some original cytobiological insight and not just a clever derivation.

Regularly, review or tutorial articles are published, often of a length greater than that of the average article. Most of these articles are a subject of a review; authors planning such articles are asked to consult with the editors at an early stage.

Most readers of a particular article will be specialists in the subject matter presented; the context within which the paper is presented should be established in the order given in Instructions for Authors. Manuscripts must be technically correct and must take proper cognizance of previous work on the same subject regardless of where it may have appeared. Such referencing is especially important for reminders of once well known ideas, proofs, or techniques that may have again become useful to readers. It is the responsibility of the author to provide adequate references; editors and referees will not do the literature search that should have been done by the authors. The references are a matter of review though.

Contributions considered include: Regular Articles (Papers), Short Communications, Review Articles, Conference Proceeding, Book Reviews and Technical Notes, which describe new laboratory methods or substantial improvements of the existing techniques. Regular articles should be about five journal pages or less in length. Short communications are usually confined to the discussion of a single concept and should be about two journal pages in length. Review articles are confined to a broad discussion and should contain the most recent knowledge about the subject.

Instructions concerning the preparation of manuscripts are given in the Information for Authors. Care in following those instructions will permit editors and referees to devote more time to thoughtful evaluation of contributions and will ultimately lead to a better, more interesting Journal.

SUBSCRIPTION

Folia Histochemica et Cytobiologica is available for paper subscription (print on demand).
To read and download articles for free as pdf document, visit http://czasopisma.viamedica.pl/fhc

Publisher: VM Media sp. z o.o. VM Group sp.k., Swietokrzyska St. 73, 80–180 Gdansk, http://www.viamedica.pl, wap.viamedica.pl

Illustration on the cover: *The cholinergic and adrenergic nerve fibers in parenchyma and the wall of blood vessels of the head of pancreas* (see: Malgorzata Radzimirska et al., pp. 54–60)

Folia Histochemica et Cytobiologica

Scientific quarterly devoted to problems of histochemistry, cytochemistry and cell & tissue biology

www.journals.viamedica.pl/folia_histochemica_cytobiologica

Vol. 58
No. 1
2020

Official Journal of the Polish Society for Histochemistry and Cytochemistry

ORIGINAL PAPERS

Foxo3a aggravates inflammation and induces apoptosis in IL-1-treated rabbit chondrocytes *via* positively regulating tenascin-c
Fei Wang, Qiubin Wang, Ming Zhu, Qi Sun 1

MiR-491-3p is down-regulated in postmenopausal osteoporosis and affects growth, differentiation and apoptosis of hFOB1.19 cells through targeting CTSS
Wen-Xiong Hu, Hua Li, Jia-Zheng Jiang 9

Expression of CD163 and HLA-DR molecules on the monocytes in chronic lymphocytic leukemia patients
Wioleta Kowalska 17

Monocytic MDSC as a source of immunosuppressive cytokines in chronic lymphocytic leukemia (CLL) microenvironment
Wioleta Kowalska, Agnieszka Bojarska-Junak 25

Search of reference biomarkers reflecting orbital tissue remodeling in the course of Graves' orbitopathy
Przemyslaw Pawlowski, Izabela Poplawska, Janusz Mysliwiec, Willem A. Dik, Anja Eckstein, Utta Berchner-Pfannschmidt, Robert Milewski, Slawomir Lawicki, Zofia Dzieciol-Anikiej, Robert Rejdak, Joanna Reszec 37

Study of DNA topoisomerase IIα expression in canine lymphomas and its potential role as a marker of sensitivity to anthracycline-based chemotherapy in dogs
Pawel Klimiuk, Wojciech Lopuszynski, Kamila Bulak, Anna Smiech, Adam Brzana 46

Cholinergic and adrenergic innervation of the pancreas in chinchilla (*Chinchilla Laniger Molina*)
Malgorzata Radzimirska, Jacek Kuchinka, Elzbieta Nowak, Wojciech Trybus, Aleksander Szczurkowski 54

FOLIA HISTOCHEMICA ET CYTOBIOLOGICA
Vol. 58, No. 1, 2020
pp. 1–8

ORIGINAL PAPER

VIA MEDICA

Foxo3a aggravates inflammation and induces apoptosis in IL-1-treated rabbit chondrocytes *via* positively regulating tenascin-c

Fei Wang[1], Qiubin Wang[1], Ming Zhu[2], Qi Sun[1]

[1]Department of Rehabilitation Medicine, The First People's Hospital of Huzhou City, Huzhou City, Zhejiang Province, 313000, China

[2]Department of Nephrology, The First People's Hospital of Huzhou City, Huzhou City, Zhejiang Province, 313000, China

Abstract

Introduction. Osteoarthritis (OA) is the most common degenerative disease in middle-aged and elderly individuals that causes joint deformity and limb disability. Accumulating evidence has suggested that the pathogenesis of OA has been related to various mechanisms such as apoptosis, inflammation, oxidative stress and metabolic disorders. The aim of this study is to clarify the role of Foxo3a in the progress of OA in an *in vitro* model.

Materials and methods. The chondrocytes were derived from rabbit, and treated with IL-1β, which was used as an *in vitro* OA model. The over-expression and down-regulation of Foxo3a were achieved by transfection with overexpression vector or shRNA, respectively. The mRNA level of iNOS in chondrocytes was quantified by qPCR. Tenascin-c (Tnc) production was measured by ELISA and apoptosis-associated proteins were analyzed by Western blotting. The MTT assay was used to assess the viability of chondrocytes.

Results. Foxo3a and iNOS expression were upregulated in IL-1β-treated chondrocytes. Foxo3a silencing decreased iNOS expression, and inhibited apoptosis of IL-1β-treated chondrocytes. The production of Tnc was significantly increased in IL-1β-treated chondrocytes and was positively regulated by Foxo3. Importantly, extracellular addition of Tnc abrogated the protective effects of Foxo3a knockdown on IL-1β — treated chondrocytes.

Conclusion. The present study indicated that down-regulation of Foxo3a protected IL-1β-treated chondrocytes by decreasing iNOS expression and suppressing chondrocytes' apoptosis *via* modulating tenascin-c, which could be regarded as a potent therapeutic target for the treatment of OA. *(Folia Histochemica et Cytobiologica 2020, Vol. 58, No. 1, 1–8)*

Key words: chondrocytes; IL-1β; osteoarthritis *in vitro*; Foxo3a; iNOS; tenascin-c; apoptosis; shRNA

Introduction

Osteoarthritis (OA) is known as a degenerative disease that gradually causes joint deformity and limb disability, which further causes a reduction in the quality of life and increases mortality [1]. OA is one of the most common diseases in middle-aged and elderly individuals. In particular, the incidence of OA is more than 60% among people over 65 years of age [2]. Once the disease occurs, a balance of extracellular matrix (ECM) synthesis/degradation is broken and ultimately leads to the destruction of joint tissue [3]. Accumulating evidence suggests that the pathogenesis of OA is linked with various mechanisms. At the cellular level, apoptosis of articular chondrocytes and articular cartilage tissue cells is induced by several factors including cytokines, chemokines, Toll-like receptor ligands, and other inflammatory mediators such as nitric oxide [4]. At the molecular level, reactive oxygen species (ROS)-mediated oxidative stress signaling in

Correspondence address: Qiubin Wang
Department of Rehabilitation Medicine,
The First People's Hospital of Huzhou City,
302, Unit B, Building 41, Jin shiji ming cheng,
Wuxing District, Huzhou City, Zhejiang Province, China
tel.: 86+0572-257-5067
e-mail: QiubinWangawe@163.com

chondrocytes, as well as mitochondrial dysfunction, metabolic disorders and other abnormal molecular signals are involved in the massive loss of cartilage, which are characteristics of OA [5]. Non-steroidal anti-inflammatory drugs (NSAIDs), the most common clinical treatment for OA, cause several serious side effects like peptic ulcer, nervous system dysfunction and bleeding after long-term use [6].

Tenascin-c (Tnc) is a member of the growing family of ECM proteins, and is expressed in normal adult tissues [7]. However, it is re-expressed during healing wounds, inflammatory responses and tumorigenesis [8, 9]. For instance, a high level of Tnc was found in cartilage, synovial tissue and synovial fluid [10]. It was also reported that Tnc promotes the proliferation and migration of cells during both OA and rheumatoid arthritis [11]. Midwood *et al.*, found that Tnc is involved in maintaining inflammation under arthritic joint disease [12].

Foxo3a, a Forkhead transcription factor of Forkhead box, class O (Foxo) subfamily, has been recently studied extensively as a critical protein that involved in the regulation of inflammation [13]. In arthritis, an increase in the expression as well as phosphorylation of Foxo3a in the blood of patients with rheumatoid arthritis was reported [14]. However, the exact role of Foxo3a in the pathogenesis of OA remains unclear. Therefore, understanding underlying mechanism of OA is helpful to explore effective molecular targets of this disease. Hence, the aim of this study was to clarify the role of Foxo3a in the progress of OA in an *in vitro* model of this disease.

Materials and methods

Animals and chondrocytes isolation. The one-year old New Zealand white rabbits were purchased from Shanghai SLAC Laboratory Animal Co., Ltd (Shanghai, China). All procedures were approved by the Medical Ethics Committee of the First Affiliated Hospital of Huzhou Normal University (Approval no. 2019008). The rabbits were housed at room temperature (23–27°C) with a 12 h light: 12 h dark cycle, and the food and water were provided *ad libitum*. Prior to the animal experiment, rabbits were anesthetized with isoflurane, and then the articular cartilage was carefully harvested from knee joints by sterile dissection. Cartilage was cut into pieces as thin as possible (approximately 1 mm^3) using SLICE!T® (Dr. Khan's Creation, Maharashtra, India), followed by digesting with enriched DMEM medium containing collagenase type II (Sigma-Aldrich Chemical Co, St. Louis, MO, USA) at the concentration of 2 mg/mL for 24 h at 37°C.

Primary chondrocytes' culture and treatment. After collagenase digestion, isolated chondrocytes were washed with Dulbecco's modified Eagle's medium (DMEM) (Gibco, Carlsbad, CA, USA) supplemented with 10% fetal bovine serum (FBS) (Gibco) and 1% penicillin/streptomycin (0.1 mg/mL and 100 Units/mL (P/S, Gibco) and cultured in 5% CO_2 humidified incubator at 37°C. The chondrocytes were cultured until the 3rd passage and were used for the induction of OA *in vitro* model by adding to the isolated chondrocytes recombinant IL-1β (Sigma-Aldrich) at the concentration of 100 ng/mL for 48 h (based on a review by Johnson *et al.* [15]).

Plasmid construction. The lentiviral short hairpin RNA (shRNA) expression constructs to silence Foxo3a (Foxo3a-shRNA) were designed using the program published online by Invitrogen (Thermo Fisher Scientific, Waltham, MA, USA). The designed Foxo3a-siRNA-expressed vector was generated by Shanghai Genechem Co., Ltd (Shanghai, China). The shRNA strands were: sense 5'-AUCUAACUCAUCUGCAAGUUU-3'; anti-sense: 5'-ACUUGCAGAUGAGUUAGAUUU-3'. As the negative control for shFoxo3a, shNC was constructed. HA-Foxo3a WT was a gift from Michael Greenberg (Addgene plasmid #1787; http://n2t.net/addgene:1787; RRID: Addgene_1787). The plasmid was amplified by EcoRI-XbaI into Flag tagged pcDNA3.1 retroviral backbone to develop pcDNA3.1-Foxo3a. pcDNA3. 1-NC was generated as a control.

Transfection. The chondrocytes were plated in 96-well plates at 10^4 cells *per* well overnight, followed by transfection with either shRNA-Foxo3a or Foxo3a overexpression vector using Lipofectamine 2000 (Invitrogen, Thermo Fisher Scientific) according to the manufacturer's instructions. The recombinant Tnc (1 μM) (Sigma-Aldrich) was added to the medium when chondrocytes were transfected.

RNA isolation, cDNA synthesis and quantitative PCR (qPCR). Total RNA from chondrocytes was extracted by TRIzol reagent (Invitrogen) following the instruction provided by the manufacturer. The RNA was reversely transcribed into complementary DNAs (cDNAs) using SuperScript IV First-Strand Synthesis System (Invitrogen) according to the manufacturer's instruction. The reverse transcription was carried out at 50°C for 1 h, and then 1 unit of RNase H (Takara, Dalian, China) was treated at 37°C for 15 min. The amplification conditions include a total of 30 cycles of pre-denaturation for 3 min at 94°C, followed by denaturation for 30 sec at 94°C, annealing at 58°C for 30 sec and extension for 60 sec at 72°C. The expression of inducible nitric oxide synthase (iNOS) was measured by SYBR-Green Master Mix (Applied Biosystems, Waltham, MA, USA) on ABIViiA7 Real-Time PCR System (Applied Biosystems). GAPDH was used as internal control for gene analysis.

The primer sequences were as follow: iNOS: 5'-CTGTGACGTCCAGCGCTACA-3', 5'-GCACGGCGATGTTGATCTCTCGCCT-3; GAPDH: 5'-GGAGAAAGCTGCTAA -3', 5'-ACGACCTGGTCCTCGGTGTA-3'.

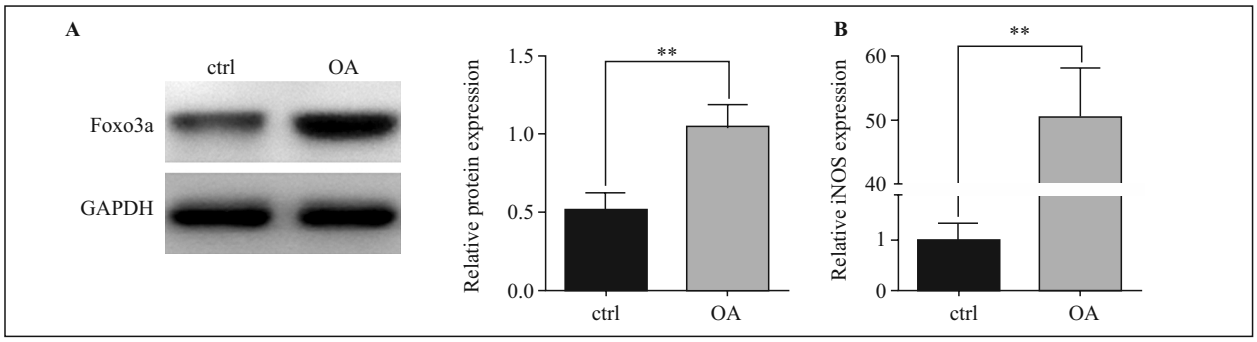

Figure 1. Foxo3a and iNOS were upregulated in IL-1β-treated chondrocytes. The chondrocytes derived from rabbit knee joints were stimulated with IL-1β (100 ng/mL) for 48 h. The protein level of Foxo3a and mRNA level of iNOS were determined by western blotting **(A)** and qPCR **(B)**, respectively. The data are presented as mean ± SD (n = 3). Symbols: 'ctrl' — untreated, control chondrocytes, 'OA' — IL-1β-treated chondrocytes. $^{**}p < 0.01$, OA *vs.* control.

Western blotting. The proteins from chondrocytes were lysed by radioimmunoprecipitation assay (RIPA) buffer. Protein assay was then used to quantify the concentration using a BCA Protein Assay Kit (Thermo Fisher Scientific). Fifty micrograms of protein were subjected to SDS-PAGE electrophoresis, and separated proteins were transferred to polyvinylidene difluoride (PVDF) membrane (Immobilon-P; EMD Millipore, Darmstadt, Germany). After that, the membrane was blocked with 5% of skill milk in TBS-T for 1 h and then incubated with 1000 time-diluted primary antibodies against Foxo3a (ARP38041-P050, Aviva Systems Biology, San Diego, CA, USA), Bax (OAED00050, Aviva Systems Biology), Bcl-2 (LS-C465574-100, LifeSpan BioSciences, Inc, Seattle, WA, USA) and cleaved Caspase-3 (NB600-1235, Novus Biologicals, LCC Centennial, CO, USA) overnight at 4°C. After washing three times in TBS-T, the membrane was incubated with secondary antibody for 1 h at room temperature. The GAPDH, as an internal control, was measured by anti-GAPDH (GTX100118, GENETEX, Inc) and its secondary antibody. Protein expression was detected using Luminata Forte Western HRP Substrate (Millipore) with a Bio-Rad ChemiDox XRS+ imaging system (Bio-Rad Laboratories, Hercules, CA, USA).

Cell viability. The viability of chondrocytes was detected using 3-(4,5)-dimethylthiahiazo(-z-yl)-3,5-di-phe-nyterazolium-bromide (MTT) (Gibco) assay based on mitochondrial reduction of MTT to formazan. Chondrocytes were pre-seeded in 96-well plate at a density of 10^4 cells/well. Next day, the chondrocytes were transfected with or without shRNA or vectors in the presence of recombinant human IL-1β (100 ng/mL). After incubation for 48 h, the medium was replaced with 200 μL of fresh medium. Then, 3 mg/mL of MTT in PBS was added into each well (20 μL/well). After incubation for 1.5 h, 150 μL of culture supernatant was removed from each well and the formazan crystal were lysed by 100 μL of MTT stop solution (0.4% HCl, 10% Triton X-100 in isopropanol). After incubation for 12 h, the absorbance was measured at 570 nm with 655 nm as reference wavelength on a microplate reader (Bio-Rad).

Measurement of Tnc level. Tnc production was measured by rabbit ELISA kit (MyBioSource, Inc, San Diego, CA, USA) according to the manufacturer's instruction. Briefly, diluted samples or standard recombinant tenascin were added into 96-well plates coated with anti-Tnc antibody for 2 h at room temperature. After washing, the detection antibody reacted at room temperature for 2 h, followed by addition of an avidin-horseradish peroxidase conjugates to bind captured antigen. The reaction was measured by the absorbance at 490 nm.

Statistical analysis. All data were expressed as means ± standard deviation (SD). Data for each experiment were acquired from at least three independent experiments. Statistical analyses were performed by using Student's t-test *via* GraphPad Prism 7 (GraphPad Software, Inc., San Diego, CA, USA), with the level of significance set at $p < 0.05$.

Results

Foxo3a and iNOS were upregulated in IL-1β-treated chondrocytes

As shown in Figure 1A, Foxo3a protein expression in IL-1β-treated chondrocytes was significantly increased compared with control chondrocytes. Importantly, the mRNA expression of inducible nitric oxide synthase (iNOS), a biomarker of severe cellular stress, in IL-1β-treated chondrocytes was also higher than that in control chondrocytes (Fig. 1B).

Foxo3a knockdown inhibited IL-1β-treated apoptosis of chondrocytes

To further investigate the mechanism underlying the role of Foxo3a in the development of OA in our *in*

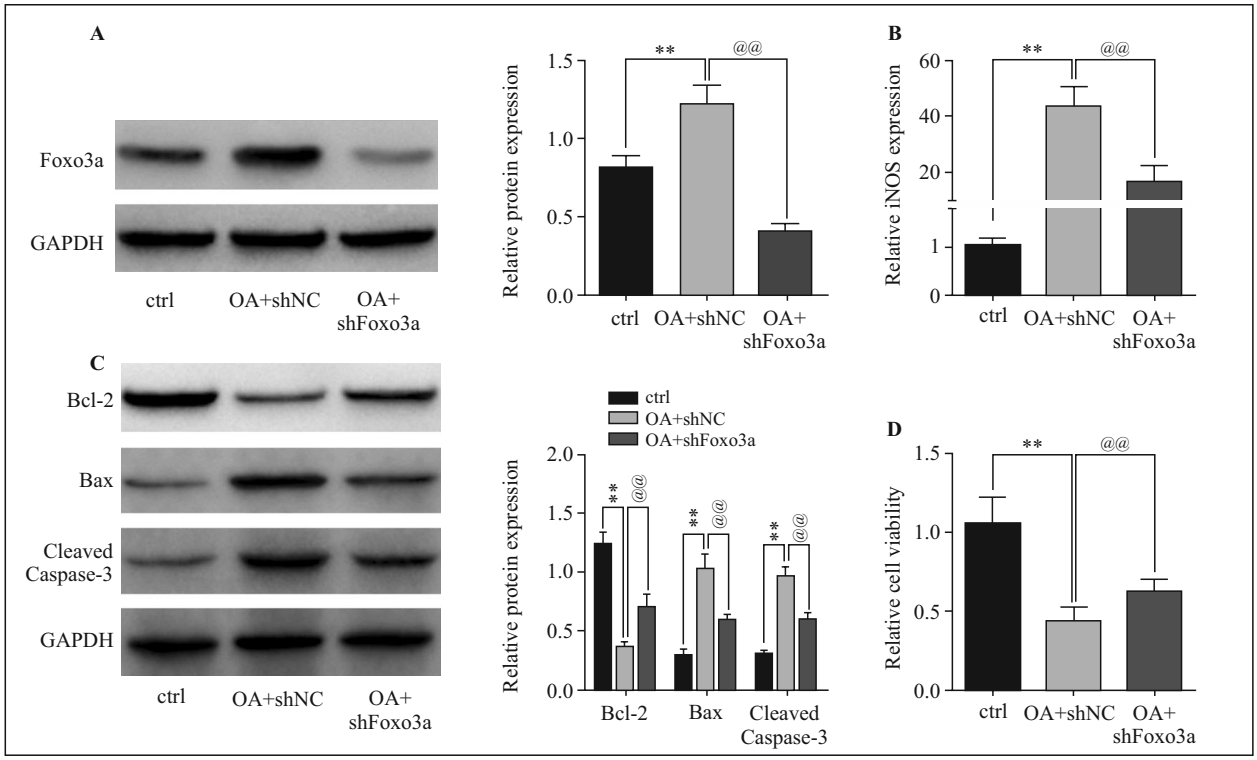

Figure 2. Foxo3a knockdown inhibited IL-1β-treated apoptosis of chondrocytes. The chondrocytes derived from rabbit were stimulated with IL-1β (100 ng/mL), followed by treatment with shNC or shFoxo3a for 48 h. The protein level of Foxo3a and mRNA level of iNOS were determined by western blotting **(A)** and qPCR **(B)**, respectively. The expression of apoptosis-associated proteins including bcl-2, bax and caspase-3 were analyzed by western blotting **(C).** The cell viability was measured by MTT assay **(D).** The data are presented as mean ± SD (n = 3). Symbols as in the description of Figure 1. $^{**}p < 0.01$, OA *vs.* control; $^{@@}p < 0.01$, OA + Sh-Foxo3a *vs.* OA + Sh-NC.

vitro model, we knocked-down Foxo3a expression in IL-1β-treated chondrocytes by shRNA transfection. It was found that shRNA treatment strongly reduced Foxo3a protein expression in IL-1β-treated chondrocytes (Fig. 2A). qPCR assay revealed that Foxo3a knockdown significantly decreased IL-1β--treated iNOS expression (Fig. 2B). The reduction of anti-apoptotic protein Bcl-2 and enhanced levels of pro-apoptotic proteins, *i.e.* cleaved caspase-3 and Bax, were observed in IL-1β-treated chondrocytes (Fig. 2C). Interestingly, Foxo3a knockdown up-regulated Bcl-2 expression and decreased the proteins levels of Bax and cleaved caspase-3 in IL-1β-treated chondrocytes as compared with cells transfected with shRNA (Fig. 2C). MTT assay analysis showed that Foxo3a knockdown prompted the decreased viability caused by IL-1β in chondrocytes (Fig. 2D). Thus, these data suggested that Foxo3a knockdown promotes IL-1--induced apoptosis of chondrocytes.

Foxo3a positively regulates Tnc expression

The level of Tnc was upregulated in IL-1β-treated chondrocytes as compared to the control (Fig. 3A). As shown in Figure 3B, the level of Tnc in IL-1β-treated chondrocytes was dramatically decreased after shRNA-Foxo3a transfection (Fig. 3B). In contrast, the level of Tnc was significantly enhanced when Foxo3a was overexpressed in IL-1β-treated chondrocytes (Fig. 3B).

The protective effects of Foxo3a knockdown on IL-1-treated chondrocytes were reversed by extracellular Tnc

To further evaluate whether Tnc was involved in the protective effects of Foxo3a knockdown in IL-1β-treated chondrocytes, Tnc was added extracellularly to the cultures of IL-1β-treated chondrocytes. It was found that the level of Tnc was appreciably increased in the presence of extracellular Tnc in IL-1β-treated chondrocytes that were transfected with Foxo3a shRNA (Fig. 4A). The decreased expression levels of iNOS, Bax and cleaved caspase-3 caused by Foxo3a knockdown were rescued by the treatment with extracellular Tnc (Figs. 4B and 4C). In contrast, shFoxo3a-enhanced Bcl-2 expression was significantly declined in the presence of extracellular Tnc in IL-1β-treated chondrocytes (Fig. 4C). It should

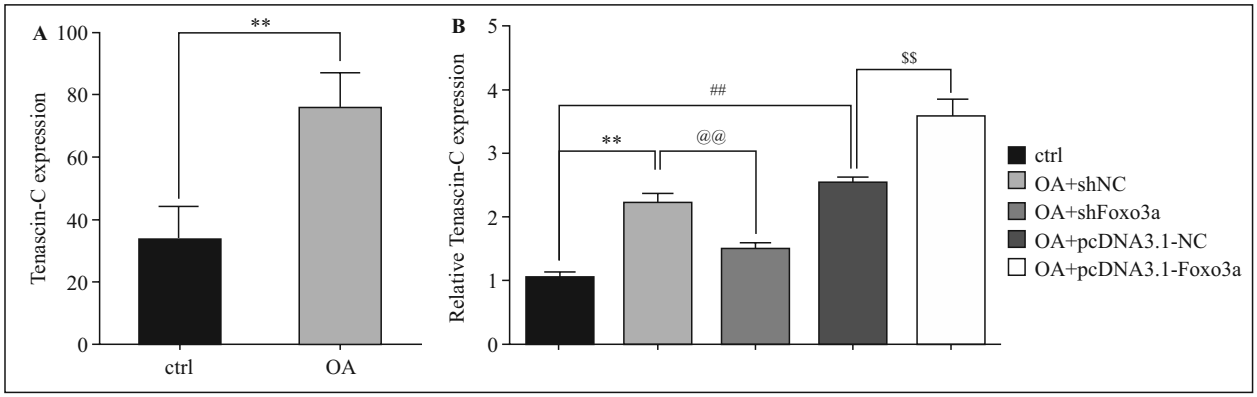

Figure 3. The expression of tenascin-c was positively regulated by Foxo3a. The chondrocytes were treated by IL-1β (100 ng/ /mL) for 48 h. The level of tenascin-c in culture medium was quantified by ELISA **(A).** The IL-1β-treated chondrocytes were transfected with shRNAs or vectors for 48 h. The release of tenascin-c was measured by ELISA **(B).** The data were represented as mean ± SD (n = 3). Symbols as in the description of Figure 1. $^{**}p < 0.01$, OA + shNC *vs.* control; $^{@@}p < 0.01$, OA + shFoxo3a *vs.* OA + shNC; $^{\#\#}p < 0.01$, OA + pcDNA3.1-NC *vs.* control; $^{\$\$}p < 0.01$, OA + pcDNA3.1-Foxo3a *vs.* Foxo3a OA + pcDNA3.1-NC.

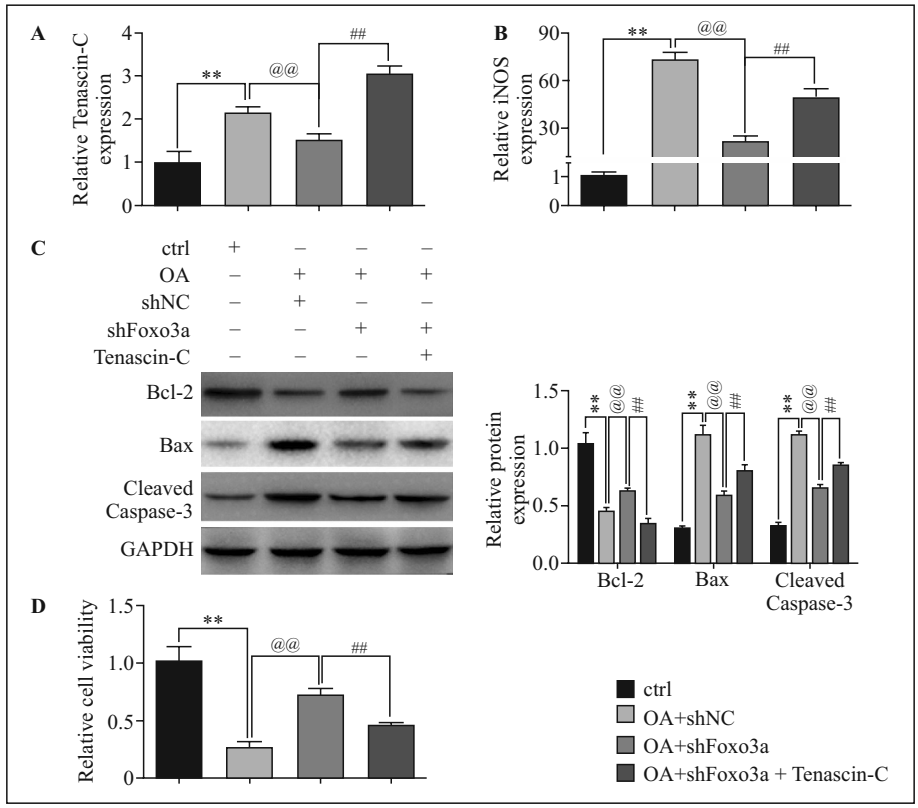

Figure 4. Extracellular tenascin-c abrogated the protective effect of down-regulated Foxo3a on IL-1β-treated chondrocytes. The chondrocytes were stimulated with IL-1β (100 ng/mL), followed by treatment of shFoxo3a in the absence or presence of tenascin-c (1 μM). The level of tenascin-c in medium and mRNA level of iNOS were determined by ELISA **(A)** and qPCR **(B)**, respectively. The expression of apoptosis-associated proteins was analyzed by western blotting **(C)**, and the cell viability was measured by MTT assay **(D)**. The data were represented as mean ± SD (n = 3). Symbols as in the description of Figure 1. $^{**}p < 0.01$, OA + shNC *vs.* control; $^{@@}p < 0.01$, OA + shFoxo3a *vs.* OA + shNC; $^{\#\#}p < 0.01$, OA + shFoxo3a + tenascin-c *vs.* OA + shFoxo3a.

be noted that Tnc treatment effectively inhibited the increased cell viability caused by shFoxo3a in IL-1β-treated chondrocytes (Fig. 4D). The evidence suggested that Foxo3a, as a positive regulator of Tnc, contributed to the apoptosis of IL-1β-treated chondrocytes.

Discussion

Currently, the treatment strategies for OA mainly involve relieving the symptoms such as joints' pain, swelling, and muscle tension to improve the quality of life. NSAIDs, prescribed for a long-term use, are currently the primary pharmacological OA treatment. However, some dangerous side effects are associated with such a treatment [16]. Therefore, safe and effective therapy for OA is urgently needed to be developed. It has been reported that Foxo3a expression is altered in various types of inflammatory diseases [17]. To our knowledge, our current study is the first to demonstrate that Foxo3a is highly expressed in IL-1β-treated chondrocytes compared with control chondrocytes, suggesting the Foxo3a might be a potential biomarker for OA.

Inducible NOS expression is induced by various factors such as inflammatory cytokines (IL-1β, IL-17, TNF-α and IFN-γ) [18], bacterial infection [19] and degradation of extracellular matrix [20]. The upstream targets of iNOS expression are associated with three main regulators including NF-κB, STAT-1 and MAPKs signaling pathways [21]. More specifically, IL-1β-induced OA is mainly associated with translocation of NF-κB into nucleus, where it binds to the promotor region of iNOS [22]. Subsequently, iNOS efficiently catalyzes the production of nitric oxide (NO) which plays a critical role in the pathogenesis of OA [23]. It has been reported that iNOS-mediated NO production in OA chondrocytes is the leading cause of cartilage destruction, and depletion of iNOS in mice inhibited the development of OA [24]. Consistently, we found in our study that iNOS expression was significantly increased in IL-1β--treated chondrocytes as compared to the control cells. It was demonstrated that NO synthesis was actively progressed in OA chondrocytes [25]. In other words, OA chondrocytes might undergo some cellular events like inflammatory response, apoptosis or oxidative stress [26]. Moreover, increased expression of iNOS and NO have been found *in vivo* in inflammatory, septic arthritis and in patients with rheumatoid arthritis [27]. Meanwhile, our data showed that enhancement of iNOS expression was suppressed by down-regulation of Foxo3a what suggests that Foxo3a could be a new clinical target for OA treatment and also for other iNOS-related inflammatory diseases.

Chondrocytes apoptosis is also regarded as the key factor in OA progression. Nitric oxide generation is known as the primary executioner of chondrocytes apoptosis through regulating caspase-3-dependent signaling [28]. Mechanically, NO-induced chondrocytes apoptosis is associated with mitochondrial dysfunction, DNA damage and iNOS signaling [29]. In this study, we provided evidence that down-regulated Foxo3a inhibited chondrocytes apoptosis through regulating caspase-3-dependent signaling, indicating that inhibition of Foxo3a expression offers a clinically-relevant perspective for the treatment of OA by regulating chondrocytes' apoptosis. However, the detailed mechanism of this phenomenon should be clarified in future study. Recently, many researchers point out that oxidative stress is a critical risk factor for the onset of OA [30]. ROS, as the mediators of oxidative stress, not only participate in the process of cell matrix degradation but also control chondrocytes' life cycle during OA [30]. On the other hand, Foxo transcription factors have been implicated in various ROS-related processes including cellular aging, proliferation, senescence or apoptosis [31]. For instance, mammalian Sterile 20-like kinase 1 (MST-1) mediates ROS-induced neuronal apoptosis *via* Foxo3a phosphorylation [32]. Foxo3a also suppressed ROS-induced apoptosis in differentiated 3T3-L1 adipocytes [33]. Hence, the mechanism underlying the protective effect of down-regulated Foxo3a on chondrocytes' apoptosis might be also associated with ROS-mediated signaling.

Tenascin-c is ECM glycoprotein which increased levels were found in the synovial fluid in OA patients [34]. Production of Tnc can also induce inflammatory mediators and promote matrix degradation in OA, and its levels could serve as a biomarker of joint damage and a trigger of further joint degradation [35, 36]. In our *in vitro* system, the level of Tnc was significantly increased in OA chondrocytes compared with control chondrocytes, which was related to Foxo3a expression. Therefore, these results suggest that Foxo3a is critically involved in the production of Tnc during OA. In other words, Foxo3a may regulate the OA-mediated inflammation *via* modulating Tnc. Furthermore, extracellular addition of Tnc abrogated the effects of Foxo3a knockdown on apoptosis and iNOS expression in IL-1β-treated chondrocytes, suggesting that Tnc promoted apoptosis in IL-1β-mediated OA chondrocytes. On the contrary, the protective effect of Tnc on human OA cartilage was observed in an *in vitro* system [37]. It was shown in Tnc$^{-/-}$ mice that cartilage repair was significantly slower than that in wild type mice, and cartilage degeneration was enhanced by deficiency of Tnc [38]. Furthermore,

Matsui's group reported that deficiency of Tnc delayed articular cartilage repair *in vivo* and treatment of full-thickness osteochondral defects by filling the defect with exogenous Tnc results in the inhibition of cartilage degeneration [39]. These different results may be affected by experimental model, experimental object or experimental conditions. In spite of this, the exact mechanisms of how Tnc plays dual roles in OA remain unclear, and needs further research.

In the present study, we provided evidence that down-regulated Foxo3a protects *in vitro* against IL-1β--mediated inflammation and IL-1β-induced chondrocytes' apoptosis. These results also revealed that those protective effects of down-regulated Foxo3a on OA were blocked by extracellular addition of Tnc, indicating that down-regulation of Foxo3a exhibited the potent cytoprotective activity in the *in vitro* OA model *via* modulating Tnc. Our study suggests potential usefulness of targeting Foxo3a as a candidate for the development of a novel and effective treatment for OA.

Funding

This work was supported by Zhejiang Provincial Basic Public Welfare Research Project (Grant No. LGF19H7000), Zhejiang Provincial Medical and Health Research Surface Project (Grant No. 2018KY777) and Zhejiang Traditional Chinese Medicine Technology Project (Grant No. 2017ZA134).

Competing interests

The authors declare that they have no competing interests.

Availability of data and materials

All data generated or analyzed during this study are included in this published article.

Authors' contribution

FW and QBW conceived and designed the experiments, MZ analyzed and interpreted the results of the experiments, QS performed the experiments.

Ethics approval and consent to participate

The animal use protocol listed below has been reviewed and approved by the Animal Ethical and Welfare Committee. Approval No. 2019008.

References

1. Nelson AE. Osteoarthritis year in review 2017: clinical. Osteoarthritis Cartilage. 2018; 26(3): 319–325, doi: 10.1016/j.joca.2017.11.014, indexed in Pubmed: 29229563.
2. Blagojevic M, Jinks C, Jeffery A, et al. Risk factors for onset of osteoarthritis of the knee in older adults: a systematic review and meta-analysis. Osteoarthritis Cartilage. 2010; 18(1): 24–33, doi: 10.1016/j.joca.2009.08.010, indexed in Pubmed: 19751691.
3. Squires GR, Okouneff S, Ionescu M, et al. The pathobiology of focal lesion development in aging human articular cartilage and molecular matrix changes characteristic of osteoarthritis. Arthritis Rheum. 2003; 48(5): 1261–1270, doi: 10.1002/art.10976, indexed in Pubmed: 12746899.
4. Goldring MB, Otero M. Inflammation in osteoarthritis. Curr Opin Rheumatol. 2011; 23(5): 471–478, doi: 10.1097/BOR.0b013e328349c2b1, indexed in Pubmed: 21788902.
5. Blanco FJ, Rego I, Ruiz-Romero C. The role of mitochondria in osteoarthritis. Nat Rev Rheumatol. 2011; 7(3): 161––169, doi: 10.1038/nrrheum.2010.213, indexed in Pubmed: 21200395.
6. Bjarnason I, Scarpignato C, Holmgren E, et al. Mechanisms of Damage to the Gastrointestinal Tract From Nonsteroidal Anti-Inflammatory Drugs. Gastroenterology. 2018; 154(3): 500–514, doi: 10.1053/j.gastro.2017.10.049, indexed in Pubmed: 29221664.
7. Chiquet-Ehrismann R. Tenascins, a growing family of extracellular matrix proteins. Experientia. 1995; 51(9-10): 853–862, doi: 10.1007/bf01921736, indexed in Pubmed: 7556567.
8. Whitby DJ, Longaker MT, Harrison MR, et al. Rapid epithelialisation of fetal wounds is associated with the early deposition of tenascin. J Cell Sci. 1991; 99 (Pt 3): 583–586, indexed in Pubmed: 1719005.
9. Tsunoda T, Inada H, Kalembeyi I, et al. Involvement of large tenascin-C splice variants in breast cancer progression. Am J Pathol. 2003; 162(6): 1857–1867, doi: 10.1016/S0002-9440(10)64320-9, indexed in Pubmed: 12759243.
10. Sofat N, Robertson SD, Hermansson M, et al. Tenascin-C fragments are endogenous inducers of cartilage matrix degradation. Rheumatol Int. 2012; 32(9): 2809–2817, doi: 10.1007/s00296-011-2067-8, indexed in Pubmed: 21874326.
11. Yoshimura E, Majima A, Sakakura Y, et al. Expression of tenascin-C and the integrin alpha 9 subunit in regeneration of rat nasal mucosa after chemical injury: involvement in migration and proliferation of epithelial cells. Histochem Cell Biol. 1999; 111(4): 259–264, doi: 10.1007/s004180050356, indexed in Pubmed: 10219625.
12. Midwood K, Sacre S, Piccinini AM, et al. Tenascin-C is an endogenous activator of Toll-like receptor 4 that is essential for maintaining inflammation in arthritic joint disease. Nat Med. 2009; 15(7): 774–780, doi: 10.1038/nm.1987, indexed in Pubmed: 19561617.
13. Nho RS, Hergert P. FoxO3a and disease progression. World J Biol Chem. 2014; 5(3): 346–354, doi: 10.4331/wjbc.v5.i3.346, indexed in Pubmed: 25225602.
14. Turrel-Davin F, Tournadre A, Pachot A, et al. FoxO3a involved in neutrophil and T cell survival is overexpressed in rheumatoid blood and synovial tissue. Ann Rheum Dis. 2010; 69(4): 755–760, doi: 10.1136/ard.2009.109991, indexed in Pubmed: 19435720.
15. Johnson CI, Argyle DJ, Clements DN. In vitro models for the study of osteoarthritis. Vet J. 2016; 209: 40–49, doi: 10.1016/j.tvjl.2015.07.011, indexed in Pubmed: 26831151.
16. Nakata K, Hanai T, Take Y, et al. Disease-modifying effects of COX-2 selective inhibitors and non-selective NSAIDs in osteoarthritis: a systematic review. Osteoarthritis Cartilage. 2018; 26(10): 1263–1273, doi: 10.1016/j.joca.2018.05.021, indexed in Pubmed: 29890262.
17. Peng SL. Forkhead transcription factors in chronic inflammation. Int J Biochem Cell Biol. 2010; 42(4): 482–485, doi: 10.1016/j.biocel.2009.10.013, indexed in Pubmed: 19850149.

18. Soufli I, Toumi R, Rafa H, et al. Overview of cytokines and nitric oxide involvement in immuno-pathogenesis of inflammatory bowel diseases. World J Gastrointest Pharmacol Ther. 2016; 7(3): 353–360, doi: 10.4292/wjgpt.v7.i3.353, indexed in Pubmed: 27602236.
19. Rodrigues JP, Caldas IS, Gonçalves RV, et al. S. mansoni-T. cruzi co-infection modulates arginase-1/iNOS expression, liver and heart disease in mice. Nitric Oxide. 2017; 66: 43–52, doi: 10.1016/j.niox.2017.02.013, indexed in Pubmed: 28268114.
20. Adler N, Schoeniger A, Fuhrmann H. Effects of transforming growth factor-βand interleukin-1βon inflammatory markers of osteoarthritis in cultured canine chondrocytes. Am J Vet Res. 2017; 78(11): 1264–1272, doi: 10.2460/ajvr.78.11.1264, indexed in Pubmed: 29076366.
21. Berenbaum F. Signaling transduction: target in osteoarthritis. Curr Opin Rheumatol. 2004; 16(5): 616–622, doi: 10.1097/01.bor.0000133663.37352.4a, indexed in Pubmed: 15314504.
22. Wang SN, Xie GP, Qin CH, et al. Aucubin prevents interleukin-1 beta induced inflammation and cartilage matrix degradation via inhibition of NF-βB signaling pathway in rat articular chondrocytes. Int Immunopharmacol. 2015; 24(2): 408–415, doi: 10.1016/j.intimp.2014.12.029, indexed in Pubmed: 25576403.
23. Studer R, Jaffurs D, Stefanovic-Racic M, et al. Nitric oxide in osteoarthritis. Osteoarthritis Cartilage. 1999; 7(4): 377–379, doi: 10.1053/joca.1998.0216, indexed in Pubmed: 10419772.
24. Xie Q, Nathan C. The high-output nitric oxide pathway: role and regulation. J Leukoc Biol. 1994; 56(5): 576–582, doi: 10.1002/jlb.56.5.576, indexed in Pubmed: 7525816.
25. Jung YK, Park HR, Cho HJ, et al. Degrading products of chondroitin sulfate can induce hypertrophy-like changes and MMP-13/ADAMTS5 production in chondrocytes. Sci Rep. 2019; 9(1): 15846, doi: 10.1038/s41598-019-52358-4, indexed in Pubmed: 31676809.
26. Yui N, Yudoh K, Fujiya H, et al. Mechanical and oxidative stress in osteoarthritis. The Journal of Physical Fitness and Sports Medicine. 2016; 5(1): 81–86, doi: 10.7600/jpfsm.5.81.
27. Dey P, Panga V, Raghunathan S. A cytokine signalling network for the regulation of inducible nitric oxide synthase expression in rheumatoid arthritis. PLoS One. 2016; 11(9): e0161306, doi: 10.1371/journal.pone.0161306, indexed in Pubmed: 27626941.
28. Hwang HS, Kim HAh. Chondrocyte apoptosis in the pathogenesis of osteoarthritis. Int J Mol Sci. 2015; 16(11): 26035–26054, doi: 10.3390/ijms161125943, indexed in Pubmed: 26528972.
29. Moncada S, Erusalimsky JD. Does nitric oxide modulate mitochondrial energy generation and apoptosis? Nat Rev Mol Cell Biol. 2002; 3(3): 214–220, doi: 10.1038/nrm762, indexed in Pubmed: 11994742.
30. Lepetsos P, Papavassiliou KA, Papavassiliou AG. Redox and NF-βB signaling in osteoarthritis. Free Radic Biol Med. 2019; 132: 90–100, doi: 10.1016/j.freeradbiomed.2018.09.025, indexed in Pubmed: 30236789.
31. Storz P. Forkhead homeobox type O transcription factors in the responses to oxidative stress. Antioxid Redox Signal. 2011; 14(4): 593–605, doi: 10.1089/ars.2010.3405, indexed in Pubmed: 20618067.
32. Yuan Z, Lehtinen MK, Merlo P, et al. Regulation of neuronal cell death by MST1-FOXO1 signaling. J Biol Chem. 2009; 284(17): 11285–11292, doi: 10.1074/jbc.M900461200, indexed in Pubmed: 19221179.
33. Kojima T, Norose T, Tsuchiya K, et al. Mouse 3T3-L1 cells acquire resistance against oxidative stress as the adipocytes differentiate via the transcription factor FoxO. Apoptosis. 2010; 15(1): 83–93, doi: 10.1007/s10495-009-0415-x, indexed in Pubmed: 19842039.
34. Hasegawa M, Nakoshi Y, Muraki M, et al. Expression of large tenascin-C splice variants in synovial fluid of patients with rheumatoid arthritis. J Orthop Res. 2007; 25(5): 563–568, doi: 10.1002/jor.20366, indexed in Pubmed: 17262825.
35. Aungier SR, Cartwright AJ, Schwenzer A, et al. Targeting early changes in the synovial microenvironment: a new class of immunomodulatory therapy? Ann Rheum Dis. 2019; 78(2): 186–191, doi: 10.1136/annrheumdis-2018-214294, indexed in Pubmed: 30552174.
36. Chockalingam PS, Glasson SS, Lohmander LS. Tenascin-C levels in synovial fluid are elevated after injury to the human and canine joint and correlate with markers of inflammation and matrix degradation. Osteoarthritis Cartilage. 2013; 21(2): 339–345, doi: 10.1016/j.joca.2012.10.016, indexed in Pubmed: 23142724.
37. Unno H. Prevention mechanism of tenascin-C for the cartilage degeneration. Jap Journal of Joint Diseases. 2016; 35(2): 131–136, doi: 10.11551/jsjd.35.131.
38. Okamura N, Hasegawa M, Nakoshi Y, et al. Deficiency of tenascin-C delays articular cartilage repair in mice. Osteoarthritis Cartilage. 2010; 18(6): 839–848, doi: 10.1016/j.joca.2009.08.013, indexed in Pubmed: 19747998.
39. Matsui Y, Hasegawa M, Iino T, et al. Tenascin-C prevents articular cartilage degeneration in murine osteoarthritis models. Cartilage. 2018; 9(1): 80–88, doi: 10.1177/1947603516681134, indexed in Pubmed: 29219023.

Submitted: 16 July, 2019
Accepted after reviews: 30 December, 2019
Available as AoP: 31 January, 2020

FOLIA HISTOCHEMICA ET CYTOBIOLOGICA
Vol. 58, No. 1, 2020
pp. 9–16

ORIGINAL PAPER

VIA MEDICA

MiR-491-3p is down-regulated in postmenopausal osteoporosis and affects growth, differentiation and apoptosis of hFOB1.19 cells through targeting CTSS

Wen-Xiong Hu, Hua Li, Jia-Zheng Jiang

Department of Orthopedics, Hainan Western Central Hospital, Hainan Province, P.R. China

Abstract

Background. Postmenopausal osteoporosis (PMO) is a common disease related to aging, which has been paid increasing attention in recent years because of its serious complications. MiR-491-3p was found to play a crucial roles in several diseases. However, the role of miR-491-3p in PMO has yet not been studied. Our research intends to explore the impact of miR-491-3p on PMO in the in vitro model.

Material and methods. The expression patterns of miR-491-3p and cathepsin S (CTSS) in patients with PMO were acquired from the GEO database. The human osteoblast cell hFOB1.19 was used to detect the function of miR-491-3p and CTSS in PMO. The viability and apoptosis of hFOB1.19 cells were measured by cell counting kit 8 and flow cytometry assays. The apoptosis and differentiation related proteins were analyzed by western blotting. The relationship between miR-491-3p and CTSS was predicted by appropriate software and affirmed by luciferase assay.

Results. MiR-491-3p expression was lower in patients with PMO. The up-regulation of miR-491-3p in hFOB1.19 cells increased their viability and differentiation and inhibited their apoptosis. CTSS, which was highly expressed in patients with PMO, was confirmed as a direct target of miR-491-3p and was found to be inversely modulated by miR-491-3p. The rescue assays showed that overexpression of CTSS suppressed the promoting effects of miR-491-3p mimic on the proliferation and differentiation of hFOB1.19 cells, and repressed the inhibitory effects of miR-491-3p mimic on apoptosis of hFOB1.19 cells.

Conclusions. The results of our study showed that miR-491-3p could ameliorate biological characteristics of hFOB1.19 cells by reducing CTSS expression suggesting that miR-491-3p/CTSS might be a potential biomarker for the diagnosis and treatment of PMO. *(Folia Histochemica et Cytobiologica 2020, Vol. 58, No. 1, 9–16)*

Key words: postmenopausal osteoporosis; osteoblastic hFOB1.19 cells; miR-491-3p; cathepsin S; proliferation; apoptosis; flow cytometry

Introduction

In recent years, an increasing number of women over the age of 50 are being affected by the postmenopausal osteoporosis (PMO), which leads to an increased economic and social burden [1]. Bone health is mainly dependent on the dynamic balance between bone formation and bone resorption. Disorders of bone metabolism easily induce bone-related diseases, especially osteoporosis, which can result in a decrease in bone density and an increase in the risk of fracture [2, 3]. Bone homeostasis is a remolding procedure regulated by three types of osteocytes, including osteoclast, osteoblast, and osteocyte [4]. PMO is considered to be a direct result of the decrease of endogenous estrogen in postmenopausal women, accompanied by a significant reduction in bone mass [5, 6]. Therefore, estrogens were widely used to treat PMO for a period of time. After hormonal therapy was found to increase the risk of heart disease and breast cancer, the use of estrogens dropped dramatically, even though the risk was low [7]. Several drugs are being used to treat PMO, including bisphosphonates, calcitonin, and other, however, they show adverse effects on the

Correspondence address: Wen-Xiong Hu
Department of Orthopedics,
Hainan Western Central Hospital,
Hainan Province, P.R. China
e-mail: Hnhwx2010@sina.cn

gastrointestinal tract [7]. Therefore, it is imperative to understand the pathogenesis of PMO and develop effective therapeutic strategies.

MicroRNAs (miRNAs), as 22-25 nucleotides non-coding small RNAs, play an indispensable role in regulating genes expression in organisms [8]. Emerging evidence shows that miRNAs are implicated in regulating numerous biological processes, such as cell growth, apoptosis, autophagy, differentiation, inflammation, invasion and migration [9–12]. In addition, the function of miRNAs in the development of PMO has attracted a lot of attention. Recent work performed by Li *et al*. demonstrated that miR-133a participated in the pathogenesis of PMO by facilitating osteoclast differentiation [13]. Moreover, the same group reported that miR-210 was implicated in the development of PMO through increasing vascular endothelial growth factor (VEGF) expression and osteoblast differentiation [14]. Thus, circulating miR-133a-3p might be regarded as an underlying non-invasive biomarker and therapy target in PMO [15]. Several reports documented the involvement of miR-491-3p in cancer, for example, miR-491-3p reduced multidrug resistance of hepatocellular carcinoma, inhibited the growth and invasion of osteosarcoma cells, regulated the chemo-sensitivity of human tongue cancer, and participated in the pathogenesis of clear cell renal cell carcinoma [16–19]. However, its role in PMO has yet not been investigated.

We found that the expression of miR-491-3p was lower in patients with PMO, while the expression of cathepsin S (CTSS) in PMO patients showed an opposite trend. Moreover, CTSS was confirmed as a target of miR-491-3p. More importantly, we revealed that miR-491-3p could promote the growth and differentiation of hFOB1.19 cells, and inhibit their apoptosis by reducing CTSS expression. Our research provides novel pairs of molecules involved in the pathogenesis of PMO with potential use for the diagnosis and therapy of this syndrome.

Materials and methods

Data sources. The expression patterns of miR-491-3p and CTSS in PMO were acquired from the GEO database following accession numbers GSE74209 and GSE56116. The GSE74209 dataset including 6 patients with PMO fractures (osteoporosis) and 6 patients with osteoarthritis ('healthy' control) was used to analyze the expression of miR-491-3p. The GSE56116 dataset containing 10 patients with PMO fractures (osteoporosis) and 3 patients with osteoarthritis ('healthy' control) was utilized to analyze the expression of CTSS.

Cell culture and transfection. Human osteoblast cell line hFOB1.19 was purchased from the Shanghai cell bank of the Chinese Academy of Medical Sciences (Shanghai, China) and cultivated in the α-MEM medium including 10% fetal bovine serum, 100 U/mL penicillin and 0.1 mg/mL streptomycin (Invitrogen, Carlsbad, CA, USA). Overexpression of miR-491-3p and CTSS were achieved by transfection of miR-491-3p mimic and pcDNA3.1-CTSS (GenePharma, Shanghai, China) into cells, respectively. The transfection concentrations were 50 nmol/L for the miR-491-3p mimic, miR-491-3p mimic NC, pcDNA3.1-CTSS and pcDNA3.1. All of them were transfected into hFOB1.19 cells by Lipofectamine 3000 reagent (Invitrogen).

Cell viability test. Cell counting kit-8 (CCK-8, Dojindo Moleular Technologies, Inc., Gathersburg, MD, USA) test was carried out to detect the viability of hFOB1.19 cells. Cells were inoculated in 96-well plates with the density of 1×10^3 cells/well. After cells adhesion, the culture medium was changed, miR-491-3p mimic or miR-491-3p mimic NC was added, and the cultivation was continued for 48 h. Then, the cells were added with 20 μL of CCK-8 reagent and cultured for another 1.5 h. Finally, microplate reader SpectraMax®iD3 (Molecular Devices, San Jose, CA, USA) was used to measure the optical density (OD) values.

Cell apoptosis test. The apoptosis of treated cells was detected by flow cytometry. Cells were collected and centrifuged. Then, cells were suspended in pre-cooling phosphate buffer saline (PBS) and centrifuged again. Subsequently, the supernatant was sucked out and cells were re-suspended with $1 \times$ binding buffer. We adjusted cell density to $1–5 \times 10^6$ cells/mL. Mixed 5 μL of Annexin V/FITC and 100 μL of cell suspension into 5 mL tube, and then the mixture was left for 5 min in the darkroom. Before detection, 10 μL of propidium iodoide (PI) and 400 μL of PBS were added into the flow tube. The results were analyzed by Flowjo software 7.6.1.

MiR-491-3p target gene prediction website. The biological prediction websites including MiRanda (http://www.microrna.org), miRWalk (http://zmf.umm.uni-heidelberg.de/apps//zmf/mirwalk2/), and TargetScan (http://www.targetscan.org/), miRDB (http://www.mirdb.org/) were used to predict the target genes of miR-491-3p.

Dual luciferase reporter assay. The fragments of CTSS-mutant-type (mut) and CTSS-wild-type (wt) were synthesized and inserted into a pmirGLO vector (GenePharma). The cells were inoculated to 24-well plates. When cells grew to 80% confluence, luciferase vector containing wt-CTSS or mut-CTSS and miR-491-3p mimic or mimic NC were co-transfected into HEK293 cells by Lipofectamine 3000 reagent (Invitrogen). After 48 h, the protein was extracted and the luciferases activity was detected by Dual-Luciferase Reporter Assay Kit (Promega, Madison, WI, USA) following the manufacturer's specification.

RNA extraction and Quantitative Real-time PCR (qRT--PCR). The whole RNA was obtained from the treated

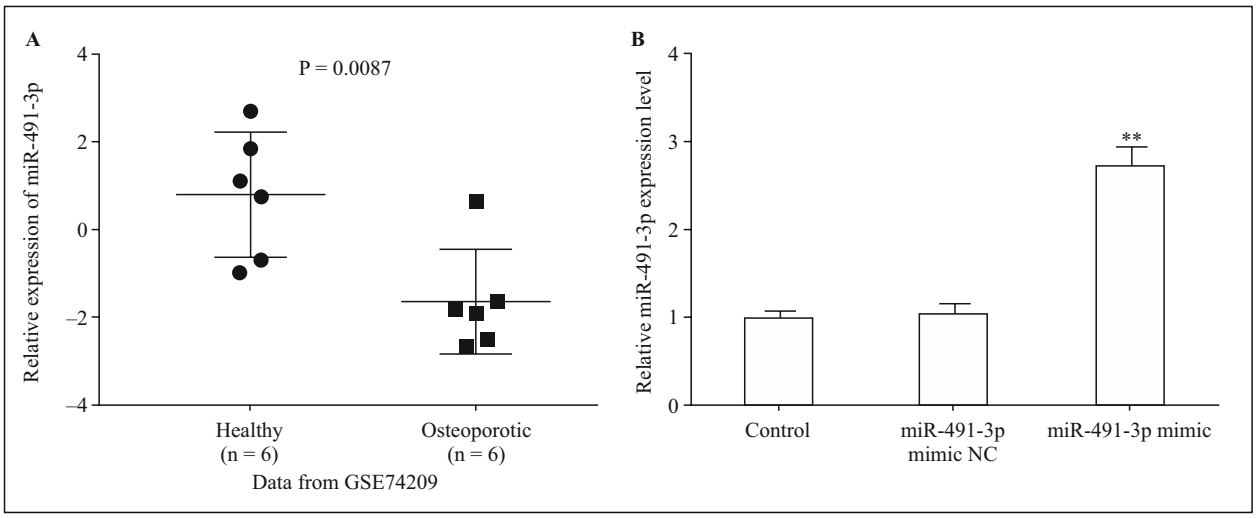

Figure 1. Determination of miR-491-3p expression. **A.** Data from GEO dataset revealed that miR-491-3p expression was lower in PMO osteoporotic patients (n = 6) compared with that of the 'healthy' people (n = 6), P = 0.0087. **B.** The relative expression of miR-491-3p in hFOB1.19 cells was measured after transfection with miR-491-3p mimic or miR-491-3p mimic NC, **P < 0.01 *vs.* control.

cells by TRIzol (Invitrogen) and reverse transcribed into cDNA by PrimeScript RT Reagent Kit and Mir-X™ miRNA First Strand Synthesis Kit (Invitrogen). Then, the expression of mRNA and miRNA were analyzed by real-time PCR with the help of SYBR Premix Ex Taq II and SYBR PrimeScriptTM miRNA RT-PCT Kit (TaKaRa, Tokyo, Japan), accordingly. Subsequently, the real-time PCR was performed on a 7900HT real-time PCR system with the following procedures: 40 circles consist of 95°C for 5 min, 95°C for 30 s, then 60°C for 45 s, 72°C for 30 min. GAPDH was considered as the internal standard for mRNA detection, and U6 was regarded as the internal standard for miRNA calculation. $2^{-\Delta\Delta Ct}$ method was used to analyze the relative expression of mRNA and miRNA. The sequences of the primers were synthesized as below: MiR-491-3p, forward: 5'-AGTGGGGAACCCTTCC-3', reverse: 5'-GAACATGTCTGCG-TATCTC-3'; U6, forward: 5'-AAAGCAAATCATCGGACGACC-3', reverse: 5'-GTACAACACATTGTTTCCTCGGA-3'; CTSS, forward: 5'-TGGATCACCACT-GGCATCTCTG-3', reverse: 5'-GCTCCAGGTTGTGAAGCATCAC-3'; GAPDH, forward: 5'-TGTGGGCATCAATGGATTTGG-3', reverse: 5'-CCCTCCAGG-GGATCTGTTTG-3'.

Western blotting. Protein samples were extracted from the treated cells by RIPA lysis buffer with protease inhibitor. 20 μg of protein within 1 × loading buffer was put into each well, isolated by sodium dodecyl sulphate-polyacrylamide gel electrophoresis and electro-transferred onto PVDF membranes under wet condition. Then 5% non-fat milk dissolved in TBST (10 mM Tris-HCl, pH7.5, 150 mM NaCl, 0.05% Tween-20) was used to block the membranes. The membranes were then incubated with primary antibodies against CTSS (1:2000), Bcl-2 (1:1000), Bax (1:2000), Cleaved caspase-3 (1:3000), Cleaved caspase-9 (1:3000), ALP (1:3000), Runx2 (1:1000), Osterix (1:5000), OPN(1:1000) and GAPDH (1:10000) (all from Abcam, Cambridge, UK) at 4°C overnight. Next, the membranes were incubated with the IgG-HRP antibody at about 25°C for 1 h. Finally, the signals were developed by ECL (HRP Substrate Luminol Reagent: HRP Substrate Peroxide Solution = 1:1) and scanned by QUANTITY ONE software 4.6.6. GAPDH was regarded as the internal standard.

Statistical analysis. All experimental data were repeated at least three times and analyzed by SPSS22.0 and Graphpad Prism 5.0 software. Student's t-test was used to analyze the difference between two samples, while the comparison among multiple groups was calculated by ANOVA followed by Dunnett (compare all groups *vs* control group) and Bofferonnie (compare selected pairs of groups) *post hoc* test. P value less than 0.05 was considered to indicate a statistically significant difference.

Results

The expression of MiR-491-3p was lower in patients with PMO

Firstly, GEO dataset was used to detect the expression of miR-491-3p in PMO. The data in Figure 1A manifested that miR-491-3p expression was lower in patients with PMO fracture (osteoporotic, n = 6) than that of the patients with osteoarthritis ("healthy" control, n = 6, P = 0.0087). Subsequently, to inves-

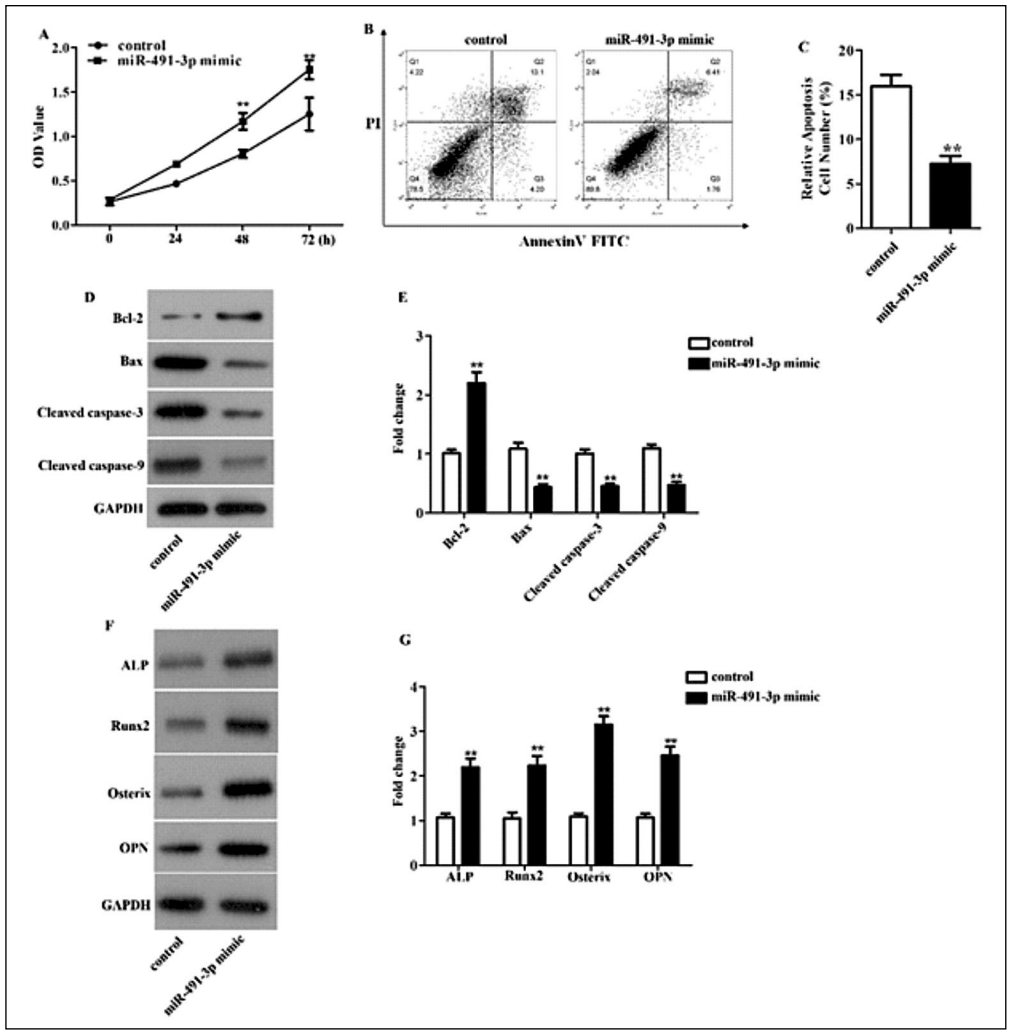

Figure 2. MiR-491-3p promoted proliferation and differentiation of hFOB1.19 cells, and inhibited their apoptosis. **A.** The proliferation of hFOB1.19 cells was measured by CCK-8 assay as described in Methods. **B–C.** The apoptosis of hFOB1.19 cells was detected by flow cytometry. **D–E.** The a presence of poptosis-related proteins in hFOB1.19 cells were analyzed by Western blotting. **F–G.** The presence of differentiation-related proteins in hFOB1.19 cells were measured by Western blotting. **P < 0.01 *vs.* control.

tigate the effects of miR-491-3p on hFOB1.19 cells, we attempted to up-regulate miR-491-3p with mimic. The data presented in Figure 1B indicated that miR-491-3p expression was significantly upregulated in hFOB1.19 cells after treatment with miR-491-3p mimic compared with that of the control cells and miR-491-3p mimic NC groups ($P < 0.01$).

Overexpression of miR-491-3p could inhibit the apoptosis of hFOB1.19 cells and promote their proliferation and differentiation

To further explore the impact of miR-491-3p on hFOB1.19 cells proliferation, apoptosis and differentiation, CCK-8, flow cytometry and western blotting assays were carried out. The data of CCK-8 tests showed that up-regulation of miR-491-3p could increase the OD values of hFOB1.19 cells compared with that of the control and the difference was significant at 48 h and 72 h (Fig. 2A, $P < 0.01$).

Flow cytometry results demonstrated that the apoptosis rate of hFOB1.19 cells was reduced nearly 60% after upregulation of miR-491-3p compared with that of the control (Figs. 2B–C, $P < 0.01$). Subsequently, the apoptotic-related proteins were analyzed by Western blotting. The results indicated that the expression of anti-apoptotic protein Bcl-2 was reduced, and the expression of pro-apoptotic proteins including Bax, Cleaved caspase-3 and Cleaved caspase-9 were increased in hFOB1.19 cells after transfection of the cells with miR-491-3p mimic (Figs. 2D–E, $P < 0.01$).

To study the effects of miR-491-3p on hFOB1.19 cells differentiation, we analyzed the changes of differentiation-related proteins with western blotting. The results indicated that after miR-491-3p mimic

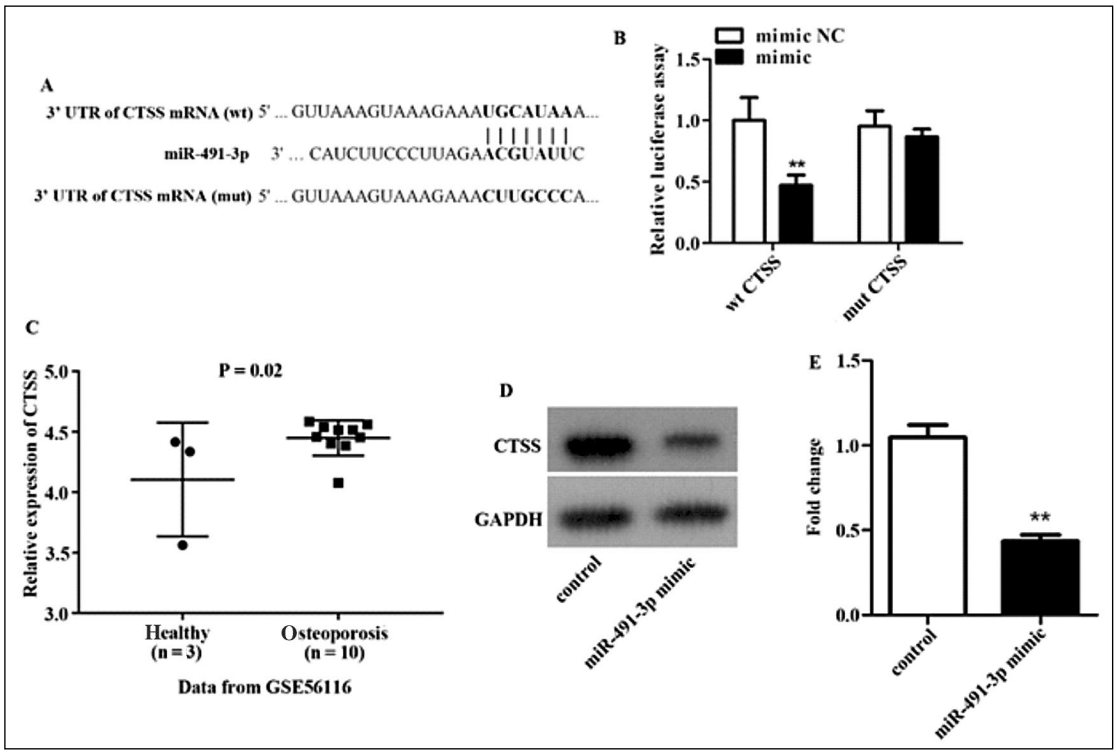

Figure 3. CTSS was highly expressed in PMO and negatively regulated by miR-491-3p. **A.** The sequences of wild type 3'UTR of CTSS, mutant type 3'UTR of CTSS, and miR-491-3p were presented. **B.** The luciferase activity of wt CTSS and mut CTSS were assessed after the cells were transfected with miR-491-3p mimic or NC. **C.** The data from GEO indicated that CTSS was clearly up-regulated in patients with PMO (n = 10) compared with that of the 'healthy' people (n = 3), P = 0.02. **D–E.** The expression of CTSS was detected after transfected with miR-491-3p mimic or NC. **P < 0.01 *vs.* control.

treatment, the expression of ALP, Runx2, Osterix and OPN significantly increased to 2.05, 2.13, 2.9, and 2.3 times of the control group, respectively (Figs. 2F–G, P < 0.01). Thus, the results of all performed tests indicated that up-regulation of miR-491-3p could increase the proliferation and differentiation of hFOB1.19 cells, and reduce the apoptosis of hFOB1.19 cells.

Cathepsin S was highly expressed in patients with PMO and negatively regulated by miR-491-3p

Based on the results from target gene prediction website and bioinformatics analysis, CTSS was selected as a target of miR-491-3p for further investigation. As presented in Figure 3A, the wt 3'UTR of CTSS contains the complementary binding sequence of miR-491-3p. Subsequently, dual luciferase reporter assay was performed to confirm the association between miR-491-3p and CTSS. The data from Figure 3B showed that the luciferase activity in wt 3'UTR of CTSS was clearly decreased after transfected with miR-491-3p mimic compared with that of the miR-491-3p mimic NC group (P < 0.01). However, miR-491-3p had little effect on luciferase activity of the mut 3'UTR of CTSS. The results further confirmed that miR-491-3p directly binds with CTSS in osteoblastic cell line. The data from GEO database indicated that CTSS was significantly up-regulated in patients with PMO fracture (osteoporotic, n = 10) compared with that of the patients in osteoarthritis ("healthy" control, n = 3, P = 0.02, Fig. 3C). Moreover, the expression of CTSS was clearly reduced in hFOB1.19 cells after transfected with miR-491-3p mimic (Figs. 3D–E, P < 0.01). The results implied that CTSS was a direct target of miR-491-3p and was negatively modulated by miR-491-3p.

CTSS suppressed the positive effects of miR-491-3p on hFOB1.19 cells

To explore the relationships between miR-491-3p and CTSS in PMO, the biological properties of hFOB1.19 cells were analyzed after they were treated with miR-491-3p mimic and pcDNA3.1-CTSS. The results shown in Figure 4A indicated that the OD values of hFOB1.19 cells were increased after treatment with miR-491-3p mimic in contrast with that of the control, while the raising tendency was reversed in miR-491-3p mimic and pcDNA3.1-CTSS group (P < 0.01). The data indicated that CTSS could suppress the ascend-

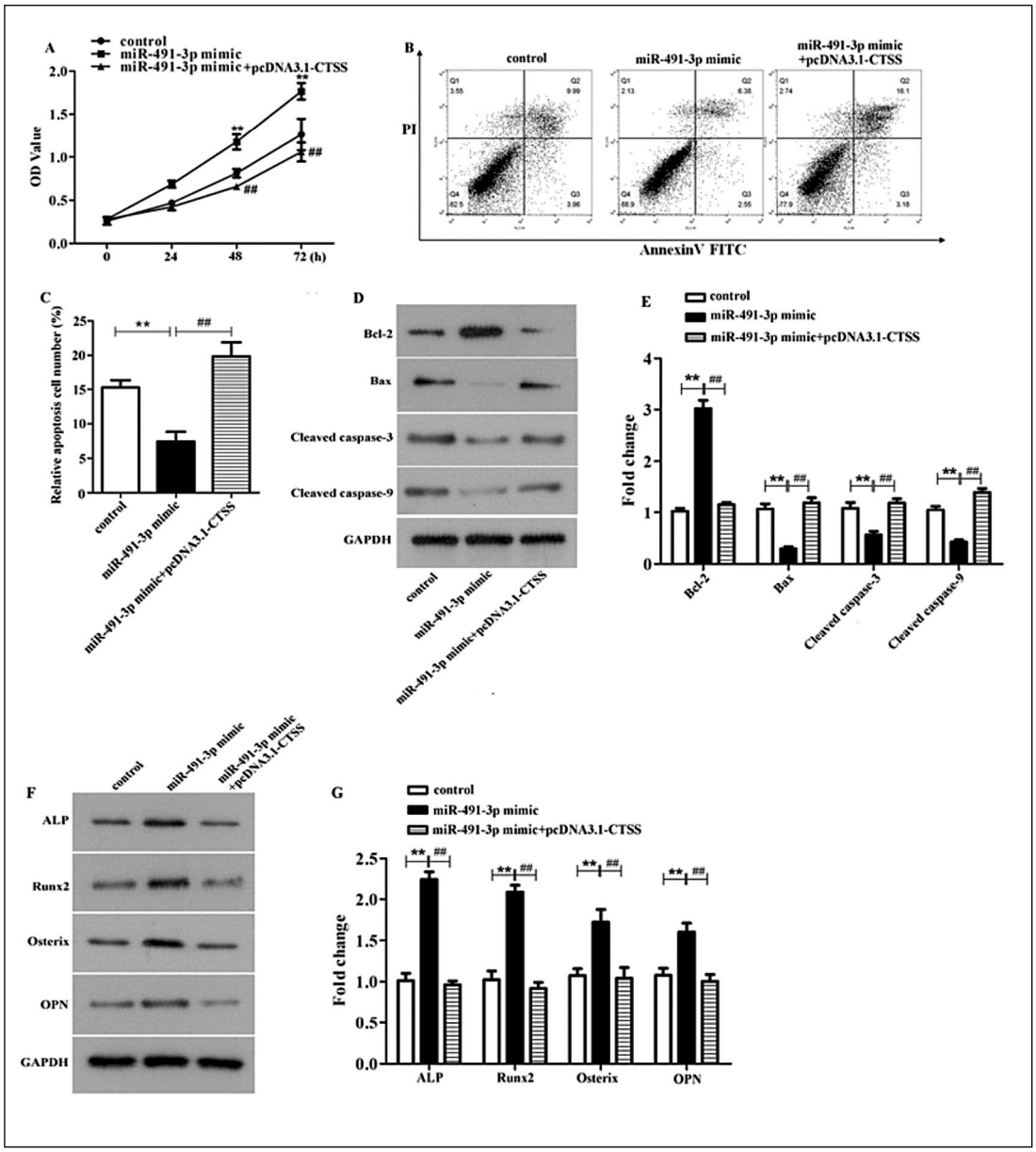

Figure 4. CTSS suppressed the promoting effects of miR-491-3p on the proliferation and differentiation of hFOB1.19 cells, and the inhibitory effects of miR-491-3p on hFOB1.19 cells apoptosis. **A.** The hFOB1.19 cells proliferation was detected by CCK-8 after their treatment with miR-491-3p mimic/miR-491-3p mimic + pcDNA3.1-CTSS. **B–C.** Flow cytometry was applied to detect the apoptosis of hFOB1.19 cells. **D–E.** The apoptosis-related proteins were measured by Western blotting. **F–G.** The expression of ALP, Runx2, Osterix and OPN were detected by Western blotting. $^{**}P < 0.01$, $^{\#\#}P < 0.01$, **represented miR-491-3p mimic *vs* control, $^{\#\#}$represented miR-491-3p mimic and pcDNA3.1-CTSS *vs* miR-491-3p mimic.

ing proliferation ability of hFOB1.19 cells induced by miR-491-3p mimic. Flow cytometry data showed that the apoptosis of hFOB1.19 cells was reduced nearly 50% after treatment with miR-491-3p mimic compared with that of the control, and increased approximately two times after treatment with miR-491-3p mimic and pcDNA3.1-CTSS compared with that of the miR-491-3p mimic group (Figs. 4B–C, $P < 0.01$). Moreover, the expression of anti-apoptotic protein Bcl-2 was reduced about 60%, and the pro-apoptotic proteins Bax, Cleaved caspase-3 and Cleaved caspase-9 were significantly increased after the cells were transfected with miR-491-3p mimic and pcDNA3.1-CTSS compared with that of the miR-491-3p mimic group ($P < 0.01$). On the contrary, the raising tendency of ALP, Runx2, Osterix and OPN expression induced by miR-491-3p mimic was reversed after the cells were transfected with miR-491-3p mimic and

pcDNA3.1-CTSS ($P < 0.01$). All the data implicate that CTSS could suppress the promoting effects of miR-491-3p on hFOB1.19 cells proliferation and differentiation, and repress the inhibitory effects of miR-491-3p on hFOB1.19 cells apoptosis.

Discussion

PMO is an insidious disease without any obvious symptoms in its early stage. Once the signs of PMO appear, the fracture has already occurred [20]. Therefore, it is essential to search effective and preventive measures and molecular markers for early diagnosis. With the development of more and more validated miRNA signatures and mature medium-throughput methods in the clinical setting, specific miRNA markers are raised potentially to conduce to human health [21]. Recently, several researchers have discovered that some miRNAs including miR-491-3p were modulated by enterovirus 71 which, apart from other virus types, may cause of major outbreaks of hand, foot, and mouth disease (HFMD) [22]. MiR-491-3p has been reported to be involved in the pathogenesis of major depression or suicide [23]. In addition, previous study has found that miR-491-3p played a vital role in the modulation of multidrug resistance in hepatocellular carcinoma through regulating ABCB1 and Sp3 expression [19]. Moreover, miR-491-3p was discovered to suppress the growth and invasiveness of osteosarcoma [18] and glioblastoma [24] cells. However, study of miR-491-3p in osteoporosis has yet not been reported. In the current study, the data indicated that miR-491-3p expression was lower in PMO patients. Importantly, there are reports which indicate that proliferation and differentiation of osteoblasts are important for the development of osteoporosis [25]. ALP, Runx2, Osterix and OPN have been demonstrated to play positive roles in promoting osteogenesis [26]. In our study, the up-regulation of miR-491-3p increased the expression of ALP, Runx2, Osterix and OPN, indicating that miR-491-3p can promote osteoblast differentiation. Cell apoptosis is an important biological process that occurs in many diseases, including PMO [27]. In our study, up-regulation of miR-491-3p attenuated the apoptosis of human osteoblastic cells. These results suggested that miR-491-3p inhibited the development of PMO by promoting the growth and differentiation of osteoblasts, and suppressing their apoptosis.

It is well known that miRNAs perform their functions through binding to mRNAs and blocking protein expression. Based on the biological predictions, bioinformatical analysis and dual luciferase reporter assay, cathepsin S was selected and confirmed as a direct target of miR-491-3p. CTSS, as a lysosomal protease, can promote the degradation of damaged or unnecessary proteins in the lysosomal pathway [28], and was reported to be involved in several diseases including atherosclerosis, tumor metastasis and osteoporosis [29]. In addition, growing evidence have indicated that CTSS regulated adipocyte and osteoblast differentiation, bone turnover, and bone microarchitecture [30]. Furthermore, CTSS was also used as a potential drug target for osteoporosis and rheumatoid arthritis [31]. In our study, CTSS was verified as a direct target of miR-491-3p, and was negatively modulated by miR-491-3p. Moreover, data from GEO dataset showed that CTSS was highly expressed in patients with PMO. Rescue assays indicated that overexpression of CTSS could limit the positive effects of miR-491-3p on osteoblastic cells. More *in vivo* experiments are needed to confirm these results, since *in vitro* experiments cannot fully simulate the situation *in vivo*.

In conclusion, our findings discovered that miR-491-3p showed a tendency of low expression in patients with PMO, while the expression trend of CTSS in PMO was just the opposite. What's more, overexpression of miR-491-3p could promote osteoblasts' proliferation and differentiation, and inhibit their apoptosis. In addition, CTSS was verified as a target gene of miR-491-3p and was found to be negatively regulated by miR-491-3p in osteoblastic cells. Further experiments implied that overexpression of CTSS could suppress the promoting effects of miR-491-3p on the phenotype of hFOB1.19 cells. To sum up, miR-491-3p could promote the differentiation and maintenance of osteoblasts by reducing CTSS expression. The results of this study provide a pair of molecules for the potential diagnosis and treatment of PMO.

References

1. Shao M. Construction of an miRNA-Regulated Pathway Network Reveals Candidate Biomarkers for Postmenopausal Osteoporosis. Comput Math Methods Med. 2017; 2017: 9426280, doi: 10.1155/2017/9426280, indexed in Pubmed: 29158773.
2. Bliuc D, Alarkawi D, Nguyen TV, et al. Risk of subsequent fractures and mortality in elderly women and men with fragility fractures with and without osteoporotic bone density: the Dubbo Osteoporosis Epidemiology Study. J Bone Miner Res. 2015; 30(4): 637–646, doi: 10.1002/jbmr.2393, indexed in Pubmed: 25359586.
3. Bliuc D, Nguyen ND, Nguyen TV, et al. Compound risk of high mortality following osteoporotic fracture and refracture in elderly women and men. J Bone Miner Res. 2013; 28(11): 2317–2324, doi: 10.1002/jbmr.1968, indexed in Pubmed: 23616397.
4. Jilka RL, O'Brien CA. The Role of Osteocytes in Age-Related Bone Loss. Curr Osteoporos Rep. 2016; 14(1): 16–25, doi: 10.1007/s11914-016-0297-0, indexed in Pubmed: 26909563.
5. Marcus R. Post-menopausal osteoporosis. Best Pract Res Clin Obstet Gynaecol. 2002; 16(3): 309–327, doi: 10.1053/beog.2002.0284, indexed in Pubmed: 12099665.

6. Seibel MJ, Dunstan CR, Zhou H, et al. Sex steroids, not FSH, influence bone mass. Cell. 2006; 127(6): 1079; author reply 1080–1079; author reply 1081, doi: 10.1016/j.cell.2006.12.002, indexed in Pubmed: 17174881.
7. Tella SH, Gallagher JC. Prevention and treatment of postmenopausal osteoporosis. J Steroid Biochem Mol Biol. 2014; 142: 155–170, doi: 10.1016/j.jsbmb.2013.09.008, indexed in Pubmed: 24176761.
8. He L, Hannon GJ. MicroRNAs: small RNAs with a big role in gene regulation. Nat Rev Genet. 2004; 5(7): 522–531, doi: 10.1038/nrg1379, indexed in Pubmed: 15211354.
9. Stefani G, Slack FJ. Small non-coding RNAs in animal development. Nat Rev Mol Cell Biol. 2008; 9(3): 219–230, doi: 10.1038/nrm2347, indexed in Pubmed: 18270516.
10. Filipowicz W, Bhattacharyya SN, Sonenberg N. Mechanisms of post-transcriptional regulation by microRNAs: are the answers in sight? Nat Rev Genet. 2008; 9(2): 102–114, doi: 10.1038/nrg2290, indexed in Pubmed: 18197166.
11. Olejniczak M, Kotowska-Zimmer A, Krzyzosiak W. Stress-induced changes in miRNA biogenesis and functioning. Cell Mol Life Sci. 2018; 75(2): 177–191, doi: 10.1007/s00018-017-2591-0, indexed in Pubmed: 28717872.
12. Yu A, Zhang T, Zhong W, et al. miRNA-144 induces microglial autophagy and inflammation following intracerebral hemorrhage. Immunol Lett. 2017; 182: 18–23, doi: 10.1016/j.imlet.2017.01.002, indexed in Pubmed: 28062218.
13. Li Z, Zhang W, Huang Y. MiRNA-133a is involved in the regulation of postmenopausal osteoporosis through promoting osteoclast differentiation. Acta Biochim Biophys Sin (Shanghai). 2018; 50(3): 273–280, doi: 10.1093/abbs/gmy006, indexed in Pubmed: 29425279.
14. Liu XD, Cai F, Liu L, et al. MicroRNA-210 is involved in the regulation of postmenopausal osteoporosis through promotion of VEGF expression and osteoblast differentiation. Biol Chem. 2015; 396(4): 339–347, doi: 10.1515/hsz-2014-0268, indexed in Pubmed: 25503465.
15. Pala E, Denkçeken T. Differentially expressed circulating miRNAs in postmenopausal osteoporosis: a meta-analysis. Biosci Rep. 2019; 39(5), doi: 10.1042/BSR20190667, indexed in Pubmed: 31023966.
16. He H, Wang L, Zhou W, et al. MicroRNA Expression Profiling in Clear Cell Renal Cell Carcinoma: Identification and Functional Validation of Key miRNAs. PLoS One. 2015; 10(5): e0125672, doi: 10.1371/journal.pone.0125672, indexed in Pubmed: 25938468.
17. Zheng G, Jia X, Peng C, et al. The miR-491-3p/mTORC2/FOXO1 regulatory loop modulates chemo-sensitivity in human tongue cancer. Oncotarget. 2015; 6(9): 6931––6943, doi: 10.18632/oncotarget.3165, indexed in Pubmed: 25749387.
18. Duan J, Liu J, Liu Y, et al. miR-491-3p suppresses the growth and invasion of osteosarcoma cells by targeting TSPAN1. Mol Med Rep. 2017; 16(4): 5568–5574, doi: 10.3892/mmr.2017.7256, indexed in Pubmed: 28849017.
19. Zhao Y, Qi X, Chen J, et al. The miR-491-3p/Sp3/ABCB1 axis attenuates multidrug resistance of hepatocellular carcinoma. Cancer Lett. 2017; 408: 102–111, doi: 10.1016/j.canlet.2017.08.027, indexed in Pubmed: 28844709.
20. Lippuner K. Medical treatment of vertebral osteoporosis. Eur Spine J. 2003; 12 Suppl 2: S132–S141, doi: 10.1007/s00586-003-0608-x, indexed in Pubmed: 13680313.
21. Backes C, Meese E, Keller A. Specific miRNA disease biomarkers in blood, serum and plasma: challenges and prospects. Mol Diagn Ther. 2016; 20(6): 509–518, doi: 10.1007/s40291-016-0221-4, indexed in Pubmed: 27378479.
22. Bian L, Wang Y, Liu Q, et al. Prediction of signaling pathways involved in enterovirus 71 infection by algorithm analysis based on miRNA profiles and their target genes. Arch Virol. 2015; 160(1): 173–182, doi: 10.1007/s00705-014-2249-2, indexed in Pubmed: 25287131.
23. Serafini G, Pompili M, Hansen KF, et al. The involvement of microRNAs in major depression, suicidal behavior, and related disorders: a focus on miR-185 and miR-491-3p. Cell Mol Neurobiol. 2014; 34(1): 17–30, doi: 10.1007/s10571-013-9997-5, indexed in Pubmed: 24213247.
24. Li X, Liu Y, Granberg KJ, et al. Two mature products of MIR-491 coordinate to suppress key cancer hallmarks in glioblastoma. Oncogene. 2015; 34(13): 1619–1628, doi: 10.1038/onc.2014.98, indexed in Pubmed: 24747968.
25. Fan JZ, Yang L, Meng GL, et al. Estrogen improves the proliferation and differentiation of hBMSCs derived from postmenopausal osteoporosis through notch signaling pathway. Mol Cell Biochem. 2014; 392(1-2): 85–93, doi: 10.1007/s11010-014-2021-7, indexed in Pubmed: 24752351.
26. An J, Yang H, Zhang Q, et al. Natural products for treatment of osteoporosis: The effects and mechanisms on promoting osteoblast-mediated bone formation. Life Sci. 2016; 147: 46–58, doi: 10.1016/j.lfs.2016.01.024, indexed in Pubmed: 26796578.
27. Yan L, Guo N, Cao Y, et al. miRNA145 inhibits myocardial infarctioninduced apoptosis through autophagy via Akt3/mTOR signaling pathway in vitro and in vivo. Int J Mol Med. 2018; 42(3): 1537–1547, doi: 10.3892/ijmm.2018.3748, indexed in Pubmed: 29956747.
28. Wilkinson RDA, Williams R, Scott CJ, et al. Cathepsin S: therapeutic, diagnostic, and prognostic potential. Biol Chem. 2015; 396(8): 867–882, doi: 10.1515/hsz-2015-0114, indexed in Pubmed: 25872877.
29. Wilder CL, Park KY, Keegan PM, et al. Manipulating substrate and pH in zymography protocols selectively distinguishes cathepsins K, L, S, and V activity in cells and tissues. Arch Biochem Biophys. 2011; 516(1): 52–57, doi: 10.1016/j.abb.2011.09.009, indexed in Pubmed: 21982919.
30. Rauner M, Föger-Samwald U, Kurz MF, et al. Cathepsin S controls adipocytic and osteoblastic differentiation, bone turnover, and bone microarchitecture. Bone. 2014; 64: 281–287, doi: 10.1016/j.bone.2014.04.022, indexed in Pubmed: 24780878.
31. Yasuda Y, Kaleta J, Brömme D. The role of cathepsins in osteoporosis and arthritis: rationale for the design of new therapeutics. Adv Drug Deliv Rev. 2005; 57(7): 973–993, doi: 10.1016/j.addr.2004.12.013, indexed in Pubmed: 15876399.

Submitted: 23 September, 2019
Accepted after reviews: 6 February, 2020
Available as AoP: 16 March, 2020

FOLIA HISTOCHEMICA ET CYTOBIOLOGICA
Vol. 58, No. 1, 2020
pp. 17–24

ORIGINAL PAPER

VIA MEDICA

Expression of CD163 and HLA-DR molecules on the monocytes in chronic lymphocytic leukemia patients

Wioleta Kowalska

Chair and Department of Clinical Immunology, Medical University of Lublin, Lublin, Poland

Abstract

Introduction. Human peripheral blood monocytes are the part of the leukemia microenvironment. We examined three monocyte subgroups: classical ($CD14^{++}CD16^{-}$), intermediate ($CD14^{++}CD16^{+}$) and non-classical ($CD14^{+}CD16^{++}$) monocytes. As these subpopulations can be also characterized by different levels of HLA-DR and CD163, we evaluated their expression on monocyte subpopulations of patients with chronic lymphocytic leukemia (CLL) and healthy individuals.

Material and methods. The monocyte subsets in peripheral blood of CLL patients (n = 40) and healthy controls (n = 10) were evaluated by flow cytometry. The monoclonal antibodies: anti-CD14 FITC, anti-CD16 PE-Cy5, anti-CD163 PE, anti-HLA-DR PE were used.

Results. The percentage of CD16-positive monocytes was significantly higher in CLL patients than in healthy donors. The highest percentage of $CD163^{+}$ monocytes is in the 'classical' ($CD14^{++}CD16^{-}$) population. In turn, the non-classical monocytes constituted the majority of cells lacking HLA-DR expression. In CLL patients, there was no statistically significant relationship between the percentage of each monocyte subpopulation and the stage according to Rai Staging of CLL.

Conclusions. The presence of CD163 on classical monocytes suggests that these cells have anti-inflammatory properties. Besides, the low expression of HLA-DR on non-classical monocytes may result in impaired ability to stimulate the immune system. *(Folia Histochemica et Cytobiologica 2020, Vol. 58, No. 1, 17–24)*

Key words: monocyte; subpopulations; CD163; HLA-DR; chronic lymphocytic leukemia

Introduction

Chronic lymphocytic leukemia (CLL) patients suffer from the immunological dysfunctions that refer not only to B cells, but also to other elements of the immune system, including T cells, NK cells, neutrophils and monocytes/macrophages [1]. The observed inhibition of antitumor response during CLL may be ascribed to cells that form the tumor microenvironment, which favor the clonal expansion of B lymphocytes and promote their survival [2]. Monocytes are mononuclear cells involved in the innate immune responses. In CLL they could have a significant influence on the regulation of the growth or elimination of cancer cells [3]. Based on differences in the expression of surface markers CD14 (receptor for lipopolysaccharide, *i.e.* LPS, LPS-R) and CD16 (FcγRIII receptor), three subpopulations of monocytes can be identified: the classical ($CD14^{++}CD16^{-}$), the intermediate ($CD14^{++}CD16^{+}$) and the non-classical ($CD14^{+}CD16^{++}$) monocytes [4–6]. Under physiological conditions, the percentage of classical monocytes constitutes about 95% of all monocytes circulating in the peripheral blood. The role of the remaining 5% of $CD16^{+}$ monocytes has not been clearly defined [7].

The disproportion between the percentage of $CD16^{-}$ and $CD16^{+}$ monocytes was observed in cancer patients [8]. It is believed that these abnormalities may have a significant impact on the proangiogenic and anti-tumor capacities of $CD16^{+}$ monocytes [9]. A higher expression of HLA-DR and CD86 molecules was observed on classical monocytes (CD16-negative) [10]. On the other hand, among CD16-positive mono-

Correspondence address: Wioleta Kowalska, PhD
Chair and Department of Clinical Immunology,
Medical University of Lublin,
Chodzki 4a, Lublin 20–093, Poland
email: w.kowalska.lub@gmail.com

cytes, the intermediate monocytes ($CD14^{++}CD16^{+}$) have a high expression of the CD163 [11]. It is currently believed that the CD163 protein is involved in the uptake of the hemoglobin-haptoglobin complex and the regulation of inflammatory processes [12, 13]. CD163 may also be in a soluble form (soluble CD163, sCD163) [14]. The role of the sCD163 molecule has not been exactly explained. However, it seems to be involved not only in the removal of hemoglobin-haptoglobin complexes but also in the anti-inflammatory response [13]. Its higher level was found in hematological cancers, including chronic lymphocytic leukemia [15]. Moreover, CD163 is certainly a marker of macrophage activity and is generally thought to be associated with downregulation of inflammation, but its biological role still has not been fully elucidated [14, 15]. Monocytes are one of the least known immune cells with a potentially important role in the pathogenesis of CLL.

The aim of our study was to evaluate the expression of CD163 and HLA-DR molecules on the monocyte subpopulations in CLL patients and healthy individuals.

Materials and methods

Characteristics of the study group. The study group consisted of 40 patients with newly diagnosed CLL at the Department of Hematooncology and Bone Marrow Transplantation of the Medical University of Lublin, Poland. The diagnosis of CLL was based on the clear recommendations developed by the International Workshop on Chronic Lymphocytic Leukemia (iwCLL) [16].

The age of patients ranged from 39 to 82 years (median: 63 ys). The study group included 24 men and 16 women. According to the Rai classification [17], patients were divided into 3 groups: the low risk group (stage 0) — 22 patients, intermediate-risk group (stage I/II) — 11 patients, high-risk group (stage III/IV) — 7 patients. Detailed characteristics of the examined group of CLL patients are presented in Table 1. The control group consisted of 10 healthy volunteers (7 men, 3 women). Age of donors ranged from 24 to 54 years (median: 47 ys).

This study was approved by the Bioethics Committee of the Medical University of Lublin (No. KE-0254/49/2016). All patients gave their written consent to participate in the research.

Blood collection and preparation of samples for flow cytometry. Approximately 5 ml of venous blood was collected into an EDTA-coated tube from each patient and healthy person. The material for the study was immediately processed. Subpopulations of monocytes circulating in the peripheral blood of CLL patients and healthy controls were determined by flow cytometry. Monocyte cell surface antigen assessments were performed with the following monoclonal antibodies conjugated with fluorochromes: anti-CD14 FITC (BD Pharmingen); anti-CD16 PE-Cy5 (BD Pharmingen); anti-HLA-DR PE (BioLegend); anti-CD163 PE (BioLegend). 100 μl of blood was taken into vials and labeled with monoclonal antibodies.

Samples were incubated for 20 minutes at room temperature. The next step was RBC lysis with FACS Lysis Solution (Becton Dickinson) for 10 minutes at room temperature. Right after centrifugation at 700 × g for 5 minutes, supernatant was poured out and the marked cells were rinsed twice with phosphate buffered saline PBS (700 × g).

A BD FACSCalibur™ flow cytometer (BD Biosciences, Franklin Lakes, NJ, USA) with CellQuestPro software (BD Biosciences) were used for cytometric analysis and data evaluation.

Statistical analysis. The statistical analysis was carried out with GraphPad Prism 5.0. software (GraphPad Software,

Table 1. Characteristics of chronic lymphocytic leukemia (CLL) patients

The criteria for differentiating patients	Number of patients
Sex	
Female (%)	16 (40%)
Male (%)	24 (60%)
Rai stage	
0	22 (55%)
I/II	11 (27.5%)
III/IV	7 (17.5%)
ZAP-70 (cut-off point 20%)	
ZAP-70-positive	17 (42.5%)
ZAP-70-negative	23 (57.5%)
CD38 (cut-off point 30%)	
CD38-positive	11 (27.5%)
CD38-negative	29 (72.5%)
	Median value (minimum-maximum)
Age at diagnosis (years)	63 (39–82)
WBC [G/l)]	25.2 (10.1–112.5)
LYM [G/l]	18.8 (5.5–106.3)
β_2M [mg/dl]	2.4 (1.36–5.39)
LDH [IU/l]	373 (266–619)
HGB [g/dl]	14.00 (8.1–17.2)
$CD19^{+}CD5^{+}ZAP\text{-}70^{+}$ (%)	13.41 (0.2–44.3)
$CD19^{+}CD5^{+}CD38^{+}$ (%)	8.43 (0.3–80.9)
$CD19^{+}CD5^{+}$ (%)	3.23 (0.9–16.6)

Abbreviations: WBC — white blood cell count; LYM — absolute lymphocyte count; LDH — lactate dehydrogenase; β2M — β2-microglobulin; HGB — hemoglobin

Inc. La Jolla, California, USA). U Mann-Whitney test or Wilcoxon test were used. Median, minimal and maximal values and IQR were used for data description. The Spearman rank correlation coefficient was used in correlation tests. The level of significance was set at $p < 0.05$.

Results

The percentage of classical monocytes in patients with CLL was significantly lower in relation to the control group ($p < 0.0001$), while the percentage of $CD14^{++}CD16^{+}$ and $CD14^{+}CD16^{++}$ monocytes was significantly higher compared to the control group ($p < 0.01$) (Fig. 1, Table 2). The percentage of $CD14^{++}CD16^{-}$ classical monocytes (median: 75.56%) was significantly higher than CD16-positive monocytes in CLL patients. The latter group includes the $CD14^{++}CD16^{+}$ intermediate subset (median: 6.34%) and non-classical $CD14^{+}CD16^{++}$ (median: 10.65%) subpopulation ($p < 0.01$) (Fig. 2, Table 2).

Of all subpopulations, classical monocytes accounted for the highest percentage of $CD163^{+}$ monocytes (median: 96.73%), while non-classical monocytes presented the lowest percentage of $CD163^{+}$ cells (median: 5.12%) (Fig. 3, Table 3).

The non-classical $CD14^{+}CD16^{++}$HLA-DR^{+} monocytes had the lowest percentage of HLA-DR^{+} cells (median: 73.36%) compared to classical HLA-DR^{+} (median: 97.73%) and intermediate HLA-DR^{+} cells (median: 96.77%) ($p < 0.0001$) (Fig. 4, Table 4).

In addition, the study showed that the percentage of subpopulations of classical, intermediate and non-classical monocytes expressing CD163 does not correlate with leukocytosis, lymphocytosis and serum $\beta 2$ microglobulin concentration ($p > 0.05$). The percentage of $CD14^{++}CD16^{-}CD163^{+}$ monocytes showed a negative correlation with the concentration of $CD5^{+}$ $CD19^{+}$ leukemia cells ($r = -0.51$; $p < 0.05$). According to the results, the percentage of $CD14^{+}$HLA-$DR^{low/neg}$ monocytes showed a negative correlation only with the percentage of $CD14^{++}CD16^{-}CD163^{+}$ monocytes among all subpopulations of monocytes ($r = -0.55$; $p < 0.05$).

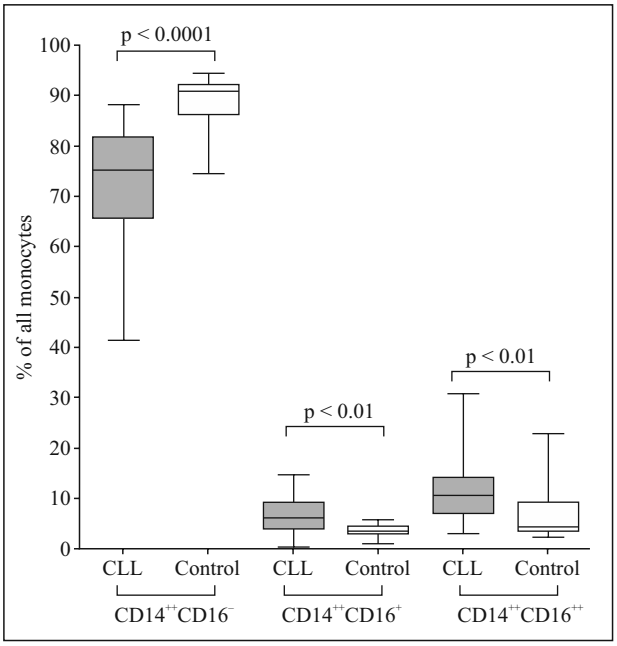

Figure 1. Comparison of the percentage of individual monocyte subpopulations: classical ($CD14^{++}CD16^{-}$), intermediate ($CD14^{++}CD16^{+}$) and non-classical ($CD14^{+}CD16^{++}$) among all monocytes in CLL patients and healthy volunteers studied by flow cytometry as described in Methods. *P* values were calculated using the non-parametric U Mann-Whitney test. Bars, line and whiskers represent median, maximum, minimum and IQR, respectively. Abbreviations: CLL — chronic lymphocytic leukemia; IQR — interquartile range.

Discussion

Among the populations of immune cells, monocytes are one of the least known cells with potentially important role in the pathogenesis of CLL [18]. Since monocytes appear to play an important role in the pathogenesis of CLL, the present study presents the

Table 2. Statistical analysis of the percentage of monocytes with the phenotypes $CD14^{++}CD16^{-}$, $CD14^{++}CD16^{+}$ and $CD14^{+}CD16^{++}$ in CLL patients and in the control group

Variables	$CD14^{++}CD16^{-}$ (%)		$CD14^{++}CD16^{+}$ (%)		$CD14^{+}CD16^{++}$ (%)	
	CLL	Control	CLL	Control	CLL	Control
Median	75.56	91.01	6.34	3.17	10.65	4.55
Min	41.42	74.66	0.24	1.14	3.03	2.25
Max	88.35	94.54	14.58	5.68	30.70	22.75
IQR	16.29	6.18	5.54	1.78	7.59	5.89

Abbreviations: CLL — chronic lymphocytic leukemia; MIN — minimum; MAX — maximum; IQR — interquartile range

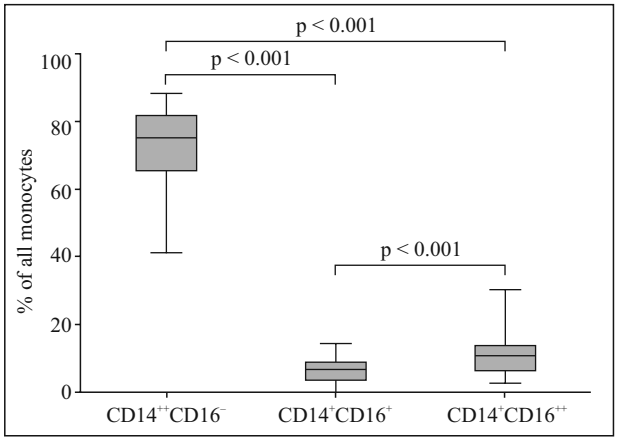

Figure 2. Comparison of the percentage of individual monocyte subpopulations among all monocytes in CLL patients was performed as described in the Legend to Figure 1. *P* values were calculated using the non-parametric Wilcoxon test. Bars, other graphical symbols and abbreviations as in the description of Figure 1.

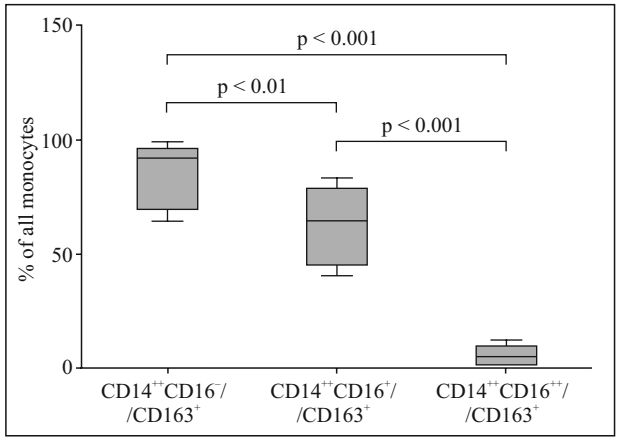

Figure 3. Comparison of the percentage of monocyte subpopulations expressing CD163 in CLL patients was performed as described in the Legend to Figure 1. *P* values were calculated using the non-parametric Wilcoxon test. Bars, other graphical symbols and abbreviations as in the description of Figure 1.

Table 3. Statistical analysis of the percentage of monocytes with the phenotypes $CD14^{++}CD16^{-}$, $CD14^{++}CD16^{+}$ and $CD14^{+}CD16^{++}$ expressing the CD163 molecule in the studied group of CLL patients

Variables	$CD14^{++}CD16^{-}/CD163^{+}$ (%)	$CD14^{++}CD16^{+}/CD163^{+}$ (%)	$CD14^{+}CD16^{++}/CD163^{+}$ (%)
Median	96.73	63.70	5.12
Min	62.10	44.87	0.30
Max	100.0	78.64	12.99
IQR	26.88	29.98	9.13

Abbreviations as in the description of Table 2.

evaluation of the proportion of the monocytes subpopulation in CLL Although the discovery of three different subpopulations of monocytes suggests the existence of the functional differences between these cells their properties are still not fully understood. Monocytes analyzed in CLL patients were divided into classical monocytes ($CD14^{++}CD16^{-}$) and monocytes expressing CD16 molecules, which are differentiated into two subpopulations: the intermediate monocytes $CD14^{++}CD16^{+}$ and the non-classical monocytes $CD14^{+}CD16^{++}$ [6].

It is assumed that the increased expression of CD16 on the surface of monocytes may correlate with their activation process [8]. An increase in the percentage of CD16-positive monocytes observed in the present study may indicate that CLL lymphocytes stimulate $CD16^{+}$ monocytes and lead to their activation. This is in line with Maffei *et al.* [19], who concluded that the increase in the percentage of non-classical monocytes may result from their stimulation by leukemic lymphocytes. According to the latter study, the $CD14^{+}CD16^{++}$

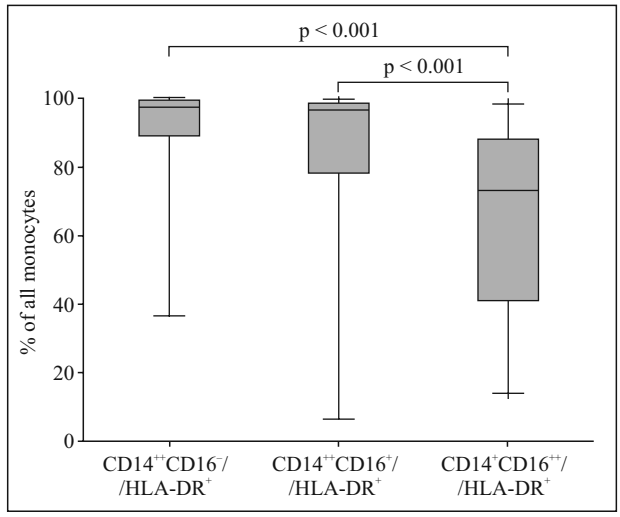

Figure 4. Evaluation of the percentage of individual HLA-DR positive monocyte subsets in patients with CLL was performed as described in the Legend to Figure 1. *P* values were calculated using the non-parametric Wilcoxon test. Bars, other graphical symbols, and abbreviations as in the description of Figure 1.

Table 4. Comparison of the percentage of classical, intermediate and non-classical monocytes with HLA-DR expression in CLL patients

Variables	$CD14^{++}CD16^{-}/HLA\text{-}DR^{+}$ (%)	$CD14^{++}CD16^{+}/HLA\text{-}DR^{+}$ (%)	$CD14^{+}CD16^{++}/HLA\text{-}DR^{+}$ (%)
MEDIAN	97.73	96.77	73.36
MIN	36.47	6.270	14.38
MAX	100.0	100.0	100.0
IQR	10.22	20.45	47.37

Abbreviations as in the description of Table 2.

monocytes do not produce cytokines in response to LPS and are unable to phagocytose [19].

In this study we observed that patients with CLL possess a higher percentage of non-classical monocytes $CD14^{+}CD16^{++}$ and a significantly higher percentage of intermediate monocytes $CD14^{++}CD16^{+}$ as compared to the healthy group. Italiani *et al.* [5] also showed a similar percentage of monocytes circulating in the peripheral blood of CLL patients, classical monocytes (85%), intermediates (5%) and non-classical (10%) [5].

It is worth mentioning that the increase in the percentage of monocytes expressing CD16 was also observed in other pathological conditions, *e.g.* during bacterial, viral or parasitic infections [20] and in acute or chronic conditions such as sepsis or atherosclerosis [8], chronic liver disease [21], rheumatoid arthritis [22], and renal diseases [23, 24].

The role of monocytes expressing CD16 during the mobilization of the immune system is not fully understood. One theory explains the differentiation of monocytes by the process of maturation and differentiation of these cells into the peripheral blood macrophages [8]. The differences in the percentage of each subpopulation of monocytes observed in CLL patients, compared to the proportion observed in healthy subjects may be due to the fact that classical monocytes may differentiate into tissue macrophages TAMs (Tumor Associated Macrophages) [25, 26].

The differences relate to, among others, the degree of expression of HLA-DR, CD86 and CD1d, which determine their ability to present antigens [8]. Furthermore, the $CD14^{++}CD16^{+}$ intermediate monocytes have a high expression of CD163 molecule [14] that inhibits activation and proliferation of T cells [27]. It is also a specific marker of monocytes/macrophages exhibiting strong anti-inflammatory properties [28]. Recent studies have shown that anti-inflammatory monocytes $CD14^{++}CD16^{+}$ are also associated with significant expression of TGF-β. This cytokine enables them to inhibit T-dependent response, and to stimulate proliferation of T regulatory cells [1].

Of all subpopulations, classical monocytes accounted for the highest percentage of $CD163^{+}$ monocytes, while non-classical monocytes had the lowest percentage of $CD163^{+}$ cells. Moniuszko *et al.* [9] also observed high expression of the CD163 molecule on classical monocytes. The percentage of $CD14^{++}CD16^{+}CD163^{+}$ monocytes was higher than the percentage of non-classical $CD163^{+}$ monocytes. It is believed that the presence of CD163 on the surface of monocytes affects the ability of these cells to inhibit the inflammatory response [8] as the $CD163^{+}$ monocytes may have anti-inflammatory properties [29]. Therefore, it is assumed that due to the disturbed antigen presentation process and abnormal maturation of dendritic cells, the activity of the immune system in patients with CLL decreases [6, 19]. Moreover, monocytes have reduced ability to stimulate the immune system, due to impaired antigen presentation to T cells [30]. Furthermore, the researchers suggest that a subpopulation of monocytes characterized by increased percentage of CD163-positive cells present in inflamed or tumor tissues can polarize to macrophages M2, in particular subtype M2d called TAM [31–33]. It is worth recalling that the presence of macrophages with the expression of CD163 in the tumor microenvironment in patients with breast cancer is unfavorable prognostic factor. Results of a recent Polish study suggest the positive correlation between the presence of CD163 macrophage and tumor size [34]. Perhaps the classical or intermediate CD163-positive monocytes differentiate into TAMs. Our studies also assessed the expression of HLA-DR on monocytes in CLL patients. The analysis showed that the percentage of cells expressing HLA-DR among classical monocytes ($CD14^{++}CD16^{-}$) is significantly higher compared with the percentage of non-classical $CD14^{+}CD16^{++}HLA\text{-}DR^{+}$. Additionally, the percentage of $CD14^{++}CD16^{+}HLA\text{-}DR^{+}$ monocytes among intermediate monocytes was significantly higher than the percentage of $CD14^{+}CD16^{++}$ $HLA\text{-}DR^{+}$. The majority of non-classical monocytes exhibit only low expression of HLA-DR ($HLA\text{-}DR^{-/low}$).

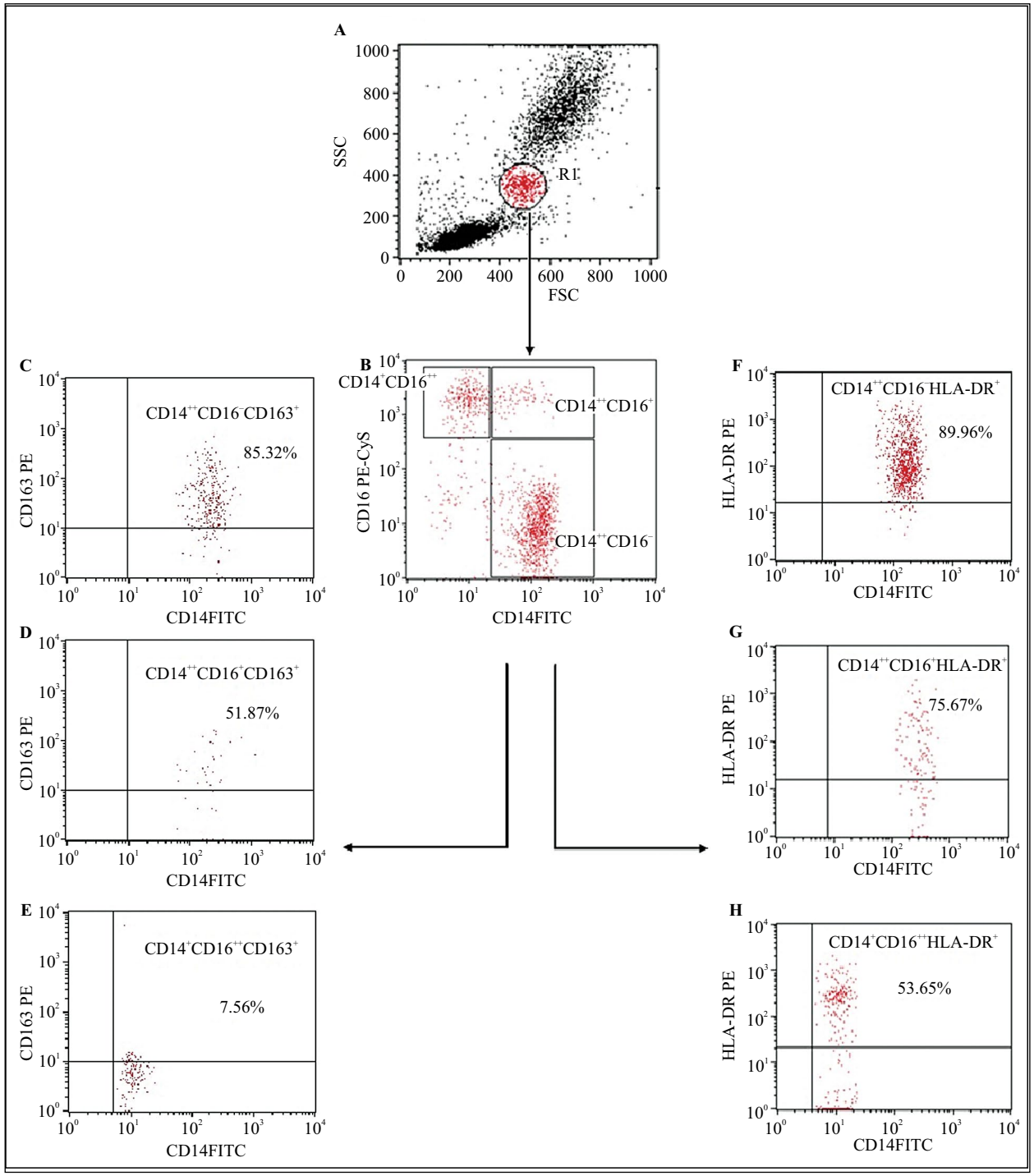

Figure 5. The dot plots of representative data from one chronic lymphocytic leukemia patient illustrate the analysis method for the identification of monocyte subpopulations in peripheral blood following three-color staining. **(A)** Monocyte population was gated (Region R1) using FSC and SSC plot. **(B)** Next, the monocytes accumulated in the R1 were analyzed for staining of monocyte subpopulations. We used dot plots of CD14 FITC *versus* CD16 PE-Cy5. The dot plot shows classical ($CD14^{++}CD16^{-}$), intermediate ($CD14^{++}CD16^{+}$) and non-classical ($CD14^{+}CD16^{++}$) monocytes. Expression of CD163 **(C, D, E)** and HLA-DR **(F, G, H)** was assessed in each of these subpopulations. Abbreviations: FSC — forward scatter; SSC — side scatter.

It suggests that these cells have a reduced ability to stimulate the immune system, due to disturbed presentation of antigens to T cells [30]. The increased number of $CD14^{+}HLA\text{-}DR^{low/neg}$ cells in the peripheral blood is present in many cancers and is related to the stage, grade, gender and tumor size [35]. Gustafson

et al. [10] observed an increased percentage of HLA-DR^{low} monocytes in patients with CLL compared to the control group (18.6% ± 11.5% *vs.* 9.9% ± 6.4%). The CD14+ HLA-DR$^{low/neg}$ monocytes secrete large amounts of IL-10 and TGF-β that stimulate regulatory T cells (Treg) proliferation and cause an alteration in the maturation of dendritic cells [10]. Moreover, an increased percentage of monocytes with low HLA-DR expression was noted in patients with acute hepatic failure, which may result in higher susceptibility to infection due to the significantly reduced immune function [21]. Monocytes exhibiting high expression of CD163 and low expression of HLA-DR may be described as a subpopulation with anti-inflammatory properties and the ability to inhibit the anti-tumor response [30, 36].

Conclusions

A statistically significant increase in the percentage of intermediate and non-classical monocytes was found in CLL patients in comparison to the control group. The highest percentage of CD163+ cells was observed in "classical" monocytes. The presence of this receptor suggests that these cells have anti-inflammatory properties. In addition, in CLL patients the highest percentage of HLA-DR$^{neg/low}$ cells expression was observed among non-classical monocytes, which means that these cells have probably impaired ability to stimulate the immune system.

Acknowledgements

The work was financed from the Young Researcher grant MNmb 519 obtained from subsidies for the development of young scientists and participants of doctoral studies at the Medical University of Lublin. The study was performed using the equipment purchased under the Project "The equipment of innovative laboratories doing research on new medicines used in the therapy of civilization and neoplastic diseases" within the Operational Program Development of Eastern Poland 2007–2013, Priority Axis I Modern Economy, Operations I.3 Innovation Promotion.

References

1. Caligaris-Cappio F. Inflammation, the microenvironment and chronic lymphocytic leukemia. Haematologica. 2011; 96(3): 353–355, doi: 10.3324/haematol.2010.039446, indexed in Pubmed: 21357715.
2. Choi MY, Kashyap MK, Kumar D. The chronic lymphocytic leukemia microenvironment: Beyond the B-cell receptor. Best Pract Res Clin Haematol. 2016; 29(1): 40–53, doi: 10.1016/j.beha.2016.08.007, indexed in Pubmed: 27742071.
3. Ab Kadir R, Zainal Ariffin SH, Megat Abdul Wahab R, et al. Characterization of mononucleated human peripheral blood cells. ScientificWorldJournal. 2012; 2012: 843843, doi: 10.1100/2012/843843, indexed in Pubmed: 22666162.
4. Ziegler-Heitbrock L. Blood monocytes and their subsets: established features and open questions. Front Immunol. 2015; 6: 423, doi: 10.3389/fimmu.2015.00423, indexed in Pubmed: 26347746.
5. Italiani P, Boraschi D. From Monocytes to M1/M2 Macrophages: Phenotypical vs. Functional Differentiation. Front Immunol. 2014; 5: 514, doi: 10.3389/fimmu.2014.00514, indexed in Pubmed: 25368618.
6. Ziegler-Heitbrock L, Ancuta P, Crowe S, et al. Nomenclature of monocytes and dendritic cells in blood. Blood. 2010; 116(16): e74–e80, doi: 10.1182/blood-2010-02-258558, indexed in Pubmed: 20628149.
7. Kzhyshkowska J, Gudima A, Moganti K, et al. Perspectives for monocyte/macrophage-based diagnostics of chronic inflammation. Transfus Med Hemother. 2016; 43(2): 66–77, doi: 10.1159/000444943, indexed in Pubmed: 27226789.
8. Łapuć I, Eljaszewicz A, Kłoczko J, et al. Rola monocytów w patogenezie przewlekłej białaczki limfocytowej. Acta Haematologica Polonica. 2014; 45(4): 340–346, doi: 10.1016/j.achaem.2014.06.001.
9. Moniuszko M, Bodzenta-Lukaszyk A, Kowal K, et al. Enhanced frequencies of CD14++CD16+, but not CD14+CD16+, peripheral blood monocytes in severe asthmatic patients. Clin Immunol. 2009; 130(3): 338–346, doi: 10.1016/j.clim.2008.09.011, indexed in Pubmed: 18952503.
10. Gustafson MP, Abraham RS, Lin Yi, et al. Association of an increased frequency of CD14+ HLA-DR lo/neg monocytes with decreased time to progression in chronic lymphocytic leukaemia (CLL). Br J Haematol. 2012; 156(5): 674–676, doi: 10.1111/j.1365-2141.2011.08902.x, indexed in Pubmed: 22050346.
11. Buechler C, Ritter M, Orsó E, et al. Regulation of scavenger receptor CD163 expression in human monocytes and macrophages by pro- and antiinflammatory stimuli. J Leukoc Biol. 2000; 67(1): 97–103, indexed in Pubmed: 10648003.
12. Onofre G, Kolácková M, Jankovicová K, et al. Scavenger receptor CD163 and its biological functions. Acta Medica (Hradec Kralove). 2009; 52(2): 57–61, indexed in Pubmed: 19777868.
13. Moestrup SK, Mβler HJ. CD163: a regulated hemoglobin scavenger receptor with a role in the anti-inflammatory response. Ann Med. 2004; 36(5): 347–354, doi: 10.1080/07853890410033171, indexed in Pubmed: 15478309.
14. Lapuc I, Bolkun L, Eljaszewicz A, et al. Circulating classical CD14++CD16- monocytes predict shorter time to initial treatment in chronic lymphocytic leukemia patients: Differential effects of immune chemotherapy on monocyte-related membrane and soluble forms of CD163. Oncol Rep. 2015; 34(3): 1269–1278, doi: 10.3892/or.2015.4088, indexed in Pubmed: 26135617.
15. Nederby L, Roug AS, Knudsen SS, et al. Soluble CD163 as a prognostic biomarker in B-cell chronic lymphocytic leukemia. Leuk Lymphoma. 2015; 56(11): 3219–3221, doi: 10.3109/10428194.2015.1026899, indexed in Pubmed: 25747973.
16. Hallek M. Chronic lymphocytic leukemia: 2017 update on diagnosis, risk stratification, and treatment. Am J Hematol. 2017; 92(9): 946–965, doi: 10.1002/ajh.24826, indexed in Pubmed: 28782884.
17. Rai KR. A critical analysis of staging in CLL. In: Gale RP, Rai KR, ed.Chronic Lymphocytic Leukemia: Recent Progress and Future Directions. New York: Alan R. Liss; 1987:253–264.

18. Herishanu Y, Katz BZ, Lipsky A, et al. Biology of chronic lymphocytic leukemia in different microenvironments: clinical and therapeutic implications. Hematol Oncol Clin North Am. 2013; 27(2): 173–206, doi: 10.1016/j.hoc.2013.01.002, indexed in Pubmed: 23561469.
19. Maffei R, Bulgarelli J, Fiorcari S, et al. The monocytic population in chronic lymphocytic leukemia shows altered composition and deregulation of genes involved in phagocytosis and inflammation. Haematologica. 2013; 98(7): 1115–1123, doi: 10.3324/haematol.2012.073080, indexed in Pubmed: 23349302.
20. Tolouei Semnani R, Moore V, Bennuru S, et al. Human monocyte subsets at homeostasis and their perturbation in numbers and function in filarial infection. Infect Immun. 2014; 82(11): 4438–4446, doi: 10.1128/IAI.01973-14, indexed in Pubmed: 25114121.
21. Abeles RD, McPhail MJ, Sowter D, et al. CD14, CD16 and HLA-DR reliably identifies human monocytes and their subsets in the context of pathologically reduced HLA-DR expression by CD14(hi) /CD16(neg) monocytes: Expansion of CD14(hi) /CD16(pos) and contraction of CD14(lo) /CD16(pos) monocytes in acute liver failure. Cytometry A. 2012; 81(10): 823–834, doi: 10.1002/cyto.a.22104, indexed in Pubmed: 22837127.
22. Luo Q, Xiao P, Li X, et al. Overexpression of CD64 on CD14CD16 and CD14CD16 monocytes of rheumatoid arthritis patients correlates with disease activity. Exp Ther Med. 2018; 16(3): 2703–2711, doi: 10.3892/etm.2018.6452, indexed in Pubmed: 30210612.
23. Schepers E, Houthuys E, Dhondt A, et al. Transcriptome analysis in patients with chronic kidney disease on hemodialysis disclosing a key role for CD16+CX3CR1+ monocytes. PLoS One. 2015; 10(4): e0121750, doi: 10.1371/journal.pone.0121750, indexed in Pubmed: 25830914.
24. Stansfield BK, Ingram DA. Clinical significance of monocyte heterogeneity. Clin Transl Med. 2015; 4: 5, doi: 10.1186/s40169-014-0040-3, indexed in Pubmed: 25852821.
25. Chen YCE, Mapp S, Blumenthal A, et al. The duality of macrophage function in chronic lymphocytic leukaemia. Biochim Biophys Acta Rev Cancer. 2017; 1868(1): 176–182, doi: 10.1016/j.bbcan.2017.03.006, indexed in Pubmed: 28347751.
26. Galletti G, Caligaris-Cappio F, Bertilaccio MTS. B cells and macrophages pursue a common path toward the development and progression of chronic lymphocytic leukemia. Leukemia. 2016; 30(12): 2293–2301, doi: 10.1038/leu.2016.261, indexed in Pubmed: 27677742.
27. Tsukamoto M, Seta N, Yoshimoto K, et al. CD14CD16+ intermediate monocytes are induced by interleukin-10 and positively correlate with disease activity in rheumatoid arthritis. Arthritis Res Ther. 2017; 19(1): 28, doi: 10.1186/s13075-016-1216-6, indexed in Pubmed: 28183329.
28. Mandl M, Schmitz S, Weber C, et al. Characterization of the CD14++CD16+ monocyte population in human bone marrow. PLoS One. 2014; 9(11): e112140, doi: 10.1371/journal.pone.0112140, indexed in Pubmed: 25369328.
29. Yang H, Wang H, Levine YA, et al. Identification of CD163 as an antiinflammatory receptor for HMGB1-haptoglobin complexes. JCI Insight. 2016; 1(7), doi: 10.1172/jci.insight.85375, indexed in Pubmed: 27294203.
30. Liu J, Zhou Y, Huang Q, et al. CD14HLA-DR expression: A novel prognostic factor in chronic lymphocytic leukemia. Oncol Lett. 2015; 9(3): 1167–1172, doi: 10.3892/ol.2014.2808, indexed in Pubmed: 25663875.
31. Allavena P, Mantovani A. Immunology in the clinic review series; focus on cancer: tumour-associated macrophages: undisputed stars of the inflammatory tumour microenvironment. Clin Exp Immunol. 2012; 167(2): 195–205, doi: 10.1111/j.1365-2249.2011.04515.x, indexed in Pubmed: 22235995.
32. Derlindati E, Dei Cas A, Montanini B, et al. Transcriptomic analysis of human polarized macrophages: more than one role of alternative activation? PLoS One. 2015; 10(3): e0119751, doi: 10.1371/journal.pone.0119751, indexed in Pubmed: 25799240.
33. Zarif JC, Hernandez JR, Verdone JE, et al. A phased strategy to differentiate human CD14+monocytes into classically and alternatively activated macrophages and dendritic cells. Biotechniques. 2016; 61(1): 33–41, doi: 10.2144/000114435, indexed in Pubmed: 27401672.
34. Medrek C, Pontén F, Jirström K, et al. The presence of tumor associated macrophages in tumor stroma as a prognostic marker for breast cancer patients. BMC Cancer. 2012; 12: 306, doi: 10.1186/1471-2407-12-306, indexed in Pubmed: 22824040.
35. Yuan XK, Zhao XK, Xia YC, et al. Increased circulating immunosuppressive CD14(+)HLA-DR(-/low) cells correlate with clinical cancer stage and pathological grade in patients with bladder carcinoma. J Int Med Res. 2011; 39(4): 1381–1391, doi: 10.1177/147323001103900424, indexed in Pubmed: 21986138.
36. Mazumdar R, Evans P, Culpin R, et al. The automated monocyte count is independently predictive of overall survival from diagnosis in chronic lymphocytic leukaemia and of survival following first-line chemotherapy. Leuk Res. 2013; 37(6): 614–618, doi: 10.1016/j.leukres.2013.02.020, indexed in Pubmed: 23522450.

Submitted: 26 October, 2019
Accepted after reviews: 21 February, 2020
Available as AoP: 16 March, 2020

FOLIA HISTOCHEMICA ET CYTOBIOLOGICA
Vol. 58, No. 1, 2020
pp. 25–36

ORIGINAL PAPER

VIA MEDICA

Monocytic MDSC as a source of immunosuppressive cytokines in chronic lymphocytic leukemia (CLL) microenvironment

Wioleta Kowalska, Agnieszka Bojarska-Junak

Chair and Department of Clinical Immunology, Medical University of Lublin, Poland

Abstract

Introduction. Myeloid derived suppressor cells (MDSCs) are one of the major components of the tumor microenvironment. The accumulation of MDSCs has been demonstrated in many types of human solid tumors. However, the relevance of this heterogeneous population in hematopoietic malignancies has only recently gained stronger attention. MDSCs are a phenotypically and functionally heterogeneous group of cells. The results of recent studies indicate that the immune dysregulation in chronic lymphocytic leukemia (CLL) affects a monocytic MDSC (M-MDSC) subpopulation. This study aimed to analyze the frequency of M-MDSCs with intracellular IL-10 and TGF-β1 expression in newly diagnosed CLL patients. We investigated the potential role of M-MDSCs in CLL by analyzing the level of IL-10 and TGF-β1 expression in circulating M-MDSCs in correlation with clinical and laboratory parameters characterizing disease activity and patients' immune status.

Material and methods. Seventy CLL patients and 17 age-matched healthy volunteers were included in this study. Flow cytometric detection of Mo-MDSCs ($CD14^+CD11b^+CD15^-HLA\text{-}DR^{-/low}$) with intracellular IL-10 and TGF-β1 expression was done.

Results. We found a significantly higher median percentage of M-MDSC with IL-10 or TGF-β1 expression in CLL patients than in healthy volunteers. The percentage of M-MDSC with intracellular IL-10 or TGF-β1 expression was significantly lower in CLL patients at stage 0 as compared to the stages I/II and III/IV according to Rai stages. The percentage of M-MDSC with intracellular TGF-β1 expression was significantly higher in ZAP-70-positive and CD38-positive patients compared with ZAP-70-negative and group of CD38-negative ones. There was also a significantly higher percentage of M-MDSC positive for intracellular TGF-β expression in patients carrying the 11q22.3 and/or the 17p13.1 deletion than in patients without these genetic aberrations. The percentage of M-MDSC IL-10-positive and M-MDSC TGF-β1-positive measured at the time of diagnosis was higher in patients requiring therapy as compared to patients without treatment during the observation period.

Conclusion. In conclusion, we have shown that an increased percentage of M-MDSC cells producing IL-10 and TGF-β1 in CLL patients may be associated with the suppression of the immune response against CLL. It can be assumed that the increased percentage of M-MDSC with an intracellular expression of IL-10 and TGF-β1 may be used in the future as the factor defining the group of patients with shorter time to onset of treatment.
(Folia Histochemica et Cytobiologica 2020, Vol. 58, No. 1, 25–36)

Key words: M-MDSC; IL-10; TGF-β; chronic lymphocytic leukemia; flow cytometry; genetic analysis

Introduction

Chronic lymphocytic leukemia (CLL) is characterized by an abnormal expansion of mature CD5+ B cells in the bone marrow and their accumulation in blood and secondary lymphoid organs [1]. The neoplastic B cells in CLL patients are dependent on interactions with their microenvironment. CLL cells fluctuate together with a microenvironment, which supports leukemia

Correspondence address: Agnieszka Bojarska-Junak, PhD
Chair and Department of Clinical Immunology
Medical University of Lublin, Chodzki 4a,
20–093 Lublin, Poland
tel. +48 81 4486420; fax +48 81 4486421
e-mail: abojarskajunak@gmail.com

cell survival and determines disease progression in CLL [2–5]. MDSCs (myeloid- derived suppressor cells) are one of the major components of the tumor microenvironment. The accumulation of MDSCs has been demonstrated in many types of human solid tumors [6]. However, the relevance of this heterogeneous population in hematopoietic malignancies has only recently gained stronger attention [7–10]. MDSCs are a phenotypically and functionally heterogeneous group of cells. In human there are two major types of MDSCs: monocytic-MDSC (M-MDSC; expressing CD14) and polymorphonuclear MDSC (PMN-MDSC; expressing CD15) [5, 11, 12]. Both subpopulations of MDSCs express the myeloid marker CD33. Unlike monocytes, MDSCs are characterized by the lack or low expression of HLA-DR [5]. M-MDSCs produce high amounts of immunosuppressive cytokines, such as IL-10 and TGF-β [13].

In CLL, malignant B lymphocytes, serve an important role in the immune response, so their interactions with other immune cells are more complex than observed in solid tumors. The results of recent studies indicate that the immune dysregulation in CLL also affects MDSCs [14, 15]. Jitschin *et al*. [16] observed the accumulation of M-MDSCs (defined as $CD14^{+}$HLA-DR^{lo} cells) in peripheral blood of CLL patients. Probably, some cytokines, such IL-10, contribute to the recruitment and accumulation of MDSCs in CLL microenvironment [17, 18]. In addition, it has been shown that CLL cells themselves constitutively produce immunosuppressive IL-10 [19]. The course of CLL is accompanied by a state of immunosuppression. The leukemic B cells achieve this mainly through the involvement of regulatory T (Treg) cells. In turn, MDSCs release IL-10 and TGF-β to exert their suppressive function by Tregs [8, 20]. The origin of M-MDSC is unknown. Some scientists believe that M-MDSCs are derived from emergency myelopoiesis that can occur during cancer development [12, 21, 22]. Other theories suggest that M-MDSCs are formed in the pathways of reprogramming monocytes [23]. Probably, this process is connected with some cytokine *milieu* (*e.g.* IL-10) [22, 24].

In a recent study, we found the accumulation of intermediate and non-classical monocytes in CLL patients. The non-classical monocytes constituted the majority of cells lacking HLA-DR expression. Moreover, non-classical monocytes presented low CD163 expression [25]. HLA-$DR^{low/-}CD163^{low/-}$ phenotype is also characteristic for M-MDSC [23].

This study aimed to analyze the frequency of M-MDSCs with intracellular IL-10 and TGF-β1 expression in newly diagnosed CLL patients. We investigated the potential role of M-MDSCs in CLL by analyzing the level of IL-10 and TGF-β1 expression in circulating M-MDSCs in correlation with clinical and laboratory parameters characterizing disease activity and patients' immune status.

Material and methods

Patients and samples. The study group comprised 70 patients with CLL diagnosis, which was based on criteria from the International Workshop on Chronic Lymphocytic Leukemia (IWCLL) [26]. All subjects were newly diagnosed. Peripheral blood (PB) samples were collected at the time of diagnosis and prior to any anticancer therapy. CLL patients were recruited between January 2016 and June 2019 in the Department of Hematooncology and Bone Marrow Transplantation of the Medical University of Lublin (Lublin, Poland). Clinical stage was determined according to the Rai classification system [27]. Thirty-seven patients were Stage 0, 11 patients were Stage I, 12 patients were Stage II, 7 patients were Stage III and 3 patients were Stage IV. The CLL group was further divided into three risk groups: Low risk (stage 0), intermediate-risk (stage I or II), and high-risk (stage III or IV). Characteristics of patients at the time of diagnosis are summarized in Table 1. Control PB samples were obtained from 17 healthy volunteers (HVs; 8 females and 9 males, aged from 35–74 years, median 56 years).

Peripheral blood (PB) samples were collected into EDTA-coated tubes and immediately processed. Peripheral blood mononuclear cells (PBMCs) were separated by density gradient centrifugation on Gradisol L (Aqua-Med, Lodz, Poland) for 25 min. at 400 *g* at room temperature (RT). Interphase cells were removed, washed twice and resuspended in phosphate-buffered saline (PBS).

Ethics statement. This study was approved by the Ethics Committee of the Medical University of Lublin (No. KE-0254/107/2013 and KE-0254/49/2016). Written informed consent was obtained from all patients with respect to the use of their blood for scientific purposes.

Detection of M-MDSC and analysis of intracellular IL-10 or TGF-β1 expression. Flow cytometry analysis of M-MDSC (defined as CD14+CD11b+CD15-HLA-DR-/low cells) was performed on PBMCs. The samples were stained with combination of fluorescent-labelled monoclonal antibodies (MoAbs): mouse anti-human 14 FITC (Clone MφP9), mouse anti-human CD11b V450 (Clone ICRF44), mouse anti-human HLA-DR PE-Cy7 (Clone L243) and CD15 APC (Clone HI98) (BD Biosciences, Franklin Lakes, NJ, USA). Cells were incubated for 20 min at RT. Following membrane staining, cells were fixed with Cytofix/Cytoperm and permeabilized with Perm/Wash buffer (BD Biosciences) according to the manufacturer's protocol. Cells were then intracellularly stained (20 min at RT) with PE anti-human

Table 1. Characteristics of the patients at CLL diagnosis

Features	No. patients (%)
Sex	
Female (%)	33 (47.1)
Male (%)	37 (52.9)
Rai Stage	
0 (%)	37 (52.9)
I (%)	11 (15.7)
II (%)	12 (17.1)
III (%)	7 (10.0)
IV (%)	3 (4.3)
ZAP-70 (cut-off 20%)[a]	
Positive (%)	24 (34.3)
Negative (%)	46 (65.7)
CD38 (cut-off 20%)[b]	
Positive (%)	25 (35.7)
Negative (%)	45 (64.3)
Cytogenetic abnormalities	
del(17p13.1) (%)	1 (1.4)
del(11q22.3) (%)	9 (12.9)
Without del(17p13.1) and del(11q22.3) (%)	60 (85.7)
Patients requiring therapy	17 (24.3)
Untreated patients	53 (74.7)
	median (range)
Age at diagnosis (years)	65 (46–85)
WBC count [G/L]	21.92 (10.11–290.46)
Lymphocyte count [G/L]	16.57 (5.21–284.9)
β_2M [mg/dl]	2.42 (1.35–5.39)
LDH [IU/l]	362.0 (178.0–492.0)
Hemoglobin [g/dl]	13.95 (8.7–16.8)
Platelets [G/L]	187.0 (23.0–414.0)
% $CD19^+/CD5^+/ZAP\text{-}70^+$ cells[a]	18.0 (0.2–50.0)
% $CD19^+/CD5^+/CD38^+$ cells[b]	16.1 (0.02–88.7)

CLL — chronic lymphocytic leukemia; WBC — white blood cell; LDH — lactate dehydrogenase; β2M — β2microglobulin. [a]Patients with ZAP-70 expression lower or higher than 20% were classified as ZAP-70 negative or positive, respectively. [b]Patients with CD38 expression lower or higher than 30% were classified as CD38 negative or positive, respectively.

LAP (TGF-β1) antibody (Clone TW4-2F8) or PE anti-human IL-10 antibody (Clone JES3-19F1) (BioLegend, San Diego, CA, USA).

Flow cytometry analysis. Samples were analyzed by flow cytometry directly following preparation. Data acquisition was performed on a FACSCanto II instrument with FACSDiva Software (BD Biosciences). For each analysis, 100,000 events were acquired and analyzed. Kaluza 2.1.1 (Beckman Coulter, Miami, FL, USA) was used for the data analysis. An acquisition gate was put on lymphocytes according to the forward scatter (FSC) and side scatter (SSC) properties. The gating strategy to identify M-MDSC with IL-10 or TGF-β1 expression is shown in Figure 1A–E. The results are expressed as the percentage of M-MDSC with intracellular IL-10 or TGF-β1 expression. Furthermore, within M-MDSC population, IL-10 and TGF-β1 cytokines were quantified regarding their mean fluorescence intensity (MFI). To establish the gating strategy, fluorescence minus one (FMO) control was used. The FMO control tube included all antibodies that were used for M-MDSC cell staining, except for the one (IL-10 PE or TGF-β1 PE) that was measured.

Analysis of T regulatory cells (CD4+CD25+FoxP3+). Treg cells were evaluated *via* analysis of the surface expression of CD4 and CD25 antigens, as well as intracellular expression of FoxP3 by flow cytometry. Tregs were stained with Human Treg Flow Kit (FOXP3 Alexa Fluor 488/CD4 PECy5/ /CD25 PE) (BioLegend) according to the manufacturer's instructions.

Analysis of CD38 and ZAP-70 expression in CLL cells. CLL cells were stained for CD38 antigen and ZAP-70 protein expression (as described previously [28]). Fresh PB samples were stained with FITC mouse anti-human CD19 (Clone SJ25C1), PE-Cy5 mouse anti-human CD5 (Clone UCHT2) and CD38 FITC (Clone HIT2) or anti-ZAP-70 PE (Clone 1E7.2) (BD Biosciences). A cut-off point for ZAP-70 positivity in leukemic cells was ≥ 20%. Patients with CD38 expression lower or higher than 30% were classified as CD38 negative or positive, respectively.

I-FISH analysis. Detection of del(17p13.1) and del(11q22.3) was a part of the routine diagnostic practice. We used a previously described method [29].

Statistical analysis. The Kruskal-Wallis test with Dunn correction or U Mann-Whitney test were used for comparative analysis of the variables. The Spearman rank correlation coefficient was used in correlation tests. Differences were considered statistically significant with p-value ≤ 0.05. Statistical analysis was calculated with Statistica 13 PL (Statistica, Krakow, PL). Graphs were processed using GraphPad Prism version 5.

Results

The percentage of M-MDSC was significantly increased in patients with CLL in comparison to the HVs (median [IQR], 2.84% [1.25–4.50%] *vs.* 8.605 [6.82–11.12%], $p < 0.001$). Moreover, we found significantly higher median percentage of M-MDSC

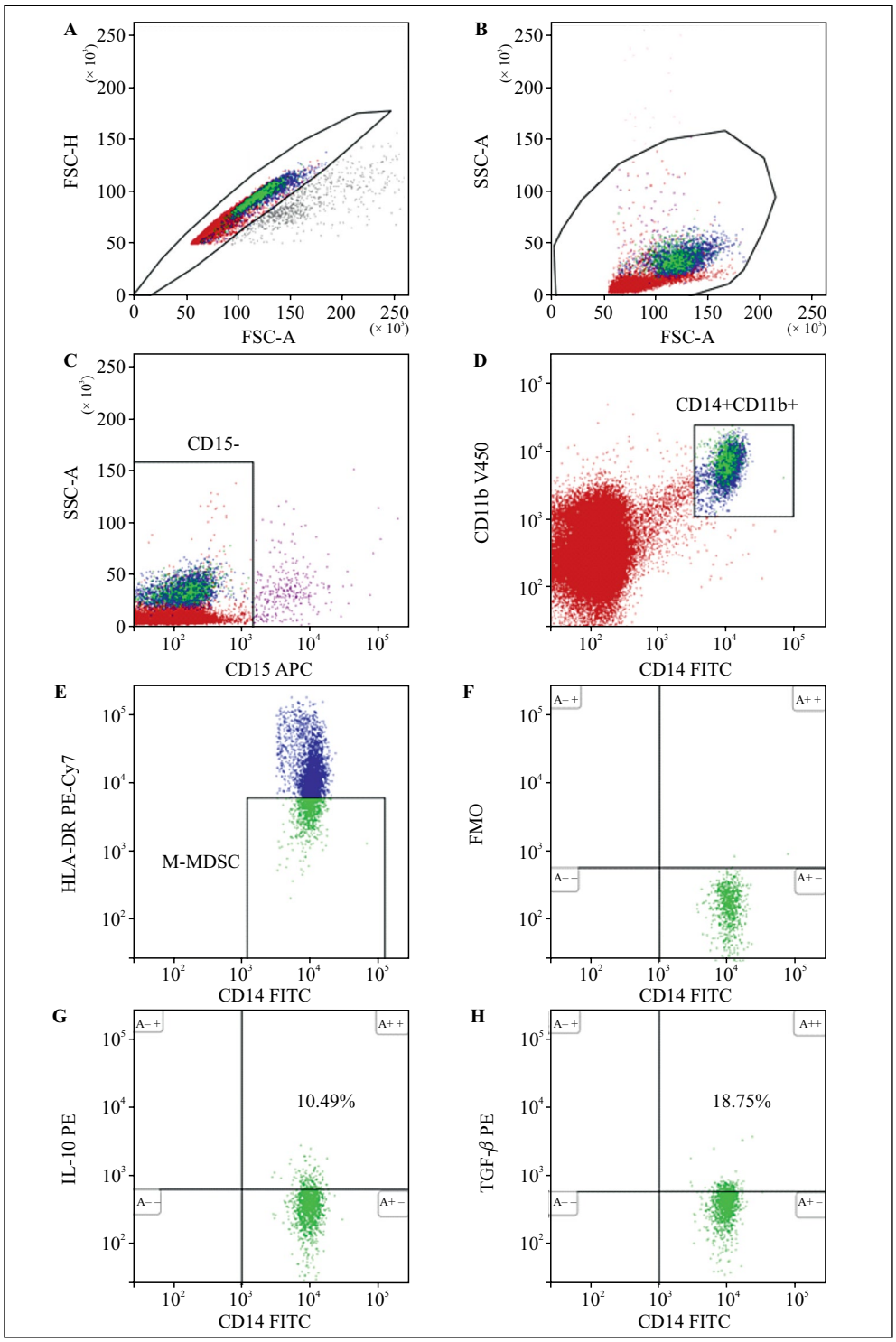

Figure 1. Representative dot plots illustrating the analytic method for the identification of M-MDSCs with the intracellular expression of IL-10 and TGF-β1. **A.** FSC-A *vs.* FSC-H dot plot: doublets' discrimination. **B.** After gating a singlet (P1 region) mononuclear cells (PBMCs) were selected based on their SSC/FSC properties. **C.** CD15 APC *vs.* SSC-A dot plot. Discrimination of $CD15^-$ from $CD15^+$ cells. **D.** Selected $CD15^-$ cells were analyzed for CD14 FITC and CD11b V450 staining. **E.** Selected $CD14^+CD11b^+$ cells were analyzed for HLA-DR PE-Cy7 expression. The dot plots (CD14 FITC *vs.* HLA-DR PE-Cy7) indicate $CD14^+CD11b^+CD15^-HLA\text{-}DR^{-/low}$ cells (M-MDSC). **F.** Dot plots indicating a FMO (*Fluorescence minus one*) control, which contains all fluorochromes in a panel except for IL-10 PE or TGF-β PE. The FMO control identifies any spread of fluorochrome in an unlabeled channel and places the gates in the correct place. **G, H.** Selected $CD14^+CD11b^+CD15^-HLA\text{-}DR^{-/low}$ cells were analyzed for IL-10 PE **(G)** or TGF-β PE staining **(H).** A++ quadrant in dot plot **(G)** shows the percentage of M-MDSCs IL-10-positive. A++ quadrant in dot plot **(H)** shows M-MDSCs with the intracellular expression of TGF-β. Data were analyzed using Kaluza 2.1.1 software.

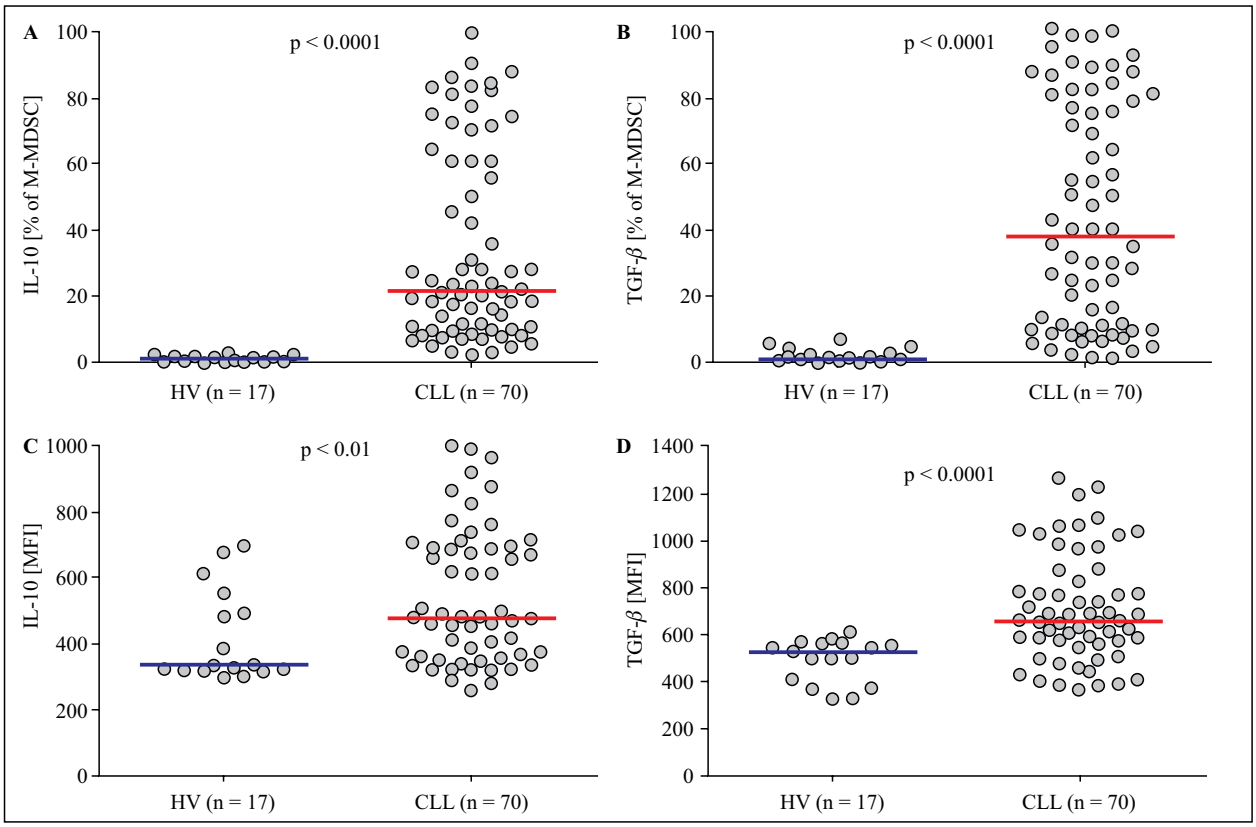

Figure 2. IL-10 and TGF-β expression in M-MDSCs from CLL patients and healthy volunteers (HV). **(A)** percentage of IL-10 positive M-MDSCs; **(B)** mean fluorescence intensity (MFI) of IL-10 in M-MDSCs. **(C)** percentage of TGF-β positive M-MDSCs; **(D)** MFI of TGF-β in M-MDSCs. The U Mann-Whitney test was used for comparative analysis.

with intracellular IL-10 expression in CLL patients than in healthy volunteers (median [IQR], 21.72% [9.81–60.93%] *vs.* 0.57% [0.06–1.31%], $p < 0.0001$; Fig. 2A). Likewise, percentage of M-MDSC with TGF-β1 (median [IQR], 37.36% [9.93–78.37%]) expression was significantly higher in comparison to the HVs (median [IQR], 1.17% [0.33–3.68%) (Fig. 2B). Furthermore, within M-MDSC population, IL-10 and TGF-β1 cytokines were quantified regarding their mean fluorescence intensity (MFI). CLL patients increased IL-10 expression level (median [IQR], 477.0 [355.3–689.3] MFI), when compared to healthy controls (median [IQR], 333.0 [318.2–522.2] MFI) ($p < 0.01$) (Fig. 2C). Likewise, TGF-β1 expression level indicated by MFI was significantly higher in M-MDSC from CLL patients when compared to HV (median [IQR], 658.4 [563.6–865.2] MFI *vs.* 526.60 [389.6–565.8] MFI, $p < 0.001$) (Fig. 2D).

The percentage of M-MDSC with intracellular IL-10 expression showed low inter-individual variability in healthy controls while in CLL patients it was much more diverse and significantly lower in patients at stage 0 as compared to the stages I/II and III/IV according to Rai stages (Fig. 3A, Table 2). Likewise, MFI was lower in patients at stage 0 (median, 456.0 MFI) as compared to the stages I/II (median, 481.90 MFI) and III/IV (median, 757.30 MFI) (Fig. 3B, Table 2). Similarly the percentage of M-MDSC with intracellular TGF-β1 expression was significantly lower in patients at stage 0 as compared to the stages I/II and III/IV according to Rai stages (Fig. 3C, Table 2). Likewise, MFI was lower in patients at stage 0 as compared to the stages I/II and III/IV (Fig. 3D, Table 2).

The percentage of M-MDSC with intracellular TGF-β1 expression was significantly higher in ZAP-70-positive patients compared with ZAP-70-negative ones (Fig. 4A, Table 3) ($p < 0.05$). Likewise, higher intracellular TGF-β1 expression determined by MFI was observed in ZAP-70+ than in ZAP-70- patients ($p < 0.05$) (Fig. 4B, Table 3). We also observed a higher percentage of M-MDSC with TGF-β1 expression in CD38-negative patients than in CD38-positive ones ($p < 0.05$) (Fig. 4C, Table 3). Likewise, MFI was higher in CD38+ than in CD38- patients; however, the difference was not statistically significant ($p > 0.05$) (Fig. 4D, Table 3). Opposing

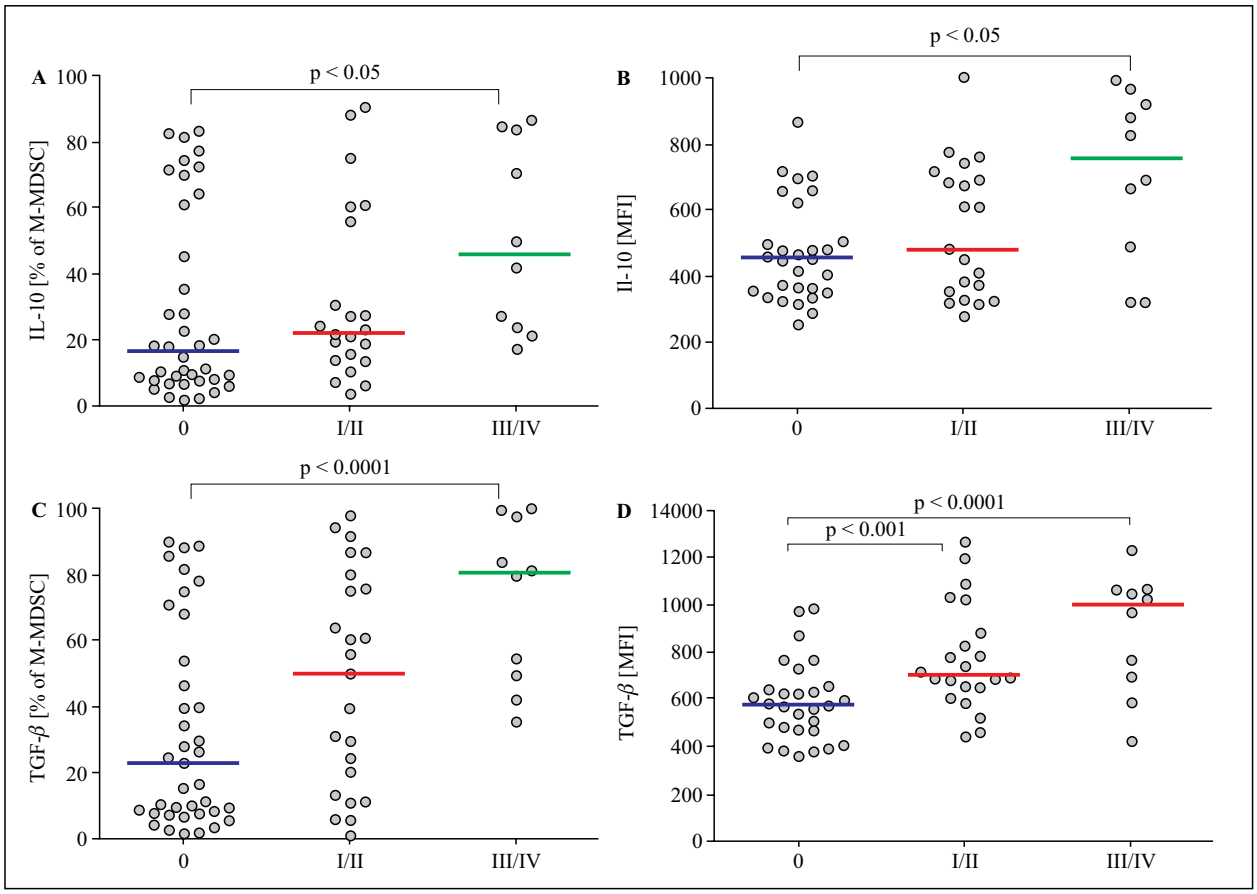

Figure 3. IL-10 and TGF-β expression in M-MDSCs from CLL patients in different disease stages. **(A)** percentage of IL-10 positive M-MDSCs; **(B)** mean fluorescence intensity (MFI) of IL-10 in M-MDSCs. **(C)** percentage of TGF-β positive M-MDSCs; **(D)** MFI of TGF-β in M-MDSCs. The Kruskal-Wallis test with Dunn correction was used for comparison or comparative analysis.

Table 2. M-MDSC with intracellular IL-10 or TGF-β1 expression in CLL patients at various disease stages (three risk groups)

$CD14^+CD11b^+CD15^-HLA\text{-}DR^{-/low}IL\text{-}10^+$						
	Stage 0 (n = 37)		**Stage I/II (n = 23)**		**Stage III/IV (n = 10)**	
	%	**MFI**	**%**	**MFI**	**%**	**MFI**
Median	17.18	456.0	22.80	481.90	46.14	757.30
Minimum	2.32	258.2	4.28	279.20	17.51	318.70
Maximum	83.77	864.6	90.63	1000.00	86.40	991.50
IQR	53.65	212.6	42.85	357.6	60.39	484.00
$CD14^+CD11b^+CD15^-HLA\text{-}DR^{-/low}TGF\text{-}\beta1^+$						
	%	**MFI**	**%**	**MFI**	**%**	**MFI**
Median	22.89	582.70	50.10	704.90	80.43	1000.00
Minimum	1.29	365.20	1.27	445.70	35.36	428.8
Maximum	89.41	987.90	97.63	1269.0	99.48	1230.0
IQR	53.01	175.60	66.76	261.70	49.69	393.40

MFI — Mean fluorescence intensity

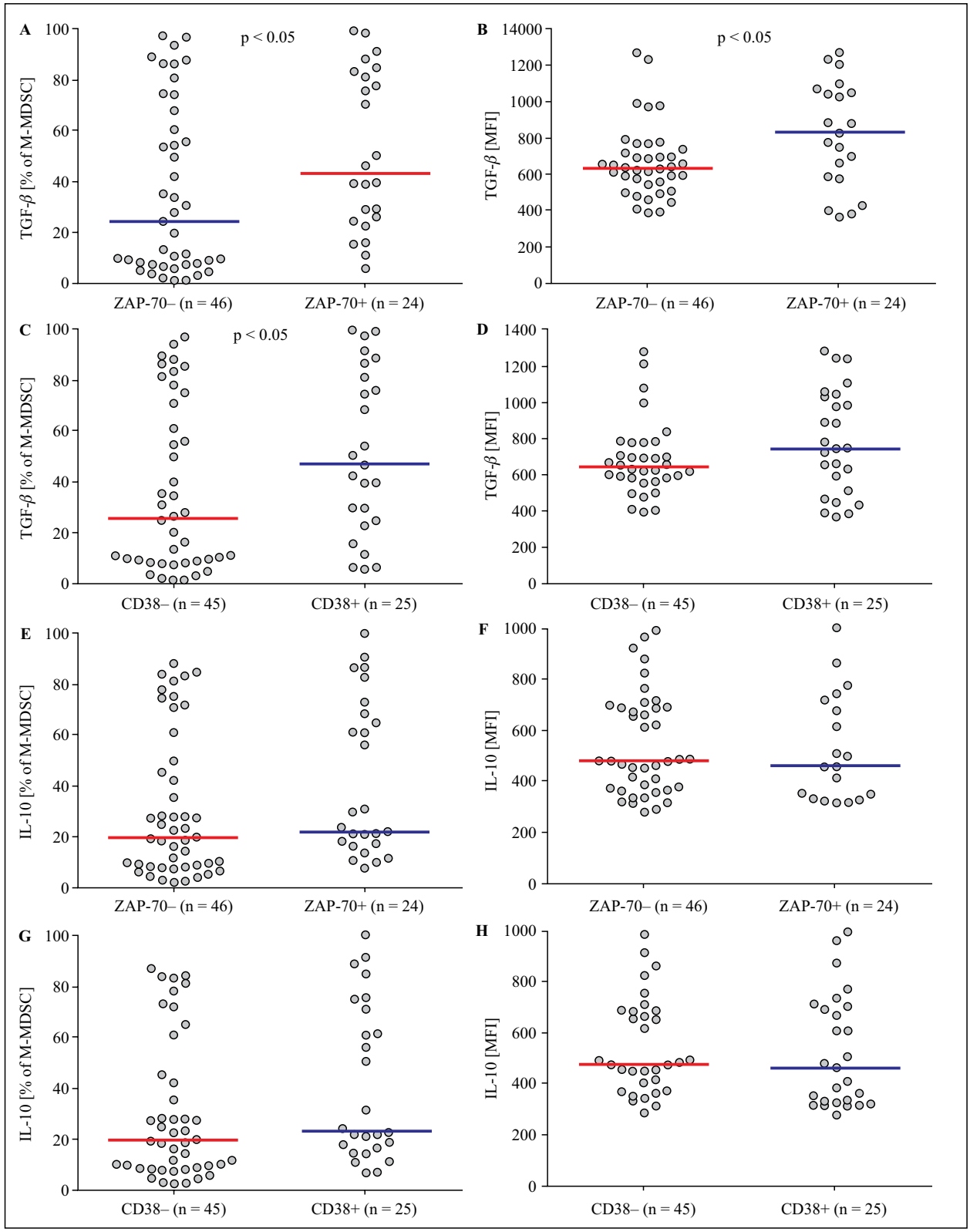

Figure 4. IL-10 and TGF-β expression in M-MDSCs from CLL patients analyzed by adverse prognostic factors. **A.** The percentage of $CD14^+CD11b^+CD15^-HLA\text{-}DR^{-/low}TGF\text{-}\beta^+$ cells in ZAP-70-negative patients compared with ZAP-70-positive patients. **B.** TGF-β expression levels indicated by the MFI (mean fluorescence intensity) in M-MDSCs from ZAP-70-negative and ZAP-70-positive patients. **C.** The percentage of $CD14^+CD11b^+CD15^-HLA\text{-}DR^{-/low}TGF\text{-}\beta^+$ cells in CD38-negative patients compared with CD38-positive patients. **D.** TGF-β expression levels indicated by the MFI in M-MDSCs from CD38- and CD38+ patients. **E.** The percentage of $CD14^+CD11b^+CD15^-HLA\text{-}DR^{-/low}IL\text{-}10^+$ cells in ZAP-70-negative patients compared with ZAP-70-positive patients. **F.** IL-10 expression levels indicated by the MFI in M-MDSCs from ZAP-70-negative and ZAP-70-positive patients. **G.** The percentage of $CD14^+CD11b^+CD15^-HLA\text{-}DR^{-/low}IL\text{-}10^+$ cells in CD38-negative patients compared with CD38-positive patients. **H.** IL-10 expression levels indicated by the MFI in M-MDSCs from CD38- and CD38+ patients. The U Mann-Whitney test was used for comparative analysis.

Table 3. Percentage of M-MDSC with the expression of IL-10 and IL-10 MFI in CLL patients classified into groups: ZAP-70+, ZAP-70-, CD38+, CD38–

M-MDSC IL10-positive								
	ZAP-70+ (n = 24)		**ZAP-70- (n = 46)**		**CD38+ (n = 25)**		**CD38- (n = 45)**	
	%	**MFI**	**%**	**MFI**	**%**	**MFI**	**%**	**MFI**
Median	21.95	458.20	20.02	478.00	22.91	465.60	19.67	478.00
Minimum	7.70	316.60	2.32	279.20	6.640	279.20	2.320	290.70
Maximum	99.84	1000.00	88.24	991.50	99.84	1000.00	86.40	991.50
IQR	48.33	382.90	41.80	318.70	55.59	380.50	36.32	296.50
M-MDSC TGF-β1-positive								
	%	**MFI**	**%**	**MFI**	**%**	**MFI**	**%**	**MFI**
Median	43.28	830.20	24.56	631.80	25.51	738.70	46.71	639.40
Minimum	6.18	365.20	1.27	387.70	1.27	365.20	5.57	392.90
Maximum	99.48	1269.00	97.63	1265.0	97.14	1269.00	99.48	1265.0
IQR	57.85	476.80	60.33	189.90	60.20	532.20	63.41	197.20

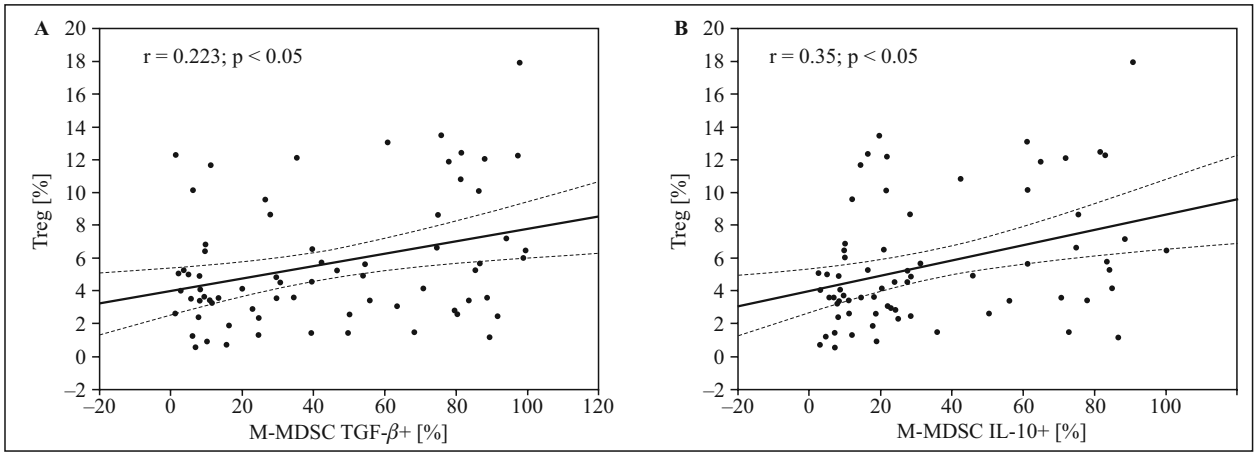

Figure 5. The relationship between the percentages of Treg lymphocytes and M-MDSCs with intracellular TGF-β **(A)** or IL-10 **(B)** expression. The Spearman rank correlation coefficient was used in correlation tests.

to what was observed for TGF-β1 differences in percentage of M-MDSC with IL-10 expression and IL-10 MFI levels were not statistically significant between ZAP-70+ and ZAP-70- patients (Fig. 4E, 4F). Likewise, the difference between CD38-negative patients and CD38-positive ones was not statistically significant ($p > 0.05$) (Fig. 4G, 4H).

The percentage of M-MDSC with TGF-β1 expression correlated positively with the peripheral blood WBC count ($r = 0.272$; $p < 0.05$) and lymphocyte count ($r = 0.260$; $p < 0.05$). In the group of patients with CLL, no significant correlations were identified between the frequency of M-MDSC TGF-β1-positive and platelet counts, hemoglobin concentration, serum LDH and β2-microglobulin levels or the age of the patients.

There was a significant correlation between the percentage of M-MDSC with intracellular TGF-β1 expression and Treg cells ($r = 0.223$; $p < 0.05$) (Fig. 5A). Likewise, percentage of M-MDSC cell with IL-10 expression correlated with frequency of Treg ($r = 0.35$; $p < 0.05$) (Fig. 5B).

Moreover, there was a significant difference in the median percentage of M-MDSC with intracellular IL-10 expression between patients carrying the 11q22.3 and/or the 17p13.1 deletion (median [IQR], 31.41% [21.29–76.96%]) and patients without these genetic aberrations (median [IQR], 20.67% [10.80–58.36%]) ($p < 0.05$) (Fig. 6A). We also observed a significantly higher percentage of M-MDSC positive for intracellular TGF-β expression in patients carrying the 11q22.3 and/or the 17p13.1 deletion (median [IQR], 55.10%

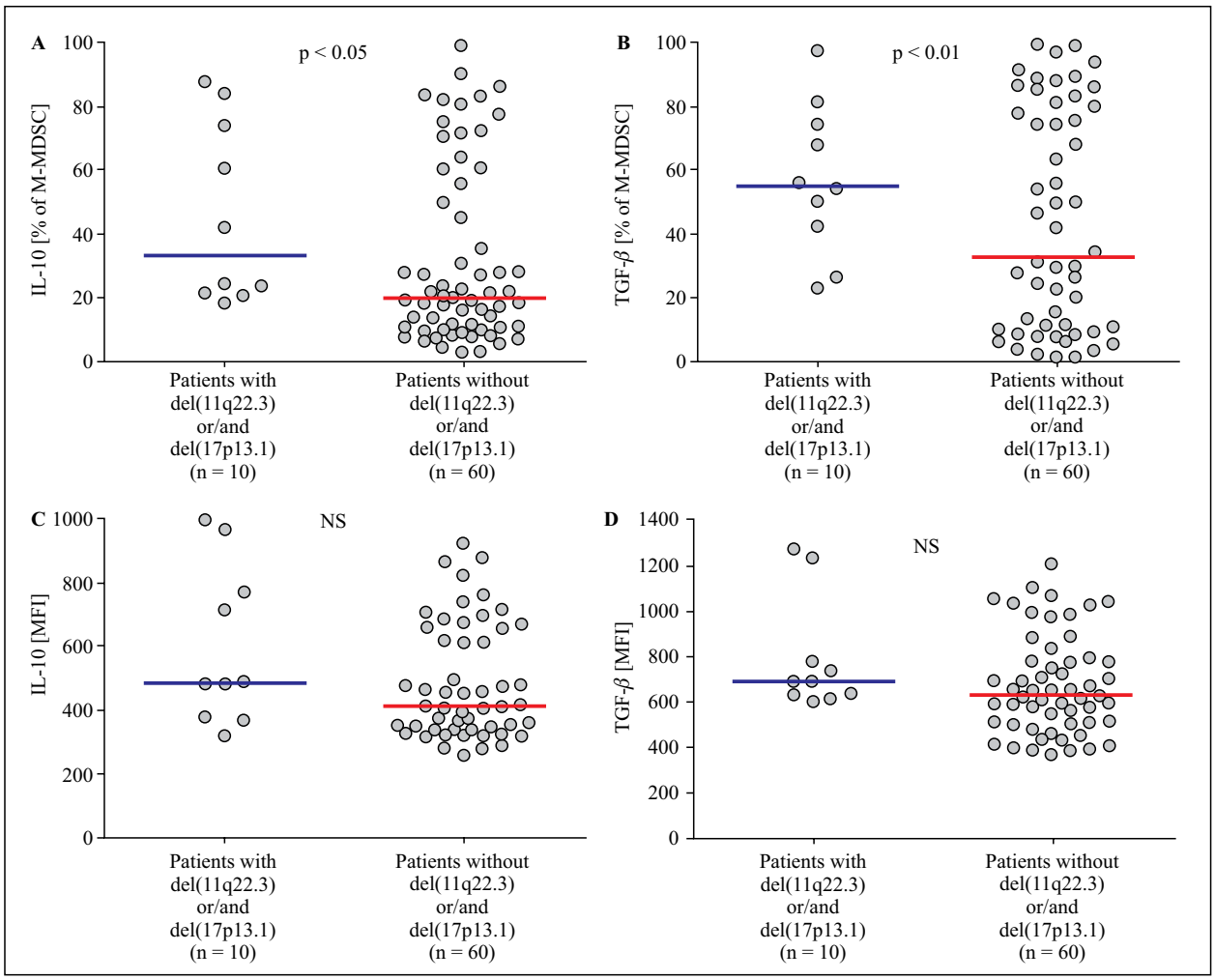

Figure 6. IL-10 and TGF-β expression in M-MDSCs from CLL patients carrying the 11q22.3 and/or the 17p13.1 deletion and patients without these genetic aberrations. **(A)** percentage of IL-10 positive M-MDSCs; **(B)** percentage of TGF-β positive M-MDSCs; **(C)** mean fluorescence intensity (MFI) of IL-10 in M-MDSCs; **(D)** MFI of TGF-β in M-MDSCs. The U Mann-Whitney test was used for comparative analysis.

[38.30–76.18%]) than in patients without these genetic aberrations (median [IQR], 32.60% [9.82–80.53%] ($p < 0.01$) (Fig. 6B).

Likewise, TGF-β1 and IL-10 expression levels indicated by the MFI were compared between patients carrying the 11q22.3 and/or the 17p13.1 deletion (TGF-β1: median [IQR], 674.4 [571.5–903.0] MFI; IL-10: median [IQR], 470.8 [366.2–822.8] MFI) and patients without these genetic aberrations (TGF-β1: median [IQR], 629.5 [495.5–808.0] MFI; IL-10: median [IQR], 411.8 [334.2–656.7] MFI). However, the difference was not statistically significant ($p > 0.05$) (Fig. 6C, 6D).

During the follow-up period (range 1–55 months), 17 patients required therapy (Table 1). The percentage of M-MDSC IL-10-positive and M-MDSC TGF-β1-positive measured at the time of diagnosis was statistically higher in patients requiring therapy as compared to patients without treatment during the observation period (IL-10: median [IQR], 27.95% [11.73–99.84%] *vs.* 21.48% [18.08–49.01%] TGF-β1: median [IQR], 49.76% [24.56–83.46%] *vs.* 39.35% [13.77–77.72%] ($p < 0.05$). However, MFI level was not statistically significant between both groups (IL-10: median [IQR], 477.0 [372.2–696.0] MFI *vs.* 375.3 [319.3–774.9] MFI; TGF-β1: median [IQR], 735.7 [477.1–927.3] MFI *vs.* 651.5 [575.5–876.9] MFI; $p > 0.05$).

Discussion

The presence of M-MDSC in the microenvironment has recently aroused great interest. M-MDSC, like regulatory T cells, is thought to contribute to the

effective reduction of anti-tumor response [30]. Unfortunately, there are very few studies available on M-MDSCs in CLL patients [16, 31–33]. Jitschin *et al*. [16] identified increased numbers of MDSCs ($CD14^+HLA\text{-}DR^{lo}$) in untreated patients with CLL. This finding is supported by our results showing the M-MDSC (defined as $CD14^+CD11b^+CD15^-HLA\text{-}DR^{-/low}$ cells) accumulation in CLL patients.

M-MDSCs have been described to express IDO (indoleamine-2,3-dioxygenase). IDO activity is an important mechanism by which effector T cells can be induced and converted to Tregs. The IDO-mediated depletion of tryptophan and subsequent production of immunosuppressive products may also lead to T cell suppression through the down-regulation of the TCR-CD3-ζ chain [34]. IDO^{high} MDSCs suppress both T-cell activation and proliferation in untreated CLL patients [16]. M-MDSCs have also been described to secrete TGF-β and IL-10, which exert direct immunosuppressive effects on T effector cells or induce the generation of Treg cells [35].

Alhakeem *et al.* [19] observed that CLL patients have a significantly higher level of IL-10 in plasma than healthy donors. They reported that IL-10 affects CLL growth indirectly by suppressing anti-CLL T-cells. In their study IL-10 reduced the generation of effector CD4 and CD8 T-cells [19]. Still little is known about the mechanisms that lead to the increasing of M-MDSC, especially in the microenvironment of leukemia [20] and lymphoma [24]. Lee *et al.* [36] found that TGF-β induced the expansion of the monocytic MDSC population, expression of immunosuppressive molecules by MDSCs, and the ability of MDSCs to suppress CD4+ T cell proliferation. In our study, we found a significantly higher percentage of M-MDSC with intracellular IL-10 or TGF-β expression in CLL patients than in healthy volunteers. Moreover, we reported a significant correlation between the percentage of M-MDSC with TGF-β or IL-10 expression and the frequency of Treg cells. In general, the accumulation of Treg lymphocytes in CLL is well documented. Their increased incidence in patients with CLL affects the severity of the disease and worse prognosis [37].

Recently, Zahran AM *et al.* [33] reported that the abundance of $CD14^+HLA\text{-}DR^{lo}$ cells is associated with frequency of ZAP-70 and CD38 cells. Expression of CD38 and ZAP-70 in cancer cells of CLL patients are typical immunophenotypic unfavorable prognostic markers of patients' life expectancy [38]. It is interesting that M-MDSC from ZAP-70-positive and CD38-positive cases expressed higher TGF-β or IL-10 levels. What is more, we were able to demonstrate a significant association of TGF or IL-10 expression in M-MDSC with del(11q22.3) and/or del(17p13.1). Deletions in the long arm of chromosomes 11 [del(11q)] or in the short arm of chromosome 17 [del(17p)] are recognized as high-risk genetic lesions [26]. Del(17p) is associated with an aggressive clinical course. Patients with leukemia cells that have del(17p) are resistant to standard chemotherapy regimens containing alkylating agents and purine analogs [26, 39, 40]. Likewise, the presence of del(11q) is associated with a clinically progressive disease in almost all CLL cases [41]. Patients with leukemia cells that have del(11q) have been associated with shorter TTFT (time to first treatment), shorter remission durations, and shorter OS (overall survival) following standard chemotherapy compared to cases without this genetic aberration [41].

Gustafson *et al*. [31] reported that the abundance of $CD14^+HLA\text{-}DR^{lo}$ cells is associated with a shorter time to CLL progression. Likewise, Liu *et al.* [32] reported that upregulation of $CD14^+HLA\text{-}DR^{low/-}$ MDSCs correlated with CLL progression and a poor prognosis for CLL patients. Recently, Zahran AM *et al.* [33] reported that the survival time was significantly shorter in patients expressed high levels of M-MDSC when compared to those with low levels. In our study patients who required therapy had a higher percentage of M-MDSC with TGF-β or IL-10 expression. Moreover, the percentage of $CD14^+HLA\text{-}DR^{-/low}$ cells with TGF-β or IL-10 expression increased with more advanced clinical stage of CLL. Undoubtedly, the existence of a relationship between the number of $CD14^+HLA\text{-}DR^{-/low}$ cells and the stage of clinical advancement of the disease indicates the possible involvement of $CD14^+HLA\text{-}DR^{-/low}$ cells in CLL progression. According to the data presented by Jitschin *et al.* [16], patients with a higher M-MDSC percentage have a more rapid accumulation of leukemia lymphocytes. In our study, the percentage of M-MDSC with TGF-β expression correlated positively with the WBC count and PB lymphocyte count.

This is the first report investigated the potential role of M-MDSCs in CLL by analyzing the level of IL-10 and TGF-β1 expression in circulating M-MDSCs in correlation with clinical and laboratory parameters characterizing disease activity and patients' immune status. We have shown that an increased percentage of M-MDSC cells producing IL-10 and TGF-β1 patients may be associated with suppression of the immune response against leukemic cells. It can be assumed that the increased percentage of M-MDSC with intracellular expression of IL-10 and TGF-β1 may in the future be the factor defining the group of patients with shorter time to onset of treatment.

Acknowledgments

This work was supported by a grant from the Medical University of Lublin (grant no. DS 458).

Authors' contributions

ABJ – designed research, performed research, analyzed and interpreted data, wrote the paper, critically revised the manuscript. WK — performed research, collected medical data, wrote the paper and critically revised the manuscript.

Conflict of interest

The authors declare that they have no conflict of interest.

References

1. Mohr A, Renaudineau Y, Bagacean C, et al. Regulatory B lymphocyte functions should be considered in chronic lymphocytic leukemia. Oncoimmunology. 2016; 5(5): e1132977, doi: 10.1080/2162402X.2015.1132977, indexed in Pubmed: 27467951.
2. Ten Hacken E, Burger JA. Microenvironment interactions and B-cell receptor signaling in Chronic Lymphocytic Leukemia: Implications for disease pathogenesis and treatment. Biochim Biophys Acta. 2016; 1863(3): 401–413, doi: 10.1016/j.bbamcr.2015.07.009, indexed in Pubmed: 26193078.
3. ten Hacken E, Burger JA. Microenvironment dependency in Chronic Lymphocytic Leukemia: The basis for new targeted therapies. Pharmacol Ther. 2014; 144(3): 338–348, doi: 10.1016/j.pharmthera.2014.07.003, indexed in Pubmed: 25050922.
4. van Attekum MHa, Eldering E, Kater AP. Chronic lymphocytic leukemia cells are active participants in microenvironmental cross-talk. Haematologica. 2017; 102(9): 1469–1476, doi: 10.3324/haematol.2016.142679, indexed in Pubmed: 28775118.
5. Ostrand-Rosenberg S, Fenselau C. Myeloid-Derived Suppressor Cells: Immune-Suppressive Cells That Impair Antitumor Immunity and Are Sculpted by Their Environment. J Immunol. 2018; 200(2): 422–431, doi: 10.4049/jimmunol.1701019, indexed in Pubmed: 29311384.
6. Gabrilovich DI, Nagaraj S. Myeloid-derived suppressor cells as regulators of the immune system. Nat Rev Immunol. 2009; 9(3): 162–174, doi: 10.1038/nri2506, indexed in Pubmed: 19197294.
7. Nicholas NS, Apollonio B, Ramsay AG. Tumor microenvironment (TME)-driven immune suppression in B cell malignancy. Biochim Biophys Acta. 2016; 1863(3): 471–482, doi: 10.1016/j.bbamcr.2015.11.003, indexed in Pubmed: 26554850.
8. Palumbo GA, Parrinello NL, Giallongo C, et al. Monocytic myeloid derived suppressor cells in hematological malignancies. Int J Mol Sci. 2019; 20(21), doi: 10.3390/ijms20215459, indexed in Pubmed: 31683978.
9. Giallongo C, Parrinello N, Brundo M, et al. Myeloid derived suppressor cells in chronic myeloid leukemia. Frontiers in Oncology. 2015; 5, doi: 10.3389/fonc.2015.00107.
10. Giallongo C, Parrinello NL, La Cava P, et al. Monocytic myeloid-derived suppressor cells as prognostic factor in chronic myeloid leukaemia patients treated with dasatinib. J Cell Mol Med. 2018; 22(2): 1070–1080, doi: 10.1111/jcmm.13326, indexed in Pubmed: 29218828.
11. Marvel D, Gabrilovich DI. Myeloid-derived suppressor cells in the tumor microenvironment: expect the unexpected. J Clin Invest. 2015; 125(9): 3356–3364, doi: 10.1172/JCI80005, indexed in Pubmed: 26168215.
12. Bronte V, Brandau S, Chen SH, et al. Recommendations for myeloid-derived suppressor cell nomenclature and characterization standards. Nat Commun. 2016; 7: 12150, doi: 10.1038/ncomms12150, indexed in Pubmed: 27381735.
13. Wang Y, Ding Y, Guo N, et al. MDSCs: Key Criminals of Tumor Pre-metastatic Niche Formation. Front Immunol. 2019; 10: 172, doi: 10.3389/fimmu.2019.00172, indexed in Pubmed: 30792719.
14. Höpken UE, Rehm A. Targeting the Tumor Microenvironment of Leukemia and Lymphoma. Trends Cancer. 2019; 5(6): 351–364, doi: 10.1016/j.trecan.2019.05.001, indexed in Pubmed: 31208697.
15. Zirlik K. MDSCs: the final frontier of the microenvironment in CLL? Blood. 2014; 124(5): 666–668, doi: 10.1182/blood-2014-06-578880, indexed in Pubmed: 25082859.
16. Jitschin R, Braun M, Büttner M, et al. CLL-cells induce IDOhi CD14+HLA-DRlo myeloid-derived suppressor cells that inhibit T-cell responses and promote TRegs. Blood. 2014; 124(5): 750–760, doi: 10.1182/blood-2013-12-546416, indexed in Pubmed: 24850760.
17. Özkan B, Lim H, Park SG. Immunomodulatory function of myeloid-derived suppressor cells during B cell-mediated immune responses. Int J Mol Sci. 2018; 19(5), doi: 10.3390/ijms19051468, indexed in Pubmed: 29762501.
18. Tcyganov E, Mastio J, Chen E, et al. Plasticity of myeloid-derived suppressor cells in cancer. Curr Opin Immunol. 2018; 51: 76–82, doi: 10.1016/j.coi.2018.03.009, indexed in Pubmed: 29547768.
19. Alhakeem SS, McKenna MK, Oben KZ, et al. Chronic lymphocytic leukemia-derived IL-10 suppresses antitumor immunity. J Immunol. 2018; 200(12): 4180–4189, doi: 10.4049/jimmunol.1800241, indexed in Pubmed: 29712773.
20. Lv M, Wang Ke, Huang XJ. Myeloid-derived suppressor cells in hematological malignancies: friends or foes. J Hematol Oncol. 2019; 12(1): 105, doi: 10.1186/s13045-019-0797-3, indexed in Pubmed: 31640764.
21. Millrud CR, Bergenfelz C, Leandersson K. On the origin of myeloid-derived suppressor cells. Oncotarget. 2017; 8(2): 3649–3665, doi: 10.18632/oncotarget.12278, indexed in Pubmed: 27690299.
22. Kumar V, Patel S, Tcyganov E, et al. The nature of myeloid-derived suppressor cells in the tumor microenvironment. Trends Immunol. 2016; 37(3): 208–220, doi: 10.1016/j.it.2016.01.004, indexed in Pubmed: 26858199.
23. Bergenfelz C, Larsson AM, von Stedingk K, et al. Systemic monocytic-MDSCs are generated from monocytes and correlate with disease progression in breast cancer patients. PLoS One. 2015; 10(5): e0127028, doi: 10.1371/journal.pone.0127028, indexed in Pubmed: 25992611.
24. Xiu B, Lin Y, Grote DM, et al. IL-10 induces the development of immunosuppressive CD14(+)HLA-DR(low/-) monocytes in B-cell non-Hodgkin lymphoma. Blood Cancer J. 2015; 5: e328, doi: 10.1038/bcj.2015.56, indexed in Pubmed: 26230952.
25. Kowalska W. Expression of CD163 and HLA-DR molecules on the monocytes in chronic lymphocytic leukemia patients. Folia Histochem Cytobiol. 2020 [Epub ahead of print], doi: 10.5603/FHC.a2020.0002, indexed in Pubmed: 32176313.
26. Hallek M, Cheson BD, Catovsky D, et al. International workshop on chronic lymphocytic leukemia. Guidelines for the

diagnosis and treatment of chronic lymphocytic leukemia: a report from the International Workshop on Chronic Lymphocytic Leukemia updating the National Cancer Institute-Working Group 1996 guidelines. Blood. 2008; 111(12): 5446–5456, doi: 10.1182/blood-2007-06-093906, indexed in Pubmed: 18216293.
27. Rai KR, Sawitsky A, Cronkite EP, et al. Clinical staging of chronic lymphocytic leukemia. Blood. 1975; 46(2): 219–234, doi: 10.1182/blood.v46.2.219.219.
28. Hus I, Podhorecka M, Bojarska-Junak A, et al. The clinical significance of ZAP-70 and CD38 expression in B-cell chronic lymphocytic leukaemia. Ann Oncol. 2006; 17(4): 683–690, doi: 10.1093/annonc/mdj120, indexed in Pubmed: 16524977.
29. Bojarska-Junak A, Hus I, Chocholska S, et al. CD1d expression is higher in chronic lymphocytic leukemia patients with unfavorable prognosis. Leuk Res. 2014; 38(4): 435–442, doi: 10.1016/j.leukres.2013.12.015, indexed in Pubmed: 24418751.
30. Awad RM, De Vlaeminck Y, Maebe J, et al. Turn back the TIMe: targeting tumor infiltrating myeloid cells to revert cancer progression. Front Immunol. 2018; 9: 1977, doi: 10.3389/fimmu.2018.01977, indexed in Pubmed: 30233579.
31. Gustafson MP, Abraham RS, Lin Yi, et al. Association of an increased frequency of CD14+ HLA-DR lo/neg monocytes with decreased time to progression in chronic lymphocytic leukaemia (CLL). Br J Haematol. 2012; 156(5): 674–676, doi: 10.1111/j.1365-2141.2011.08902.x, indexed in Pubmed: 22050346.
32. Liu J, Zhou Y, Huang Q, et al. CD14HLA-DR expression: A novel prognostic factor in chronic lymphocytic leukemia. Oncol Lett. 2015; 9(3): 1167–1172, doi: 10.3892/ol.2014.2808, indexed in Pubmed: 25663875.
33. Zahran AM, Moeen SM, Thabet AF, et al. Monocytic myeloid-derived suppressor cells in chronic lymphocytic leukemia patients: a single center experience. Leuk Lymphoma. 2020 [Epub ahead of print]: 1–8, doi: 10.1080/10428194.2020.1728747, indexed in Pubmed: 32077360.
34. Li F, Zhao Y, Wei L, et al. Tumor-infiltrating Treg, MDSC, and IDO expression associated with outcomes of neoadjuvant chemotherapy of breast cancer. Cancer Biol Ther. 2018; 19(8): 695–705, doi: 10.1080/15384047.2018.1450116, indexed in Pubmed: 29621426.
35. Groth C, Hu X, Weber R, et al. Immunosuppression mediated by myeloid-derived suppressor cells (MDSCs) during tumour progression. Br J Cancer. 2019; 120(1): 16–25, doi: 10.1038/s41416-018-0333-1, indexed in Pubmed: 30413826.
36. Lee CR, Lee W, Cho S, et al. Characterization of multiple cytokine combinations and TGF-β on differentiation and functions of myeloid-derived suppressor cells. IJMS. 2018; 19(3): 869, doi: 10.3390/ijms19030869.
37. Lad DP, Varma S, Varma N, et al. Regulatory T-cell and T-helper 17 balance in chronic lymphocytic leukemia progression and autoimmune cytopenias. Leuk Lymphoma. 2015; 56(8): 2424–2428, doi: 10.3109/10428194.2014.986479, indexed in Pubmed: 25393804.
38. Rassenti LZ, Jain S, Keating MJ, et al. Relative value of ZAP-70, CD38, and immunoglobulin mutation status in predicting aggressive disease in chronic lymphocytic leukemia. Blood. 2008; 112(5): 1923–1930, doi: 10.1182/blood-2007-05-092882, indexed in Pubmed: 18577710.
39. Shindiapina P, Brown JR, Danilov AV. A new hope: novel therapeutic approaches to treatment of chronic lymphocytic leukaemia with defects in TP53. Br J Haematol. 2014; 167(2): 149–161, doi: 10.1111/bjh.13042, indexed in Pubmed: 25040077.
40. Brander D, Islam P, Barrientos JC. Tailored Treatment Strategies for Chronic Lymphocytic Leukemia in a Rapidly Changing Era. Am Soc Clin Oncol Educ Book. 2019; 39: 487–498, doi: 10.1200/EDBK_238735, indexed in Pubmed: 31099686.
41. Puiggros A, Blanco G, Espinet B. Genetic abnormalities in chronic lymphocytic leukemia: where we are and where we go. Biomed Res Int. 2014; 2014: 435983, doi: 10.1155/2014/435983, indexed in Pubmed: 24967369.

Submitted: 28 February, 2020
Accepted after reviews: 24 March, 2020
Available as AoP: 30 March, 2020

FOLIA HISTOCHEMICA ET CYTOBIOLOGICA
Vol. 58, No. 1, 2020
pp. 37–45

ORIGINAL PAPER

VIA MEDICA

Search of reference biomarkers reflecting orbital tissue remodeling in the course of Graves' orbitopathy

Przemyslaw Pawlowski[1, 2, 3], Izabela Poplawska[1], Janusz Mysliwiec[4], Willem A. Dik[5], Anja Eckstein[6], Utta Berchner-Pfannschmidt[6], Robert Milewski[7], Slawomir Lawicki[8], Zofia Dzieciol-Anikiej[9], Robert Rejdak[10, 11], Joanna Reszec[1]

[1]Department of Medical Pathomorphology, Cathedral of Biostructure, Medical University of Bialystok, Poland
[2]Department of Pediatric Ophthalmology and Strabismus, Medical University of Bialystok, Bialystok, Poland
[3]Department of Ophthalmology, Ludwik Rydygier District Hospital in Suwalki, Poland
[4]Department of Nuclear Medicine, Medical University of Bialystok, Bialystok, Poland
[5]Department of Immunology, Laboratory Medical Immunology, Erasmus MC, University Medical Centre Rotterdam, Rotterdam, The Netherlands
[6]Molecular Ophthalmology, Department of Ophthalmology, University Hospital Essen/University of Duisburg-Essen, Essen, Germany
[7]Department of Statistics and Medical Informatics, Medical University of Bialystok, Bialystok, Poland
[8]Department of Population Medicine and Civilization Diseases Prevention, Medical University of Bialystok, Bialystok, Poland
[9]Department of Rehabilitation, Medical University of Bialystok, Bialystok, Poland
[10]Department of General Ophthalmology, Medical University of Lublin, Lublin, Poland
[11]Department of Experimental Pharmacology, Medical Research Centre, Polish Academy of Sciences, Warsaw, Poland

Abstract

Introduction. Graves' orbitopathy (GO) is a complication in Graves' disease (GD) that causes disfigurement and sometimes blindness. The pathogenesis of GO remains unknown, while its symptoms demonstrate dependence between the thyroid gland and the orbit. The ongoing inflammatory process in retrobulbar tissue results in its remodeling characterized by increased volume of the orbital contents involving adipose tissue, with fibrosis and adipogenesis as predominant features. This study was aimed at the immunohistochemical verification of potential contribution and correlation between orbital expressions of IGF-1R, CD34, Foxp-3, PPAR-γ and CD4, CD68, TGF-β, FGF-β in severe and mild (long-lasting) GO.

Material and methods. Forty-one orbital tissue specimens — 22 patients with severe GO, 9 patients with mild GO and 10 patients undergoing blepharoplasty as a control group — were processed by routine immunohistochemistry.

Results. Increased IGF-1R, CD34 and Foxp-3 expression was found in both severe and mild GO, yet a significant correlation between CD34 and CD4, CD68, TGF-β, FGF-β expressions was observed in long-lasting GO.

Conclusions. CD34 expression is proposed to be the marker of orbital tissue remodeling in the course of mild GO. *(Folia Histochemica et Cytobiologica 2020, Vol. 58, No. 1, 37–45)*

Key words: Graves' orbitopathy; CD34; IGF-1R; PPAR-γ; CD68; TGF-β; FGF-β; Foxp-3; tissue remodeling; autoimmunity; IHC

Correspondence address: Przemyslaw Pawlowski, MD, PhD
Department of Medical Pathomorphology,
Cathedral of Biostructure,
Medical University of Bialystok,
13 Waszyngtona Street, 15–269 Bialystok, Poland
tel./fax: +48 85 8795945
e-mail: przemyslaw.pawlowski@umb.edu.pl

Introduction

The pathogenesis of Graves' orbitopathy (GO) remains enigmatic as does the connection between the thyroid and orbit [1, 2]. GO is characterized by a volume increase of the orbital adipose tissue and orbital remodeling, but the cells and molecules that drive orbital adipogenesis and remodeling remain uncertain. Previously, CD34(+) fibrocytes, monocyte-lineage bone marrow-derived cells, were found to infiltrate the orbit in GO where they could transform into CD34(+) orbital fibroblasts [3, 4]. Moreover, it has been reported that CD34(+) fibrocytes express functional TSH receptor, the central autoantigen in Graves' disease (GD) [5, 6]. In addition to the TSH receptor, orbital fibrocytes (OF) express the insulin-like growth factor 1 receptor (IGF-1R) and the role of TSHR/IGF-1R crosstalk has been recently emphasized in the pathogenesis of GO [7–9]. Previous study had shown that IGF-1R levels were three-fold higher on the orbital fibroblasts (OF) from GO patients compared with control fibroblasts [10]. Most recently, Zhao *et al.* showed that IGF-1 significantly promoted the cell proliferation and lipid accumulation in stromal cells derived from GO-orbital adipose tissue [11]. Furthermore, Zhao *et al.* have demonstrated that the protein level of peroxisome proliferator-activated receptor-γ (PPAR-γ), involved in insulin action, adipocyte differentiation, lipid metabolism and inflammation, is up-regulated in adipose-derived stromal cells when treated with IGF-1, which involved activation of IGF-1R and subsequent PI3K signaling [11]. These data illustrate that the IGF-1/IGF-1R axis represents a pro-proliferative and pro-adipogenic pathway in orbital tissue from GO [11].

Regulatory T cells (Tregs) are crucial in suppressing aberrant pathological immune responses, including auto-immune responses [12]. To maintain homeostasis, Tregs use different mechanisms, including the secretion of inhibitory cytokines, but also by cell surface expression of molecules such as cytotoxic T lymphocyte-associate protein 4 (CTLA-4) that is a critical negative regulator of T cell immunity. Development and functioning of Tregs is controlled by the transcription factor Forkhead box P3 (Foxp-3), while the absence or dysfunction, reduced number of CD4+CD25+Foxp-3+ Tregs associated with auto-immune disease, including GD [13, 14]. Previously, we found enhanced Foxp-3 mRNA expression in GO orbital tissue samples and the positive correlation observed with CD3 infiltration along with diminished CTLA-4 expression suggesting that inadequate Treg function contributes to the pathogenesis of severe GO [15].

The limitations in our understanding of extrathyroidal Graves' disease immunophenotype result in unsatisfying treatment of severe GO. Therefore, we performed a detailed immunohistochemical study that aimed at comparing the expression pattern of CD34, IGF-1R, Foxp-3, and PPAR-γ in the orbital fat/connective tissue of patients with mild/long-lasting and severe/active GO in relation to tissue infiltrating cells and remodeling properties (CD4, CD68, TGF-β, FGF-β) in these two subgroups of patients with GO.

Material and methods

Patients and controls. Human orbital tissue samples from twenty seven patients with GO (26 females and 1 male) classified according to the European Group on Graves' Orbitopathy [16], who underwent orbital decompression procedures, were obtained from the orbital tissue bank at the Department of Ophthalmology, University of Essen, Essen, Germany. The mean age of patients at the time of surgery was 44.5 years (range 26–47).

Control, age-matched, fat/connective tissue was obtained from 10 individuals (9 females and 1 male) undergoing orbital surgery for blepharoplasty and without history of GO or any orbital inflammatory disease. Surgical specimens were immediately snap-frozen in liquid nitrogen and stored in –80°C until use.

The clinical activity score of GO (CAS) was estimated according to Mourits *et al.* [17]. The severity of the eye disease was estimated using NOSPECS classification (no signs or symptoms; only signs, on symptoms; signs only; proptosis; eye muscle involvement; corneal involvement; and sight visual acuity reduction) [16].

Patients with severe GO (NOSPECS IV–VI), required orbital bony decompression due to optic nerve compression and limited extraocular muscle functions (22 specimens). Mean duration of thyroid disease was 2.5 ± 1.5 years (mean ± SD) and 1.2 ± 1 year for GO. Before the surgery all patients received > 1 cycle of steroid treatment and orbital irradiation. The mean clinical activity score was 8.5 ± 2.5.

Patients with mild GO (n = 9) (NOSPECS III–IV) underwent orbital bony decompression to reduce proptosis. Mean duration of thyroid disease was 3.9 ± 2 years and 3.3 ± 1.9 for GO. Steroid treatment and orbital irradiation characteristics in this group were similar to the patients with severe GO. The mean clinical activity score was 2.2 ± 0.8.

The study was approved by the Medical Ethics Committee of the University of Essen, Germany. All procedures performed in studies involving human participants were in accordance with the ethical standards of the institutional and/or national research committee and with the 1964 Helsinki declaration and its later amendments or comparable ethical standards.

Table 1. Antibodies used in the study for immunohistochemical stainings. For negative control phosphate-buffered saline (PBS) was used instead of primary antibody, no staining was detected when the primary antibody was omitted

Antibody	Type of antibody	Dilution	Positive control
IGF-1Rα	Monoclonal mouse anti-human Santa Cruz Biotechnology Antibody (1H7): sc-461	1:100	Thyroid gland tissue
CD34	Monoclonal rabbit anti-human Abcam Antibody (EP373Y): ab81289	1:100	Normal kidney vessels tissue
Foxp-3	Monoclonal mouse anti-human Santa Cruz Biotechnology Antibody (2A11G9): sc-53876	1:150	Human lymph node tissue
PPAR-γ	Monoclonal mouse anti-human Santa Cruz Biotechnology Antibody (E-8): sc-7273	1:50	Human placenta tissue

Immunohistochemistry. Formalin-fixed, paraffin-embedded human orbital cryosections (4 μm thick) were subjected to heat-induced antigen retrieval in EnVision Flex Target Retrieval Solution (DAKO, Glostrup, Denmark) in high pH (Tris/EDTA buffer, pH = 9) for the evaluation of CD34 and Foxp-3, and in low pH (0.01M sodium citrate buffer, pH = 6.0) for IGF-IR and PPAR-γ expression. Following the reduction of endogenous peroxidase activity by immersion in 3% hydrogen peroxidase in methanol for 10 minutes and blockade of nonspecific antigens, slides were incubated with primary antibodies, as indicated in Table 1, overnight at refrigerator temperature (4°C). Visualization reagent EnVision/HRP (DAKO Omnis) was applied for 20 minutes followed by DAB+ Chromogen (DAKO Omnis) solution for 10 minutes. The slides were counterstained with hematoxylin and evaluated under the light microscope. The results of the immunostaining were evaluated in 15 random fields under 20× magnification per each sample by two independent pathologist blindly. The immunohistochemical assessment of CD4, CD68, TGF-β and FGF-β was evaluated and described earlier in our previous study [18]. The results were expressed as the percentage of IGF-1R$^+$, CD34$^+$, PPAR-γ^+ orbital fibroblasts (OF) and Foxp-3$^+$ associated T lymphocytes by the positive staining as follows: ≤ 10% positive cells — negative (−), between 11% and 50% (+), and ≥ 51% positive cells (++). Although both nuclear and cytoplasmic expressions were observed, it was necessary to use a unified semi-quantitative rating system in order to determine possible dependencies in co-expression.

Statistical analysis. The results were analyzed using Statistica 12.0 for Windows (StatSoft, Poland). Owing to asymmetric data distribution, nonparametric tests were used. Significance levels were calculated in accordance with Kruskal-Wallis test (differences between the control and examined group). The correlations between the examined parameters were assessed with Spearman's rank correlation test. A p-value < 0.05 was regarded as significant.

Results

In this study we assessed IGF-1R, CD34, Foxp-3 and PPAR-γ expression in the orbital tissue in severe and mild GO compared between each other and with control cases. Obtained results were correlated with CAS of GO patients and with CD4, CD68, TGF-β and FGF-β expression.

CD34 expression

CD34 expression was found in OF in orbital connective tissue of GO patients (Fig. 1A–B). 80% of the evaluated control samples were negative for CD34 expression, while all mild GO cases were evaluated as + while in severe GO cases ~23% of the orbital tissues were scored as + and ~ 77% were rated as ++ (Table 2 and 3).

Foxp-3 expression

Foxp-3 expression (Fig. 1C) was found in associated T lymphocytes from orbital connective tissue of both control and GO patients. From the orbital tissues obtained from the control group, half of them revealed a Foxp-3 staining scored as + while the other half was scored as ++ (Table 2). Within the group of mild GO all orbital tissues were evaluated as + while in the severe GO group ~59% of the orbital tissues were scored as ++, ~32% as + and ~9% as negative (Table 2 and Table 3).

IGF-1R expression

IGF-1R was undetectable in the orbital tissue from all control cases (Table 2). However, IGF-1R expression

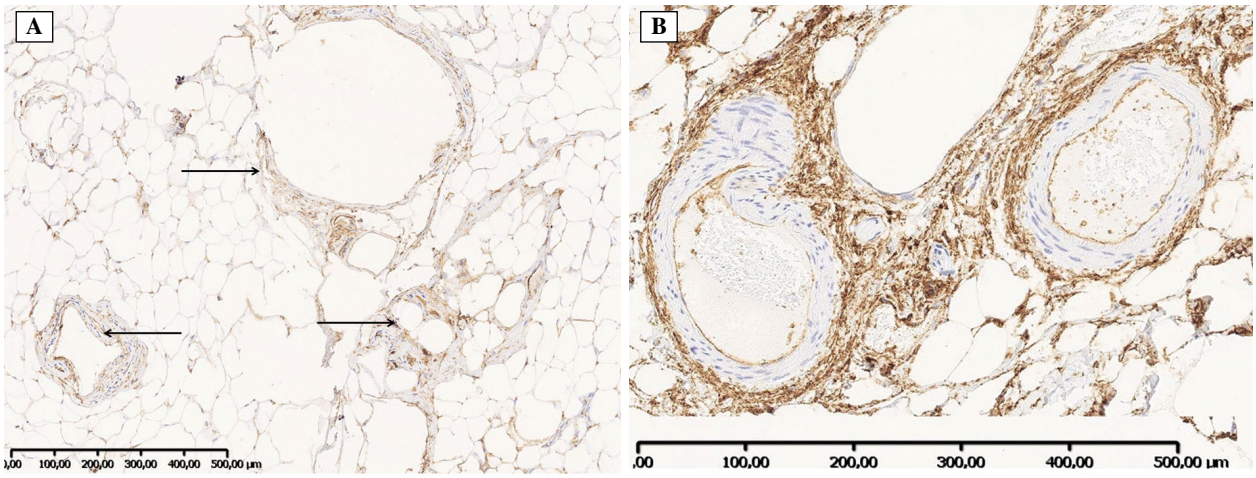

Figure 1A–B. The expression of CD34 in fibroblasts of orbit connective tissue in mild Graves' orbitopathy (GO) **(A)** and severe GO **(B).** The immunohistochemical (IHC) staining was performed as described in Methods. Arrowheads indicate immunoreactivity.

Table 2. The descriptive statistics of evaluated score for immunohistochemical staining of the respective antigens in control and Graves' orbitopathy (GO) patients with mild and severe disease activity. The p-value presented in the Kruskal-Wallis test column is a comparison of the given sub-group with the control group

Antigen and disease activity	n	Mean	SD	Median	Min	Max	Q1	Q3	p (Kruskal-Wallis)
IGF-1R, severe GO	22	1.9	0.4	2.0	1.0	2.0	2.0	20.	p = 0.0000
IGF-1R mild GO	9	0.9	0.6	1.0	0.0	2.0	1.0	1.0	p = 0.0000
IGF-1R control	10	0.0	0.0	0.0	0.0	0.0	0.0	0.0	
CD34 severe GO	22	1.8	0.4	2.0	1.0	2.0	2.0	2.0	p = 0.0000
CD34 mild GO	9	1.0	0.0	1.0	1.0	1.0	1.0	1.0	p = 0.0000
CD34 contr.	10	0.2	0.4	0.0	0.0	1.0	0.0	0.0	
Foxp-3 severe GO	22	1.5	0.7	2.0	0.0	2.0	1.0	2.0	p = 0.0351
Foxp-3 mild GO	9	1.0	0.0	1.0	1.0	1.0	1.0	1.0	p = 0.0351
Foxp-3 contr.	10	1.5	0.5	1.5	1.0	2.0	1.0	2.0	
PPAR-γ severe GO	22	1.4	0.5	1.0	1.0	2.0	1.0	2.0	p = 0.3213
PPAR-γ mild GO	9	1.2	0.4	1.0	1.0	2.0	1.0	1.0	p = 0.3213
PPAR-γ contr.	10	1.5	0.7	2.0	0.0	2.0	1.0	2.0	

was found in OF in connective tissue and surrounding the blood vessels in GO specimen (Fig. 1D–E). ~77% of mild GO cases were evaluated as + while in case of patients with severe GO ~77% of the orbital tissue were scored as ++ (Table 2 and Table 3).

PPAR-γ expression

PPAR-γ expression was also found in OF in orbital connective tissue of control and GO patients (Fig. 1F–G). 60% of the orbital tissues from the control group showed a positive staining estimated as ++, while 30% were scored as + and 10% as negative (Table 2). Within the mild GO subgroup ~78% of the orbital tissues were scored as + and ~22% as ++ (Table 2). Orbital tissues from the severe GO group were scored as + in ~64% of the cases and the remaining 36% were scored as ++ (Table 2 and Table 3).

Correlation of IGF-1R and CD34 with CAS

Using the Spearman's rank correlation we found that IGF-1R expression was positively and strongly correlated with CAS (R= 0.6521, p = 0.00007) in the whole group of GO patients. CD34 expression also correlated positively with CAS in the total GO (p = 0.03). However,

Table 3. Number of patients and the percentage of IGF-1R, CD34, Foxp-3 and PPAR-γ expression within scores 0 (-), 1 (+), and 2 (++) in the examined groups of control subjects and Graves' orbitopathy patients

IGF-1R expression	Control	Mild GO	Severe GO	Sum
0	**10** (100%)	**1** (11.1%)	**0**	11
1	**0**	**7** (77.8%)	**5** (22.7%)	12
2	**0**	**1** (11.1%)	**17** (77.3%)	18
CD34 expression	**Control**	**Mild GO**	**Severe GO**	**Sum**
0	**8** (80.0%)	**0**	**0**	8
1	**2** (20.0%)	**9** (100%)	**5** (22.7%)	16
2	**0**	**0**	**17** (77.3%)	17
Foxp-3 expression	**Control**	**Mild GO**	**Severe GO**	**Sum**
0	**0**	**0**	**2** (9.1%)	2
1	**5** (50%)	**9** (100%)	**7** (31.8%)	21
2	**5** (50%)	**0**	**13** (59.1%)	18
PPAR-γ expression	**Control**	**Mild GO**	**Severe GO**	**Sum**
0	**1** (10%)	**0**	**0**	1
1	**3** (30%)	**7** (77.8%)	**14** (63.7%)	24
2	**6** (60%)	**2** (22.2%)	**8** (36.4%)	16

Immunohistochemistry score: 0 — less than 10% positive in 15 representative high power fields (HPF); 1 — 10%–50% positive cells in 15 HPF; 2 — more than 50% positive cells in 15 HPF.

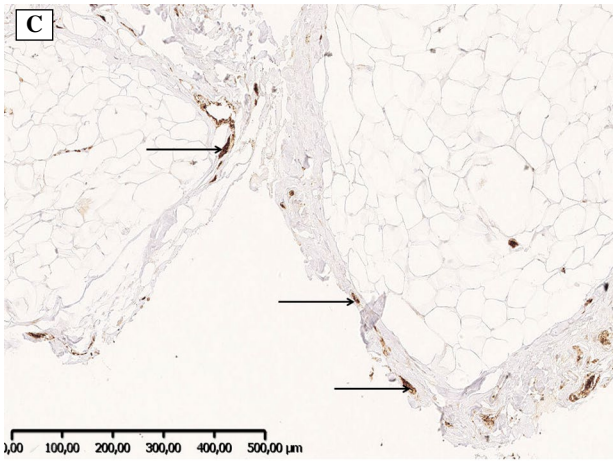

Figure 1C. The expression of FoxP3 on lymphocytes surrounding blood vessels within orbital connective tissue in Graves' orbitopathy (arrows). The IHC staining was performed as described in Methods.

neither Foxp-3 nor PPAR-γ expression showed any correlation with CAS of GO patients (Table 4).

Correlation with CD4, CD68, FGF-β and TGF-β

In addition, using the Spearman's rank correlation we examined the relationship between the expression of

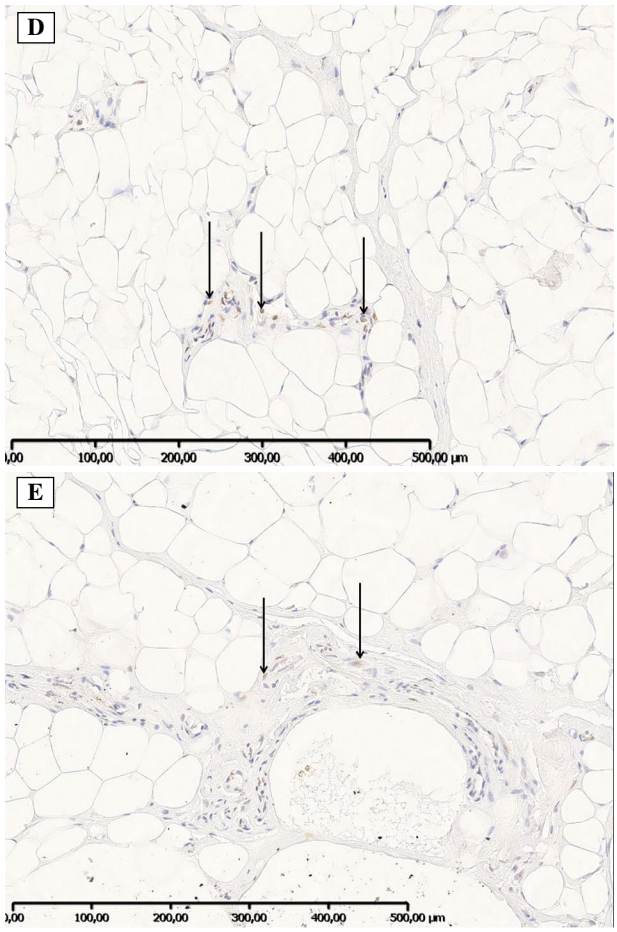

Figure 1D–E. IGF-IR immunoreactivity (arrows) in fibroblasts of orbital connective tissue obtained from patients with mild GO (**D**) and severe GO (**E**). The IHC staining was performed as described in Methods.

IGF-1R or CD34 with immunohistochemical staining analysis for CD4, CD68, FGF-β and TGF-β which had been conducted on the same orbital tissues in one of our previous studies [13]. A positive correlation was found between IGF-1R or CD34 and all parameters, when GO cases were considered without further subdivision into mild and severe subgroups (Table 5). In mild GO a statistical significant correlation was observed between the expression of CD34 and CD4, CD68, TGF-β or FGF-β. Further, a clear trend towards a positive correlation was observed between the expression of CD34 and TGF-β in severe GO ($p = 0.07613$). IGF-1R expression only revealed positive and significant correlations with FGF-β in mild GO and with CD4 in severe GO (Table 5).

Discussion

In GO the ongoing inflammatory process in the retrobulbar tissue results in adipogenesis, volume increase

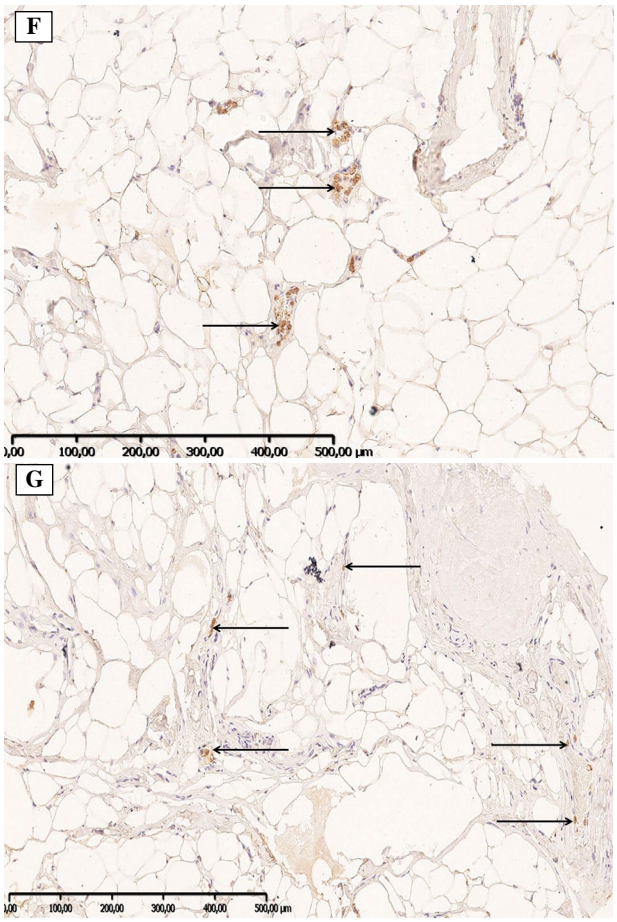

Figure 1F–G. PPAR-γ immunoreactivity expression in fibroblasts of orbital connective tissue in mild GO (**F**) and severe GO (**G**). The IHC staining was performed as described in Methods.

Table 4. Spearman's correlation of clinical activity score (CAS) values with examined parameters in patients with Grave's orbitopathy

	CAS	
	R value	**P value**
IGF-1R expression	0.6521	0.00007
CD34 expression	0.3872	0.03127
Foxp-3 expression	0.2948	0.10738
PPAR-γ expression	0.1384	0.45664

of the orbital adipose-connective tissue and, in the end, remodeling characterized by fibrosis. These processes encompass both changes in cellular composition and extracellular matrix within the orbital tissue, which are controlled by stimulatory factors such as growth factors and cytokines released by infiltrating immune cells [2, 18, 19].

Table 5. Spearman's rank correlations of CD4, CD68, FGF-β and TGF-β with IGF-1R or CD34 expression without dividing into groups and within mild and severe Grave's orbitopathy (GO)

	Without dividing into groups (n = 31)			
	R value		**P value**	
	CD4 expression			
IGF-1R expression	0.6277		0.00001	
CD34 expression	0.5334		0.00033	
	CD68 expression			
IGF-1R expression	0.5445		0.00016	
CD34 expression	0.4442		0.00361	
	FGF-β expression			
IGF-1R expression	0.6455		0.00000	
CD34 expression	0.5330		0.00033	
	TGF-β expression			
IGF-1R expression	0.7989		0.00000	
CD34 expression	0.6369		0.00001	
	Mild GO (n = 9)		**Severe GO (n = 22)**	
	R value	**P value**	**R value**	**P value**
	CD4 expression			
IGF-1R expression	0.6754	0.2237	0.5587	0.00846
CD34 expression	0.5334	0.00033	0.0925	0.1476
	CD68 expression			
IGF-1R expression	0.3487	0.1876	0.0654	0.3256
CD34 expression	0.4442	0.00361	0.2421	0.5421
	FGF-β expression			
IGF-1R expression	-0.7043	0.02298	0.6054	0.2877
CD34 expression	0.5330	0.02298	0.4334	0.1233
	TGF-β expression			
IGF-1R expression	0.7155	0.0928	0.1054	0.2227
CD34 expression	0.6369	0.00001	–0.3953	0.07613

Tsui *et al.* suggested that cross-talk between the TSH and IGF-1 receptors plays a role in GO pathogenesis [10], which has been further supported by findings of numerous other scientific groups [7, 9, 20]. Interestingly, IGF-1 promotes cell proliferation and lipid accumulation within orbital adipose tissue-derived stromal cells from patients with GO [11]. Recently we revealed that IGF-1 stimulation of peripheral blood mononuclear cells (PBMC) derived from GO patients resulted in significant increase of Treg frequency, thus demonstrating Treg-enhancing effects of IGF-1 [21]. This effect of IGF-1 may also impact Treg numbers locally within the orbital tissue

from GO and therefore we compared the expression pattern of the IGF-1R with that of Foxp-3 in this current study. We demonstrated the medium Foxp-3 expression (11% to 50% positive cells) in all orbital tissues from patients with mild GO, whereas in severe GO majority of patients (~59% of cases revealed a staining pattern of ≥ 50% positive cells). It could suggest that orbital accumulation of Foxp-3 could suppress CD4+ mediated inflammatory process in mild GO more than in severe GO and it might be not sufficient in overcoming severe GO.

In accordance, Kahaly *et al*. observed that peripheral blood T-cells from GO patients more strongly upregulated Foxp-3 and CD25 upon stimulation with rabbit anti-T-lymphocyte globulin (rATG) than T-cells from patients with Graves' disease without orbital involvement as well as healthy controls [22]. In addition, recently Bilbao *et al*. found that human IGF-1 stimulates proliferation of Tregs [23]. Thus, Tregs as immunosuppressive cells, generally suppress or downregulate induction and proliferation of effector T cells, maintaining tolerance to self-antigens and preventing autoimmune reactions [24]. Therefore, within GO orbital tissue Tregs might be upregulated by IGF-1R stimulation.

Recent research has found that the cytokine TGF-β is essential for Tregs to differentiate from naïve CD4+ cells and is important in maintaining Treg homeostasis [25]. The overexpression of this protein induces the differentiation and expansion of Tregs [11]. The relationship between the disease duration, as in patients with mild GO, and TGF-β secretion was demonstrated in our previous studies [18]. Moreover, previously we found enhanced Foxp-3 mRNA expression in GO orbital tissue which correlated with CD3 expression and serum CRP levels suggesting its involvement in the pathogenesis of severe GO [15]. In accordance, Chen *et al*. showed that IGF-1R inhibition diminished trafficking of CD4+ T cells as well as IGF-1 actions in fibroblasts [26]. Moreover, Frostad *et al*. found that IGF-1 has a costimulatory effect on proliferation of progenitors derived from human umbilical cord CD34+ cells [27]. In the context of these studies we have demonstrated the significant correlation between IGF-1R and CD4 expression in patients with severe GO confirming the assumption about the positive relationship between them.

Previous papers suggested, that IGF-1R signaling may accelerate severity of GO which may be related to its enhanced expression by orbital fibroblasts and T-lymphocytes from GO patients. The production of T-cell chemoattractants, hyaluronan and adipogenesis by orbital fibroblasts/stromal cells upon IGF-1R activation and the role of circulating stimulatory IGF-1R autoantibodies (IGF1R-Abs), however controversial [28]), were also detected [11, 29, 30]. Notwithstanding, Bilbao *et al*. demonstrated that IGF-1 directly targets human and mouse Tregs thereby stimulating their proliferation. In addition, they demonstrated that systemically delivered IGF-1 suppressed autoimmune symptoms in mouse models of multiple sclerosis and type-1 diabetes, which involved local Treg recruitment and modulation of Treg transcriptome [23]. Moreover, Zhao *et al*. claimed that the IGF-1/IGF-1R axis represents a pro-proliferative and pro-adipogenic pathway in orbital tissue from GO [11]. Indeed, our results indicate that elevated IGF-1R expression may exert an important role in the pathogenesis of severe GO, as orbital tissue from most severe GO patients (~77% of cases) revealed robust staining for IGF-1R (≥ 50% positive cells) whereas in mild GO the expression of IGF-1R was far less pronounced (78% revealed a staining pattern of between 11% and 50% positive cells). Moreover the negative correlation between IGF-1R and FGF-1β in mild GO could suggest that the pro-proliferative and pro-fibroblastic (pro-adipogenic) properties of IGF-1R stimulation may be milder or altered in this GO group. Yet, to elucidate the exact contribution of orbital IGF-1R expression in GO further studies are required.

The signaling pathways of adipogenesis have been shown to involve both TSH-R and IGF-1R and it appears both TSH-R and IGF-1R share the same intracellular AKT/PI3K signaling to affect adipogenesis probably by co-localization of these two receptors on orbital fibroblasts [8]. In addition, PPAR-γ involved in adipocyte differentiation, lipid metabolism and inflammation is a potent stimulator for adipogenesis in GO as well. Recently, Alevizaki *et al.* observed that the distribution of the Pro(12)Ala PPAR-γ gene polymorphism is equally present in patients with GD with or without GO [31]. However, among patients with GO this polymorphism is associated with less-severe and less-active disease. Alevizaki *et al.* concluded that the PPAR-γ gene does not seem to be involved in the predisposition for GO. Interestingly, Zhao *et al.* demonstrated that activation of IGF-1R and PI3K signaling pathways resulted in PPAR-γ up-regulation in adipose tissue-derived stromal cells [11]. Yet, in our experiments we did not find any significant relation between PPAR-γ and the other molecules studied. However, the steroid treatment our patients received may have hampered PPAR-γ expression in both groups of GO analyzed. Nevertheless, comparison of PPAR-γ staining in patients with mild GO *versus* severe GO revealed that more mild long lasting cases had a score 1 (~78% of cases) than severe active cases (~63% of cases), suggestive of its role in a long term tissue remodeling and less-active disease.

Recently, CD34+ fibrocytes were found to express functional TSH receptor, the central antigen in GD [4, 6, 32]. Kozdon *et al.* observed that CD34 protein was expressed by 45% up to 70% of the GO orbital fibroblasts [33]. Furthermore, CD4+ T cells secrete cytokines that stimulate the production of mucopolysaccharides by orbital fibroblasts, which contributes to edema in the extraocular muscles [33]. In orbital tissue from mild GO we found a positive correlation between CD34 expressing cells and CD4+ T-cell and macrophage (CD68+) infiltration. Furthermore, the positive relationship of CD34+ cells with TGF-β and FGF-β expression in longer-lasting GO, suggest that T cells and macrophages may mediate an immune response stimulating orbital fibroblasts, consequently CD34+ cells may thus exhibit a key role in orbital tissue remodeling in these patients [18]. Despite the increased expression of IGF-1R, CD34 and Foxp-3 in both mild and severe GO we observed a positive correlation between IGF-1R, CD34 and CAS coefficient, which may indicate that these molecules are expressed at higher level in patients with acute disease.

In conclusion, our observations support involvement of the IGF-1 receptor, Foxp-3 expressing Tregs, and CD34+ expressing cells (fibroblasts/fibrocytes) in the development of both mild and severe GO. Fibrosis in mild GO is associated with TGF-β and FGF-β expression, which is mediated by helper T cells and macrophages and correlates with CD34 expression. Thus, due to the multidirectional relationship with other molecules and factors, CD34 expression rather than IGF-1R or Foxp-3 is proposed to represent a marker of orbital tissue remodeling in the course of GO.

Declaration of interest

The authors report no conflicts of interest. The authors alone are responsible for the content and writing of the article.

Funding

This research was supported by a grant of Medical University of Bialystok grant no. N/ST/ZB/16/003/1194.

References

1. Wang Y, Smith TJ. Current concepts in the molecular pathogenesis of thyroid-associated ophthalmopathy. Invest Ophthalmol Vis Sci. 2014; 55(3): 1735–1748, doi: 10.1167/iovs.14-14002, indexed in Pubmed: 24651704.
2. Smith T, Hegedüs L. Graves' Disease. New England Journal of Medicine. 2016; 375(16): 1552–1565, doi: 10.1056/nejmra1510030.
3. Douglas RS, Afifiyan NF, Hwang CJ, et al. Increased generation of fibrocytes in thyroid-associated ophthalmopathy. J Clin Endocrinol Metab. 2010; 95(1): 430–438, doi: 10.1210/jc.2009-1614, indexed in Pubmed: 19897675.
4. Smith TJ, Padovani-Claudio DA, Lu Y, et al. Fibroblasts expressing the thyrotropin receptor overarch thyroid and orbit in Graves' disease. J Clin Endocrinol Metab. 2011; 96(12): 3827–3837, doi: 10.1210/jc.2011-1249, indexed in Pubmed: 21956421.
5. Li He, Fitchett C, Kozdon K, et al. Independent adipogenic and contractile properties of fibroblasts in Graves' orbitopathy: an in vitro model for the evaluation of treatments. PLoS One. 2014; 9(4): e95586, doi: 10.1371/journal.pone.0095586, indexed in Pubmed: 24751986.
6. Gillespie EF, Papageorgiou KI, Fernando R, et al. Increased expression of TSH receptor by fibrocytes in thyroid-associated ophthalmopathy leads to chemokine production. J Clin Endocrinol Metab. 2012; 97(5): E740–E746, doi: 10.1210/jc.2011-2514, indexed in Pubmed: 22399514.
7. Krieger CC, Place RF, Bevilacqua C, et al. TSH/IGF-1 receptor cross talk in graves' ophthalmopathy pathogenesis. J Clin Endocrinol Metab. 2016; 101(6): 2340–2347, doi: 10.1210/jc.2016-1315, indexed in Pubmed: 27043163.
8. Khong JJ, McNab AA, Ebeling PR, et al. Pathogenesis of thyroid eye disease: review and update on molecular mechanisms. Br J Ophthalmol. 2016; 100(1): 142–150, doi: 10.1136/bjophthalmol-2015-307399, indexed in Pubmed: 26567024.
9. Wiersinga WM. Autoimmunity in Graves' ophthalmopathy: the result of an unfortunate marriage between TSH receptors and IGF-1 receptors? J Clin Endocrinol Metab. 2011; 96(8): 2386–2394, doi: 10.1210/jc.2011-0307, indexed in Pubmed: 21677036.
10. Tsui S, Naik V, Hoa N, et al. Evidence for an association between thyroid-stimulating hormone and insulin-like growth factor 1 receptors: a tale of two antigens implicated in Graves' disease. J Immunol. 2008; 181(6): 4397–4405, doi: 10.4049/jimmunol.181.6.4397, indexed in Pubmed: 18768899.
11. Zhao P, Deng Y, Gu P, et al. Insulin-like growth factor 1 promotes the proliferation and adipogenesis of orbital adipose-derived stromal cells in thyroid-associated ophthalmopathy. Exp Eye Res. 2013; 107: 65–73, doi: 10.1016/j.exer.2012.11.014, indexed in Pubmed: 23219871.
12. Sakaguchi S. Regulatory T cells: history and perspective. Methods Mol Biol. 2011; 707: 3–17, doi: 10.1007/978-1-61737-979-6_1, indexed in Pubmed: 21287325.
13. Klatka M, Grywalska E, Partyka M, et al. Th17 and Treg cells in adolescents with Graves' disease. Impact of treatment with methimazole on these cell subsets. Autoimmunity. 2014; 47(3): 201–211, doi: 10.3109/08916934.2013.879862, indexed in Pubmed: 24443787.
14. Ban Y, Tozaki T, Tobe T, et al. The regulatory T cell gene FOXP3 and genetic susceptibility to thyroid autoimmunity: an association analysis in Caucasian and Japanese cohorts. J Autoimmun. 2007; 28(4): 201–207, doi: 10.1016/j.jaut.2007.02.016, indexed in Pubmed: 17418529.
15. Pawlowski P, Wawrusiewicz-Kurylonek N, Eckstein A, et al. Disturbances of modulating molecules (FOXP3, CTLA-4/CD28/B7, and CD40/CD40L) mRNA expressions in the orbital tissue from patients with severe graves' ophthalmopathy. Mediators Inflamm. 2015; 2015: 340934, doi: 10.1155/2015/340934, indexed in Pubmed: 25653477.
16. Bartalena L, Baldeschi L, Boboridis K, et al. European Group on Graves' Orbitopathy (EUGOGO). The 2016 European Thyroid Association/European Group on Graves' Orbitopathy Guidelines for the Management of Graves' Orbitopathy. Eur Thyroid J. 2016; 5(1): 9–26, doi: 10.1159/000443828, indexed in Pubmed: 27099835.
17. Mourits MP, Prummel MF, Wiersinga WM, et al. Clinical activity score as a guide in the management of patients with

Graves' ophthalmopathy. Clin Endocrinol (Oxf). 1997; 47(1): 9–14, doi: 10.1046/j.1365-2265.1997.2331047.x, indexed in Pubmed: 9302365.
18. Pawlowski P, Reszec J, Eckstein A, et al. Markers of inflammation and fibrosis in the orbital fat/connective tissue of patients with Graves' orbitopathy: clinical implications. Mediators Inflamm. 2014; 2014: 412158, doi: 10.1155/2014/412158, indexed in Pubmed: 25309050.
19. Dik WA, Virakul S, van Steensel L. Current perspectives on the role of orbital fibroblasts in the pathogenesis of Graves' ophthalmopathy. Exp Eye Res. 2016; 142: 83–91, doi: 10.1016/j.exer.2015.02.007, indexed in Pubmed: 26675405.
20. Smith TJ, Hegedüs L, Douglas RS. Role of insulin-like growth factor-1 (IGF-1) pathway in the pathogenesis of Graves' orbitopathy. Best Pract Res Clin Endocrinol Metab. 2012; 26(3): 291–302, doi: 10.1016/j.beem.2011.10.002, indexed in Pubmed: 22632366.
21. Pawlowski P, Grubczak K, Kostecki J, et al. Decreased Frequencies of Peripheral Blood CD4+CD25+CD127-Foxp3+ in Patients with Graves' Disease and Graves' Orbitopathy: Enhancing Effect of Insulin Growth Factor-1 on Treg Cells. Horm Metab Res. 2017; 49(3): 185–191, doi: 10.1055/s-0042-122780, indexed in Pubmed: 28222462.
22. Kahaly GJ, Shimony O, Gellman YN, et al. Regulatory T-cells in Graves' orbitopathy: baseline findings and immunomodulation by anti-T lymphocyte globulin. J Clin Endocrinol Metab. 2011; 96(2): 422–429, doi: 10.1210/jc.2010-1424, indexed in Pubmed: 21147887.
23. Bilbao D, Luciani L, Johannesson B, et al. Insulin-like growth factor-1 stimulates regulatory T cells and suppresses autoimmune disease. EMBO Mol Med. 2014; 6(11): 1423–1435, doi: 10.15252/emmm.201303376, indexed in Pubmed: 25339185.
24. Bettelli E, Carrier Y, Gao W, et al. Reciprocal developmental pathways for the generation of pathogenic effector TH17 and regulatory T cells. Nature. 2006; 441(7090): 235–238, doi: 10.1038/nature04753, indexed in Pubmed: 16648838.
25. Schmidt, A., Éliás, S., Joshi, R. N., & Tegnér, J. . In vitro differentiation of human CD4+ FOXP3+ induced regulatory T cells (iTregs) from naïve CD4+ T cells using a TGF-β-containing protocol. J Visual Exp. 2016; 118: e55015.
26. Chen H, Mester T, Raychaudhuri N, et al. Teprotumumab, an IGF-1R blocking monoclonal antibody inhibits TSH and IGF-1 action in fibrocytes. J Clin Endocrinol Metab. 2014; 99(9): E1635–E1640, doi: 10.1210/jc.2014-1580, indexed in Pubmed: 24878056.
27. Frostad S, Bjerknes R, Abrahamsen JF, et al. Insulin-like growth factor-1 (IGF-1) has a costimulatory effect on proliferation of committed progenitors derived from human umbilical cord CD34+ cells. Stem Cells. 1998; 16(5): 334–342, doi: 10.1002/stem.160334, indexed in Pubmed: 9766813.
28. Minich WB, Dehina N, Welsink T, et al. Autoantibodies to the IGF1 receptor in Graves' orbitopathy. J Clin Endocrinol Metab. 2013; 98(2): 752–760, doi: 10.1210/jc.2012-1771, indexed in Pubmed: 23264397.
29. Douglas RS, Gianoukakis AG, Kamat S, et al. Aberrant expression of the insulin-like growth factor-1 receptor by T cells from patients with Graves' disease may carry functional consequences for disease pathogenesis. J Immunol. 2007; 178(5): 3281–3287, doi: 10.4049/jimmunol.178.5.3281, indexed in Pubmed: 17312178.
30. Varewijck AJ, Boelen A, Lamberts SWJ, et al. Circulating IgGs may modulate IGF-I receptor stimulating activity in a subset of patients with Graves' ophthalmopathy. J Clin Endocrinol Metab. 2013; 98(2): 769–776, doi: 10.1210/jc.2012-2270, indexed in Pubmed: 23295466.
31. Alevizaki M, Mantzou E, Cimponeriu A, et al. The Pro 12 Ala PPAR gamma gene polymorphism: possible modifier of the activity and severity of thyroid-associated orbitopathy (TAO). Clin Endocrinol (Oxf). 2009; 70(3): 464–468, doi: 10.1111/j.1365-2265.2008.03343.x, indexed in Pubmed: 18624999.
32. Smith TJ. TSH-receptor-expressing fibrocytes and thyroid-associated ophthalmopathy. Nat Rev Endocrinol. 2015; 11(3): 171–181, doi: 10.1038/nrendo.2014.226, indexed in Pubmed: 25560705.
33. Kozdon K, Fitchett C, Rose GE, et al. Mesenchymal stem cell-like properties of orbital fibroblasts in graves' orbitopathy. Invest Ophthalmol Vis Sci. 2015; 56(10): 5743–5750, doi: 10.1167/iovs.15-16580, indexed in Pubmed: 26325413.

Submitted: 24 October, 2018
Accepted after reviews: 26 February, 2020
Available as AoP: 16 March, 2020

FOLIA HISTOCHEMICA ET CYTOBIOLOGICA
Vol. 58, No. 1, 2020
pp. 46–53

ORIGINAL PAPER

VIA MEDICA

Study of DNA topoisomerase IIα expression in canine lymphomas and its potential role as a marker of sensitivity to anthracycline-based chemotherapy in dogs

Pawel Klimiuk[1], Wojciech Lopuszynski[2], Kamila Bulak[2], Anna Smiech[2], Adam Brzana[3]

[1]Veterinary Diagnostic Laboratory VetDiagnostyka, Lublin, Poland

[2]Sub-Department of Pathomorphology and Forensic Veterinary Medicine, Department and Clinic of Animal Internal Diseases, University of Life Sciences in Lublin, Poland

[3]Regional Veterinary Inspectorate in Opole, Regional Veterinary Laboratory, Opole, Poland

Abstract

Introduction. Canine lymphoma remains one of the most chemotherapy-responsive neoplasia in dogs. Many factors affect the prognosis in dogs treated for lymphoma, but indications for a specific treatment regimen in individual animals with lymphoma are poorly defined. Topoisomerase IIα (TOPIIα) is a key enzyme in DNA replication and a molecular target for TOPIIα inhibitors, including anthracyclines. The aim of this study was to determine the expression of TOPIIα in canine malignant lymphomas. The relationship between TOPIIα expression in canine lymphomas and potential sensitivity of neoplastic cells to anthracycline-based chemotherapy is discussed.

Materials and method. Samples of formalin-fixed paraffin-embedded lymph nodes from 47 dogs with different subtypes of non-Hodgkin's (34 B-cell and 13 T-cell) lymphoma were immunohistochemically labeled with anti-TOPIIα. The number of positive cells and the intensity of the reaction were taken into account in order to assess TOPIIα expression.

Results. TOPIIα expression was evident in all cases, although differences in the number of positive cells and intensity of the reaction were demonstrated between B-cell and T-cell lymphoma groups as well as within individual groups. Based on the established scoring system, in the B-cell lymphoma group statistically higher expression of TOPIIα was found compared to the T-cell lymphoma group ($P = 0.006$). In B-cell lymphoma group moderate (41.18%) and strong (32.35%) TOPIIα expression predominated, whereas among T-cell lymphoma group the majority were cases with a weak (46.15%) TOPIIα expression.

Conclusion. These preliminary results indicate that further studies are needed to determine the prognostic value of TOPIIα expression with regard to the sensitivity of canine B-cell lymphomas to anthracycline-based chemotherapy regimen. Nevertheless, this study indicates the possibility of choosing the appropriate treatment of canine lymphoma based on TOPIIα expression. *(Folia Histochemica et Cytobiologica 2020, Vol. 58, No. 1, 46–53)*

Key words: topoisomerase IIα; dog, lymphoma; immunohistochemistry; chemotherapy

Introduction

Nearly 90% of hematological malignancies and about 5–7% of all neoplasia in dogs are malignant lymphomas, in which chemotherapy is the treatment of choice [1–4]. The main diagnostic test for suspected lymphoma is cytopathological examination of fine needle aspirates collected from enlarged lymph nodes and, according to the WHO guidelines, histopathological examination of the surgically removed lymph node supplemented with

Correspondence address: Wojciech Lopuszynski, DVM PhD
Sub-Department of Pathomorphology
and Forensic Veterinary Medicine,
Department and Clinic of Animal Internal Diseases,
University of Life Sciences in Lublin, Poland
e-mail: wojciech.lopuszynski@up.lublin.pl

the immunophenotype assessment [5–8]. Canine lymphomas are very sensitive to chemotherapy, as evidenced by numerous studies which indicate that complete remission (CR) is obtained in about 65% to 98% of treated animals [9–16]. In some cases, the remission lasts up to 36 months [9]. Despite the availability of numerous therapy regimens, it is difficult to determine the prognosis, select the optimal treatment method and predict the response to the therapy in each individual patient [12, 17–19]. When selecting a therapy protocol, factors such as lymphoma immunophenotype, histological type and grade of malignancy as well as clinical stage are usually taken into consideration [20–24]. In many cases the response to the treatment regimen is not satisfactory due to the partial remission (PR) or rapid relapse, which implies the need to adjust the treatment protocol with other cytotoxic drugs [9, 10]. Due to the high cytotoxicity and side effects of drugs used in chemotherapy and the varied response to the treatment protocol, attempts are being made to implement individualized treatment. Targeted therapy aims to adapt the treatment regimen to the type of neoplasia as well as to the individual patient. The therapeutic effect of specific cytotoxic drug differs among individuals despite the same histological type of lymphoma [9, 10, 25–28]. Therefore, prognostic factors that allow the determination of a predictable response to the treatment protocol remain in the area of clinical interest. The potential predictive value of protein markers whose expression changes in the course of neoplastic transformation is of particular interest. One of such markers is DNA topoisomerase IIα (TOPIIα) belonging to the family of enzymes involved in DNA replication [29]. The TOPIIα function is associated with condensation and chromosome formation, reorganization of double-stranded DNA and segregation of newly formed chromosomes. TOPIIα expression is variable, associated with the phase of the cell cycle. TOPIIα expression increases in S phase, reaching peak in G2 and M phase, and then decreases at the end of mitosis (G1 phase). TOPIIα during the complicated 7-step process leads to the separation of two strands of DNA, allowing cell division [30–33]. The inhibition of the TOPIIα function results in permanent links between the DNA strands, and finally in blocking of transcription and replication. Cells with damaged DNA are eliminated by apoptosis [34–37]. TOPIIα is therefore a molecular target for antineoplastic drugs such as anthracyclines, which are TOPIIα inhibitors [38]. The most commonly used anthracycline drugs to treat lymphomas in dogs are doxorubicin and epirubicin [9, 16, 39, 40]. *In vivo* and *in vitro* studies carried out on neoplastic cell lines in humans have shown that the sensitivity of neoplastic cells to anthracycline drugs depends on TOPIIα cellular expression [25, 30, 34, 35, 41]. In addition, one study carried out on women with breast cancer treated with mastectomy followed by adjuvant anthracycline chemotherapy showed that the mortality rate was higher and the free survival time was shorter in patients with TOPIIα-negative tumors as compared to patients with a positive TOPIIα status [31]. A retrospective study on human B-cell lymphomas managed with anthracycline-based chemotherapy revealed that TOPIIα expression was significantly associated with the response to chemotherapy, but not to disease-free or overall survival [25]. In veterinary oncology, TOPIIα inhibitors are relatively widely used in various chemotherapy protocols with no data on the determination of TOPIIα expression levels in canine lymphomas. The aim of the study was to determine the expression of TOPIIα in malignant lymphomas in dogs in relation to the potential sensitivity of neoplastic cells to anthracycline-based chemotherapy.

Material and methods

Animals and design of the study. Dogs of different sex and different age with a suspect of multicentric lymphoma based on clinical symptoms, chest x-rays, abdominal ultrasound, fine needle aspiration biopsy and laboratory tests were considered for inclusion. The studied material consisted of samples of enlarged canine popliteal lymph nodes. Forty-seven samples of lymph nodes were ultimately included upon the histopathological confirmation of lymphoma (stage III and IV according to WHO Clinical Staging System for Lymphosarcoma in Domestic Animals). The animals were not treated with chemotherapy or steroids prior to collection of the lymph nodes. The study design was approved by the local ethics committee.

Histopathological examination. Surgically removed lymph nodes were fixed for 24 hours in 10% formalin, pH = 7.2, and then carried out by alcohol solutions, acetone and xylene to paraffin blocks in a tissue processor (Leica TP-1020). Four μm thick tissue sections were stained with hematoxylin and eosin. The morphological evaluation of stained tissue sections was based on WHO classification criteria [6].

Immunohistochemical evaluation. To determine the lymphoma immunophenotype and to evaluate TOPIIα expression, tissue sections were applied to Super Frost slides (Menzel-Glaser) and then incubated at 56°C for 12 hours. Tissue sections were dewaxed in xylene and then carried out by decreasing concentrations of alcohols to distilled water. Tissue sections were then immersed in a 0.3% hydrogen peroxide solution for 15 minutes to block endogenous peroxidase. Incubation with primary antibodies was carried out at 37°C in a humidity chamber for 60 minutes. The following primary antibodies were used in the study: polyclonal rabbit anti-CD3 (Dako, Glostrup, Denmark) diluted 1:300; monoclonal mouse anti-CD79α clone HM57 (Dako, Glostrup, Denmark) diluted 1:100, and mono-

clonal mouse anti-topoisomerase IIα clone Ki-S1 (Dako Glostrup, Denmark) diluted 1:200. Heat-induced antigen retrieval was performed in a specific buffer with proper pH, followed by cooling for 20 min at room temperature. For immunohistochemical examination, a system for detection of antigen-antibody complexes was used based on secondary antibodies conjugated with biotin directed against primary antibodies (HRP, K0690, Dako, Glostrup, Denmark). The enzyme labeling the reaction site was horseradish peroxidase conjugated with streptavidin and tetrahydrochloride-3'-3-diaminobenzidine (DAB) used as a chromogen (SK-4100, Vector Laboratories, Peterborough, UK). Tissue sections were counterstained with Mayers' hematoxylin and covered with PERTEX (Histolab). In all immunohistochemical reactions, a double-control system was used: a negative control in which the incubation with the primary antibody was replaced with appropriate IgG sera and a positive control in which the incubation was carried out on palatine tonsil tissue for CD3 and CD79α and human breast ductal carcinoma for TOPIIα with a proven positive reaction with the given antibody. Determination of lymphoma immunophenotype was performed by estimating the expression of CD3 and CD79α (membrane and cytoplasmic reaction) in tissue sections. The histogenesis of lymphomas was defined as T-cell lymphomas with dominant CD3 expression and B-cell lymphomas with dominant CD79α expression. A computer-assisted microscopic image analysis system was used to quantify the expression of TOPIIα. The system included: a light microscope (Nikon Eclipse E-600, Nikon Instruments, Tokyo, Japan) coupled with a digital camera (Nikon DS-Fi1, Nikon Instruments) and a personal computer (PC) with image analysis software (NIS-Elements BR-2.20, Laboratory Imaging, Praha, Czech Republic). The evaluation of TOPIIβ expression was performed by two independent pathologists based on analysis of at least 500 cells in different fields of view at a magnification of 400 ×. According to the scoring system proposed by Remmele *et al*. for estrogen receptors, the number of cells with a positive reaction was estimated, where 0 = no positive cells, 1 = ≤ 25% positive cells, 2 = 26–50% positive cells, 3 = 51–75% positive cells, 4 = more than 75% positive cells, and the reaction intensity was evaluated, where 0 — no reaction, 1 — mild reaction, 2 — moderate reaction, 3 — intense reaction [42]. The final result was the product of the parameters (percentage of positive cells × colored reaction intensity). Based on the obtained number of points and the criteria proposed by Hajduk *et al*. the expression intensity of TOPIIα was determined, where 0–1 meant no expression (–), 2–3 meant weak (+), 4–8 moderate (++), and 9–12 strong (+++) expression of TOPIIα [31].

Statistical analysis. The obtained results were subjected to statistical analysis. The levels of TOPIIα expression between B-cell and T-cell lymphoma groups and between individual subtypes were compared using the Mann-Whitney U test. The minimum level of significance was set at $P < 0.05$. Statistical analysis was carried out using STATISTICA v 9.1 (StatSoft, Poland).

Table 1. Morphological characterization of canine lymphomas in the studied group

Type and subtype of lymphoma	No. of cases	Percentage (%)
B-cell	34	72.34
Diffuse Large B-cell (DLBCL)	26	55.32
Burkitt-type	5	10.63
Marginal zone	3	6.38
T-cell	13	27.66
T-cell not otherwise specified	9	19.15
Nodal T-zone	2	4.26
Lymphoblastic	2	4.26
Total	47	100.00

Results

The age of dogs ranged from 4 to 14 years (average age 7 years). There were 23 female dogs (49%) and 24 male dogs (51%). The studied population consisted of purebred dogs with 38 individuals (80.85%), and among them the most numerous were German Shepherds (17%) and boxers (14.9%). Mixed-breed dogs constituted 19.15% of the studied population.

On the basis of immunohistochemical examination 34 (72.34%) B-cell lymphomas and 13 (27.66%) T-cell lymphomas were diagnosed (Table 1). The following subtypes of lymphoma were recognized: diffuse large B-cell lymphoma (DLBCL) in 26 of all cases (55.32%), Burkitt-type lymphoma — in 5 of all cases (10.63%), marginal zone B-cell lymphoma — in 3 of all cases (6.38%), peripheral T-cell lymphoma not otherwise specified (PTCL) — in 9 of all cases (19.15%), nodal T-zone lymphoma (TZL) — in 2 of all cases (4.26%), and lymphoblastic lymphoma (T-LBL) — in 2 of all cases (4.26%).

TOPIIα expression was evident in all cases with a diffuse granular nuclear pattern, although the variability in the reaction intensity and the number of positive cells were demonstrated (Fig. 1). Higher expression of TOPIIα was observed at the periphery of the examined lymph nodes, and a weaker reaction was obtained in the central areas of the lymph nodes. Based on the established TOPIIα expression scoring system, in the B-cell lymphoma group the most numerous were cases with moderate TOPIIα expression (14 cases, 41.18%), whereas in the T-cell lymphoma group, weak expression predominated (6 cases, 46.15%). B-cell lymphomas with strong TOPIIα expression included 11 cases

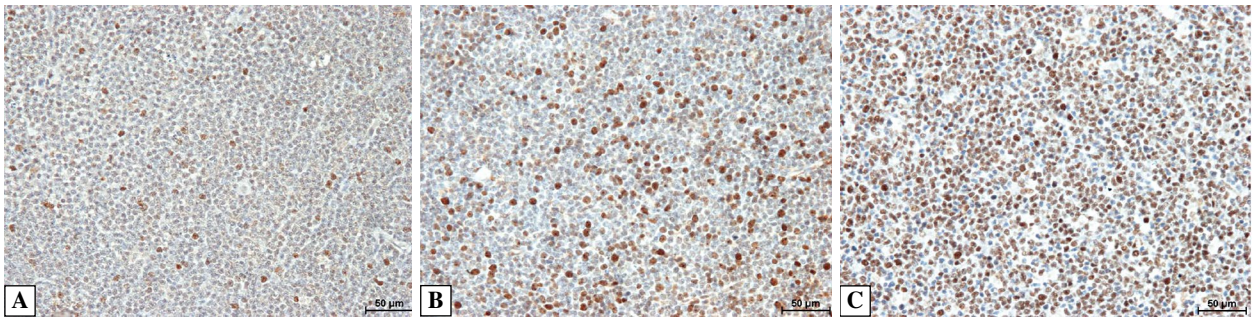

Figure 1. Diversity of TOPIIα expression in canine lymph nodes with diffuse large B-cell lymphoma. **(A)** weak expression (score 2–3), **(B)** moderate expression (score 4–8), **(C)** strong expression (score 9–12). Immunohistochemistry, anti-TOPIIα, clone Ki-S1, Mayer's hematoxylin counterstain. Bar = 50 μm.

Table 2. TOPIIα expression in the studied groups of canine lymphomas

TOPIIα expression	B-cell lymphoma (No. of cases = 34)	T-cell lymphoma (No. of cases = 13)
(–)	0 0.00%	2 15.38%
Weak (+)	9 26.47%	6 46.15%
Moderate (++)	14 41.18%	5 38.46%
Strong (+++)	11 32.35%	0 0.00%
	U = 107.0 P = 0.006	

(32.35%), while weak expression was found in 9 cases (26.47%). In the T-cell lymphoma group no cases with strong TOPIIα expression were found. Concurrently, in the B-cell lymphoma group no cases with lacking TOPIIα expression were recorded (Table 2). In the B-cell lymphoma group statistically higher expression of TOPIIα was found compared to the T-cell lymphoma group (P = 0.006). In all analyzed lymphoma subtypes there were differences in TOPIIα expression. The moderate and strong TOPIIα expression predominated in the most numerous subtype of DLBCL (Table 3). In the case of Burkitt-type lymphoma, strong or moderate expression was found in all cases, in the absence of weak-expression cases. In the PTCL group; however, cases with weak and moderate TOPIIα expression predominated, as in the case of TZL and T-LBL. Unfortunately, too few cases in particular subtypes made statistical analysis between lymphoma subtypes impossible.

Discussion

In this study conducted on a group of 47 dogs with non-Hodgkin's lymphomas, the majority were B-cell lymphomas, whereas T-cell lymphomas were less frequent, as confirmed by other literature data [6, 7, 16, 27, 43]. In the vast majority of cases (45 dogs), positive immunohistochemical reaction with varied intensity was observed. Only in 2 cases in the studied group the TOPIIα expression was lacking. Statistically

Table 3. Results of immunochistochemical assessment of TOPIIα in studied subtypes of B-cell and T-cell canine lymphomas

TOPIIα expression	B-cell lymphoma			T-cell lymphoma		
	DLBCL[a]	Burkitt-type	MZL[b]	PTCL[c]	TZL[d]	T-LBL[e]
No. of cases	26	5	3	9	2	2
No expression (–)	0 0.00%	0 0.00%	0 0.00%	1 11.11%	1 50.00%	0 0.00%
Weak (+)	7 26.92%	0 0.00%	2 66.67%	4 44.44%	1 50.00%	1 50.00%
Moderate (++)	11 42.31%	2 40.00%	1 33.33%	4 44.44%	0 0.00%	1 50.00%
Strong (+++)	8 30.77%	3 60.00%	0 0.00%	0 0.00%	0 0.00%	0 0.00%

[a]DLBCL — diffuse large B-cell lymphoma; [b]MZL — marginal zone B-cell lymphoma; [c]PTCL — peripheral T-cell lymphoma not otherwise specified; [d]TZL — nodal T-zone lymphoma; [e]T-LBL — T-cell lymphoblastic lymphoma

higher TOPIIα expression was demonstrated in the B-cell lymphoma group (P = 0.006) in which moderate (41.18%) and strong (32.35%) TOPIIα expression predominated, whereas among T-cell lymphomas the majority were lymphomas with a weak (46.15%) TOPIIα expression. The obtained results may indicate a potentially greater chemosensitivity of canine B-cell lymphomas to the action of TOPIIα inhibitors. Based on the literature data the use of TOPIIα inhibitors in dogs with B-cell lymphomas results in a better therapeutic effect and a longer-lasting remission compared to dogs with T-cell lymphomas. In the study of Beaver *et al*. the use of a single dose of doxorubicin in dogs with B-cell lymphoma resulted in a CR in 86% of dogs and a PR in 13.8% of dogs, whereas in dogs with T-cell lymphoma remission was obtained only in 50% of treated animals [27]. Similar dependencies have been demonstrated in other studies in which single or multi-drug protocols containing TOPIIα inhibitors were used [10, 11, 16, 23, 44–48]. In addition, differences in the response to different treatment protocols were observed in individual dogs with the B-cell or T-cell lymphoma. In one study, dogs with B-cell lymphoma treated with doxorubicin in combination with L-asparaginase and prednisone 71% of animals achieved CR while in 13% PR occurred. Remission time ranged from a few days to 414 days, and the total survival time ranged from several days to 566 days [9]. Study in dogs with T-cell lymphoma showed that 88% of dogs treated with the chemotherapy protocol consisted of cyclophosphamide, doxorubicin hydrochloride (hydroxydaunorubicin), vincristine sulfate (Oncovin), and prednisone (CHOP protocol) achieved CR, 8% of dogs had PR, and 4% of dogs had no response. Remission time ranged from 84 to 126 days, and the overall survival time varied from 167 to 244 days [11]. Similar differences in response to treatment using different protocols containing TOPIIα inhibitors in relation to various subtypes of B-cell and T-cell lymphomas have been demonstrated in other studies [12, 21, 26, 27, 49]. Our study revealed that both B-cell and T-cell lymphoma group showed differentiated TOPIIα expression. Noteworthy is also the fact that a weak expression of TOPIIα was found in 26.47% of B-cell lymphomas in our study. This study showed that cases of low TOPIIα expression and lack of TOPIIα expression were observed in specific lymphoma subtypes. In the case of DLBCL diagnosed in 26 dogs, the percentage of weak-expression cases was 26.92%, and in the case of PTCL diagnosed in 9 dogs, nearly half (44.44%) had weak expression. This may explain why some dogs with B-cell lymphoma do not respond or partially respond to TOPIIα inhibitors. It is worth mentioning that cytotoxic drugs can cause numerous side effects and in extreme cases can lead to the patient's death [16, 40, 44, 51]. Unfortunately, despite the use of numerous lymphoma classifications, it is currently not possible, based solely on histopathological examination and the lymphoma immunophenotype, to determine the most effective therapy for individual patient. Based on the histological malignancy grade and taking into account the clinical stage of the disease, the biological behavior of the lymphoma can be predicted with high probability, and thus the choice of therapeutic treatment can be made, while in some cases, the therapy may be discontinued. However, the updated Kiel classification for lymphomas does not answer the question whether the use of a specific cytotoxic drug within a selected scheme used for a specific type of lymphoma with respect to a particular patient will bring satisfactory results [22, 23, 50]. In many cases, the use of the same chemotherapy protocol in two different patients with the same histological type of lymphoma gave different treatment effects, with different periods of remission and survival time [9, 10, 19, 26, 27]. The diversity of TOPIIα expression in this study, despite the predominance of moderate to strong TOPIIα expression in B-cell lymphoma, does not show that the lymphoma immunophenotype and histological type are closely related to the level of TOPIIα expression.

There is currently growing interest in the potential prognostic value of markers that are the molecular target for cytotoxic drugs. One such marker is DNA topoisomerase IIα, whose inhibitors are cytotoxic drugs from the anthracycline group, including commonly used doxorubicin [30, 32]. Doxorubicin is one of the drugs included in the CHOP protocol considered the most effective treatment protocol in non-Hodgkin's lymphoma in dogs [18, 19, 27]. The second most commonly used scheme in the treatment of lymphoma is the COP protocol including prednisolone, cyclophosphamide and vincristine. It is assumed that the addition of doxorubicin to the treatment protocol increases its effectiveness, but this effect is observed only in individual dogs [19, 52]. An explanation for the observed differences in the effects of implemented treatment in clinical trials seems to be the diverse TOPIIα expression found in our study, both between B-cell and T-cell lymphoma group and their subtypes. In addition, the adverse reactions associated with the use of doxorubicin are observed. The most common is the cardiotoxicity that develops with long-term use and chemotherapy-induced myelotoxicity [14, 40, 51, 53]. The possibility of determining in which patients the use of doxorubicin would be beneficial and in which its use would not bring satisfactory results

seems to be crucial in choosing the optimal treatment protocol and minimizing the possibility of side effects.

Immunohistochemical studies on the predictive and prognostic value of TOPIIα expression have been conducted in human medicine [33, 36, 41]. Special interest among researchers was aroused by the expression of TOPIIα in breast cancer in women. The reason for this interest is the fact that one of the main drugs used in the treatment of breast cancer are anthracycline [30, 31]. A variable response was observed for its use in the treatment of women with the same histological type of breast cancer [31]. Immunohistochemical studies have shown different TOPIIα expression in various histological types of breast tumors and in the same histological types of breast cancer of different women [35]. Similar observations were also made in patients with various types of soft tissue sarcomas, testicular, ovarian, lung and gastric cancer [54–60]. Despite the widespread use of doxorubicin in the treatment of various types of neoplasia (including lymphomas) in animals, no preliminary studies have yet been conducted in veterinary medicine to assess the sensitivity of particular types of neoplasia to anthracyclins. There are also no literature reports describing TOPIIα expression in various types of neoplasia in dogs. In vitro and in vivo studies performed on human neoplastic cell lines showed that cells with higher TOPIIα expression exhibit greater sensitivity to anthracyclines, whereas cells with lower expression of TOPIIα have a significantly lower sensitivity [25, 34]. In clinical trials, human patients with breast cancer overexpressing TOPIIα showed a better response to treatment with anthracyclines than those with low TOPIIα expression [30, 31, 35]. In addition, in human medicine for the evaluation of the TOPIIα expression itself, attempts were made to determine the TOPIIα gene amplification and its correlation with the TOPIIα expression at the cellular level. Nevertheless, there is no unambiguous consensus between TOPIIα gene amplification and TOPIIα expression, which may indicate the existence of other mechanism than amplification that affect TOPIIα overexpression [30]. This may suggest that assessing TOPIIα expression in tissues is more useful than determining TOPIIα gene amplification.

In the conducted study, a human monoclonal antibody was used to assess TOPIIα expression and this antibody demonstrated cross-reactivity with a dog tissue. The author's original scoring system was used to assess the expression of TOPIIα, in which both the number of positive cells and the intensity of the reaction were taken into account. Doubts of many authors arouse the lack of a uniform pattern that allows objectively evaluate and interpret the expression of TOPIIα. The problem is to determine the so-called cut-off point where the expression of TOPIIα can be assessed as weak, moderate or strong. Most authors in human medicine determine the observed correlations between the expression of TOPIIα and the response to treatment with anthracyclines, without a measurable determination of the level of this expression. Hajduk *et al*. investigating the expression of TOPIIα in breast cancer cells assumed that the lack of expression is when the number of positive cells does not exceed 5%, weak 6–30%, moderate 31–60%, while strong expression is more than 60% of positive cells [31]. Pentheroudakis *et al*. in studies on TOPIIα expression in diffuse large B-cell lymphomas (DLBCL) in human patients, assessed that strong-expressive TOPIIα lymphomas are those in which positive cells account for more than 80% of all cells, the others (less than 80%) are lymphomas with weak expression of TOPIIα. In the study group, lymphomas with strong TOPIIα expression accounted for as much as 91% of all DLBCL [25]. In the study of Hajduk *et al.* a positive correlation was observed between the increase in TOPIIα expression and the increase in response to anthracycline treatment [31]. It is considered unreasonable to use anthracycline-based chemotherapy with weak TOPIIα expression. This means that the use of doxorubicin in dogs with weak TOPIIα expression may not bring noticeable therapeutic effects or may lead to a significant reduction in the effectiveness of therapy with other cytotoxic drugs leading to the increased risk of multidrug resistance in cells [1].

This study corresponds to the trend of research on prognostic factors in the chemotherapy of dogs with lymphoma [17, 61]. This is the first paper describing the importance and potential role of determining the TOPIIα expression in veterinary oncology. The study has been conducted in a small number of cases; however, given the mechanism of anti-tumor effects of TOPIIα inhibitors, it shows that immunohistochemical determination of TOPIIα expression might be helpful in the selection of the optimal treatment regimen for non-Hodgkin's lymphomas in dogs. However, further studies are needed to assess the relationship between TOPIIα expression and other prognostic factors, including the histological type, proliferation rate, grade and clinical stage of the disease. Clinical trials are also necessary to assess the correlation between TOPIIα expression and long-term clinical outcomes including the survival time and remission rates in animal patients treated with different chemotherapy protocols containing TOPIIα inhibitors.

References

1. Zandvliet M. Canine lymphoma: a review. Veterinary Quarterly. 2016; 36(2): 76–104, doi: 10.1080/01652176.2016.1152633.

2. Vail D, Pinkerton M, Young K. Hematopoietic tumours. In: Withrow SJ, Vail DM, Page RL, eds. Withrow & MacEwen's Small Animal Clinical Oncology. 5th ed. St Louis, MO: Elsevier; 2013: 608.
3. Brønden LB, Nielsen SS, Toft N, et al. Data from the Danish veterinary cancer registry on the occurrence and distribution of neoplasms in dogs in Denmark. Vet Rec. 2010; 166(19): 586–590, doi: 10.1136/vr.b4808, indexed in Pubmed: 20453236.
4. Merlo DF, Rossi L, Pellegrino C, et al. Cancer incidence in pet dogs: findings of the Animal Tumor Registry of Genoa, Italy. J Vet Intern Med. 2008; 22(4): 976–984, doi: 10.1111/j.1939-1676.2008.0133.x, indexed in Pubmed: 18564221.
5. Sapierzyński R, Kliczkowska-Klarowicz K, Jankowska U, et al. Cytodiagnostics of canine lymphomas - possibilities and limitations. Pol J Vet Sci. 2016; 19(2): 433–439, doi: 10.1515/pjvs-2016-0055, indexed in Pubmed: 27487521.
6. Valli VE, San Myint M, Barthel A, et al. Classification of canine malignant lymphomas according to the World Health Organization criteria. Vet Pathol. 2011; 48(1): 198–211, doi: 10.1177/0300985810379428, indexed in Pubmed: 20861499.
7. Ponce F, Marchal T, Magnol JP, et al. A morphological study of 608 cases of canine malignant lymphoma in France with a focus on comparative similarities between canine and human lymphoma morphology. Vet Pathol. 2010; 47(3): 414–433, doi: 10.1177/0300985810363902, indexed in Pubmed: 20472804.
8. Teske E, van Heerde P. Diagnostic value and reproducibility of fine-needle aspiration cytology in canine malignant lymphoma. Vet Q. 1996; 18(3): 112–115, doi: 10.1080/01652176.1996.9694630, indexed in Pubmed: 8903146.
9. Al-Nadaf S, Rebhun RB, Curran KM, et al. Retrospective analysis of doxorubicin and prednisone as first-line therapy for canine B-cell lymphoma. BMC Vet Res. 2018; 14(1): 356, doi: 10.1186/s12917-018-1688-5, indexed in Pubmed: 30458771.
10. Curran K, Thamm DH. Retrospective analysis for treatment of naïve canine multicentric lymphoma with a 15-week, maintenance-free CHOP protocol. Vet Comp Oncol. 2016; 14 Suppl 1: 147–155, doi: 10.1111/vco.12163, indexed in Pubmed: 26279153.
11. Rebhun RB, Kent MS, Borrofka SA, et al. CHOP chemotherapy for the treatment of canine multicentric T-cell lymphoma. Vet Comp Oncol. 2011; 9(1): 38–44, doi: 10.1111/j.1476-5829.2010.00230.x, indexed in Pubmed: 21303452.
12. Flory AB, Rassnick KM, Erb HN, et al. Evaluation of factors associated with second remission in dogs with lymphoma undergoing retreatment with a cyclophosphamide, doxorubicin, vincristine, and prednisone chemotherapy protocol: 95 cases (2000-2007). J Am Vet Med Assoc. 2011; 238(4): 501–506, doi: 10.2460/javma.238.4.501, indexed in Pubmed: 21320021.
13. Brodsky EM, Maudlin GN, Lachowicz JL, et al. Asparaginase and MOPP treatment of dogs with lymphoma. J Vet Intern Med. 2009; 23(3): 578–584, doi: 10.1111/j.1939-1676.2009.0289.x, indexed in Pubmed: 19645842.
14. Daters AT, Mauldin GE, Mauldin GN, et al. Evaluation of a multidrug chemotherapy protocol with mitoxantrone based maintenance (CHOP-MA) for the treatment of canine lymphoma. Vet Comp Oncol. 2010; 8(1): 11–22, doi: 10.1111/j.1476-5829.2009.00199.x, indexed in Pubmed: 20230577.
15. Rassnick KM, Bailey DB, Malone EK, et al. Comparison between L-CHOP and an L-CHOP protocol with interposed treatments of CCNU and MOPP (L-CHOP-CCNU-MOPP) for lymphoma in dogs. Vet Comp Oncol. 2010; 8(4): 243–253, doi: 10.1111/j.1476-5829.2010.00224.x, indexed in Pubmed: 21062406.
16. Simon D, Nolte I, Eberle N, et al. Treatment of dogs with lymphoma using a 12-week, maintenance-free combination chemotherapy protocol. J Vet Intern Med. 2006; 20(4): 948––954, doi: 10.1892/0891-6640(2006)20[948:todwlu]2.0.co;2, indexed in Pubmed: 16955821.
17. Legendre AM. Treatment of dogs with lymphoma: a work in progress. J Vet Intern Med. 2007; 21(6): 1166–1167, doi: 10.1892/0891-6640(2007)21[1166:todwla]2.0.co;2, indexed in Pubmed: 18196720.
18. Baskin CR, Couto CG, Wittum TE. Factors influencing first remission and survival in 145 dogs with lymphoma: a retrospective study. J Am Anim Hosp Assoc. 2000; 36(5): 404–409, doi: 10.5326/15473317-36-5-404, indexed in Pubmed: 10997515.
19. Chun R. Lymphoma: which chemotherapy protocol and why? Top Companion Anim Med. 2009; 24(3): 157–162, doi: 10.1053/j.tcam.2009.03.003, indexed in Pubmed: 19732735.
20. Moore A. Treatment of T cell lymphoma in dogs. Veterinary Record. 2016; 179(11): 277–277, doi: 10.1136/vr.103456.
21. Valli VE, Kass PH, San Myint M, et al. Canine lymphomas: association of classification type, disease stage, tumor subtype, mitotic rate, and treatment with survival. Vet Pathol. 2013; 50(5): 738–748, doi: 10.1177/0300985813478210, indexed in Pubmed: 23444036.
22. Bienzle D, Vernau W. The diagnostic assessment of canine lymphoma: implications for treatment. Clin Lab Med. 2011; 31(1): 21–39, doi: 10.1016/j.cll.2010.10.001, indexed in Pubmed: 21295720.
23. Ponce F, Magnol JP, Ledieu D, et al. Prognostic significance of morphological subtypes in canine malignant lymphomas during chemotherapy. Vet J. 2004; 167(2): 158–166, doi: 10.1016/j.tvjl.2003.10.009, indexed in Pubmed: 14975390.
24. Carter RF, Harris CK, Withrow SJ, et al. Chemotherapy of canine lymphoma with histopathological correlation: Doxorubicin alone compared to COP as first treatment regimen. J Am Anim Hosp Assoc. 1987; 23: 587–596.
25. Pentheroudakis G, Goussia A, Voulgaris E, et al. High levels of topoisomerase IIalpha protein expression in diffuse large B-cell lymphoma are associated with high proliferation, germinal center immunophenotype, and response to treatment. Leuk Lymphoma. 2010; 51(7): 1260–1268, doi: 10.3109/10428194.2010.483749, indexed in Pubmed: 20497003.
26. Childress MO, Ramos-Vara JA, Ruple A. Retrospective analysis of factors affecting clinical outcome following CHOP-based chemotherapy in dogs with primary nodal diffuse large B-cell lymphoma. Vet Comp Oncol. 2018; 16(1): E159–E168, doi: 10.1111/vco.12364, indexed in Pubmed: 29152834.
27. Beaver LM, Strottner G, Klein MK. Response rate after administration of a single dose of doxorubicin in dogs with B-cell or T-cell lymphoma: 41 cases (2006-2008). J Am Vet Med Assoc. 2010; 237(9): 1052–1055, doi: 10.2460/javma.237.9.1052, indexed in Pubmed: 21034344.
28. Chun R, Garrett LD, Vail DM. Evaluation of a high-dose chemotherapy protocol with no maintenance therapy for dogs with lymphoma. J Vet Intern Med. 2000; 14(2): 120–124, doi: 10.1892/0891-6640(2000)014<0120:eoahcp>2.3.co;2, indexed in Pubmed: 10772481.
29. Nitiss J. Targeting DNA topoisomerase II in cancer chemotherapy. Nature Reviews Cancer. 2009; 9(5): 338–350, doi: 10.1038/nrc2607.
30. Sosinska-Mielcarek K, Jassem J. Predictive role of topoisomerase IIβexpression in anthracycline based breast cancer chemotherapy. Nowotwory. Journal of Oncology. 2005; 55(3): 252–256.
31. Hajduk M, Olszewski WP, Smietana A. Evaluation of the predictive value of topoisomerase II alpha in patients with breast carcinoma. Pol J Pathol. 2009; 60(3): 115–123, indexed in Pubmed: 20069504.
32. Nitiss J. Targeting DNA topoisomerase II in cancer chemotherapy. Nature Reviews Cancer. 2009; 9(5): 338–350, doi: 10.1038/nrc2607.
33. Zijlstra JG, de Jong S, de Vries EG, et al. Topoisomerases, new targets in cancer chemotherapy. Med Oncol Tumor

Pharmacother. 1990; 7(1): 11–18, doi: 10.1007/bf03000485, indexed in Pubmed: 2160032.
34. Burgess DJ, Doles J, Zender L, et al. Topoisomerase levels determine chemotherapy response in vitro and in vivo. Proc Natl Acad Sci U S A. 2008; 105(26): 9053–9058, doi: 10.1073/pnas.0803513105, indexed in Pubmed: 18574145.
35. Villman K, Sjöström J, Heikkilä R, et al. TOP2A and HER2 gene amplification as predictors of response to anthracycline treatment in breast cancer. Acta Oncol. 2006; 45(5): 590–596, doi: 10.1080/02841860500543182, indexed in Pubmed: 16864174.
36. Smith PJ, Souβ S. Multilevel therapeutic targeting by topoisomerase inhibitors. Br J Cancer Suppl. 1994; 23: S47–S51, indexed in Pubmed: 8075006.
37. Bodley A, Liu LF, Israel M, et al. DNA topoisomerase II-mediated interaction of doxorubicin and daunorubicin congeners with DNA. Cancer Res. 1989; 49(21): 5969–5978, indexed in Pubmed: 2551497.
38. Mordente A, Meucci E, Martorana GE, et al. Topoisomerases and Anthracyclines: Recent Advances and Perspectives in Anticancer Therapy and Prevention of Cardiotoxicity. Curr Med Chem. 2017; 24(15): 1607–1626, doi: 10.2174/0929867323666161214120355, indexed in Pubmed: 27978799.
39. Wang SL, Lee JJ, Liao AT. Comparison of efficacy and toxicity of doxorubicin and mitoxantrone in combination chemotherapy for canine lymphoma. Can Vet J. 2016; 57(3): 271–276, indexed in Pubmed: 26933263.
40. Valerius KD, Ogilvie GK, Mallinckrodt CH, et al. Doxorubicin alone or in combination with asparaginase, followed by cyclophosphamide, vincristine, and prednisone for treatment of multicentric lymphoma in dogs: 121 cases (1987-1995). J Am Vet Med Assoc. 1997; 210(4): 512–516, indexed in Pubmed: 9040837.
41. Dwarakanath BS, Khaitan D, Mathur R. Inhibitors of topoisomerases as anticancer drugs: problems and prospects. Indian J Exp Biol. 2004; 42(7): 649–659, indexed in Pubmed: 15339028.
42. Remmele W, Stegner HE. [Recommendation for uniform definition of an immunoreactive score (IRS) for immunohistochemical estrogen receptor detection (ER-ICA) in breast cancer tissue]. Pathologe. 1987; 8(3): 138–140, indexed in Pubmed: 3303008.
43. Valli VE, Vernau W, de Lorimier LP, et al. Canine indolent nodular lymphoma. Vet Pathol. 2006; 43(3): 241–256, doi: 10.1354/vp.43-3-241, indexed in Pubmed: 16672571.
44. Morgan E, O'Connell K, Thomson M, et al. Canine T cell lymphoma treated with lomustine, vincristine, procarbazine, and prednisolone chemotherapy in 35 dogs. Vet Comp Oncol. 2018; 16(4): 622–629, doi: 10.1111/vco.12430, indexed in Pubmed: 30117253.
45. Sorenmo K, Overley B, Krick E, et al. Outcome and toxicity associated with a dose-intensified, maintenance-free CHOP-based chemotherapy protocol in canine lymphoma: 130 cases. Vet Comp Oncol. 2010; 8(3): 196–208, doi: 10.1111/j.1476-5829.2010.00222.x, indexed in Pubmed: 20691027.
46. Rassnick KM, Bailey DB, Malone EK, et al. Comparison between L-CHOP and an L-CHOP protocol with interposed treatments of CCNU and MOPP (L-CHOP-CCNU-MOPP) for lymphoma in dogs. Vet Comp Oncol. 2010; 8(4): 243–253, doi: 10.1111/j.1476-5829.2010.00224.x, indexed in Pubmed: 21062406.
47. Rebhun RB, Lana SE, Ehrhart EJ, et al. Comparative analysis of survivin expression in untreated and relapsed canine lymphoma. J Vet Intern Med. 2008; 22(4): 989–995, doi: 10.1111/j.1939-1676.2008.0143.x, indexed in Pubmed: 18647159.
48. Edwards DS, Henley WE, Harding EF, et al. Breed incidence of lymphoma in a UK population of insured dogs. Vet Comp Oncol. 2003; 1(4): 200–206, doi: 10.1111/j.1476-5810.2003.00025.x, indexed in Pubmed: 19379181.
49. Sierra Matiz OR, Santilli J, Anai LA, et al. Prognostic significance of Ki67 and its correlation with mitotic index in dogs with diffuse large B-cell lymphoma treated with 19-week CHOP-based protocol. J Vet Diagn Invest. 2018; 30(2): 263–267, doi: 10.1177/1040638717743280, indexed in Pubmed: 29192554.
50. Sayag D, Fournel-Fleury C, Ponce F. Prognostic significance of morphotypes in canine lymphomas: A systematic review of literature. Vet Comp Oncol. 2018; 16(1): 12–19, doi: 10.1111/vco.12320, indexed in Pubmed: 28524622.
51. Hallman BE, Hauck ML, Williams LE, et al. Incidence and risk factors associated with development of clinical cardiotoxicity in dogs receiving doxorubicin. J Vet Intern Med. 2019; 33(2): 783–791, doi: 10.1111/jvim.15414, indexed in Pubmed: 30697816.
52. Keller ET, MacEwen EG, Rosenthal RC, et al. Evaluation of prognostic factors and sequential combination chemotherapy with doxorubicin for canine lymphoma. J Vet Intern Med. 1993; 7(5): 289–295, doi: 10.1111/j.1939-1676.1993.tb01021.x, indexed in Pubmed: 8263847.
53. Volkova M, Russell R. Anthracycline cardiotoxicity: prevalence, pathogenesis and treatment. Curr Cardiol Rev. 2011; 7(4): 214–220, doi: 10.2174/157340311799960645, indexed in Pubmed: 22758622.
54. Miura Y, Kaira K, Sakurai R, et al. High expression of topoisomerase-II predicts favorable clinical outcomes in patients with relapsed small cell lung cancers receiving amrubicin. Lung Cancer. 2018; 115: 42–48, doi: 10.1016/j.lungcan.2017.11.010, indexed in Pubmed: 29290260.
55. González-Molleda L, Wang Y, Yuan Y. Potent antiviral activity of topoisomerase I and II inhibitors against Kaposi's sarcoma-associated herpesvirus. Antimicrob Agents Chemother. 2012; 56(2): 893–902, doi: 10.1128/AAC.05274-11, indexed in Pubmed: 22106228.
56. Faggad A, Darb-Esfahani S, Wirtz R, et al. Topoisomerase IIalpha mRNA and protein expression in ovarian carcinoma: correlation with clinicopathological factors and prognosis. Mod Pathol. 2009; 22(4): 579–588, doi: 10.1038/modpathol.2009.14, indexed in Pubmed: 19270648.
57. Dimov ND, Zynger DL, Luan C, et al. Topoisomerase II alpha expression in testicular germ cell tumors. Urology. 2007; 69(5): 955–961, doi: 10.1016/j.urology.2007.01.068, indexed in Pubmed: 17482942.
58. Chekerov R, Klaman I, Zafrakas M, et al. Altered expression pattern of topoisomerase IIalpha in ovarian tumor epithelial and stromal cells after platinum-based chemotherapy. Neoplasia. 2006; 8(1): 38–45, doi: 10.1593/neo.05580, indexed in Pubmed: 16533424.
59. Withoff S, van der Zee AG, de Jong S, et al. DNA topoisomerase IIalpha and -beta expression in human ovarian cancer. Br J Cancer. 1999; 79(5-6): 748–753, doi: 10.1038/sj.bjc.6690120, indexed in Pubmed: 10070864.
60. Giaccone G, van Ark-Otte J, Scagliotti G, et al. Differential expression of DNA topoisomerases in non-small cell lung cancer and normal lung. Biochim Biophys Acta. 1995; 1264(3): 337–346, doi: 10.1016/0167-4781(95)00171-9, indexed in Pubmed: 8547322.
61. Argyle DJ, Pecceu E. Canine and feline lymphoma: challenges and opportunities for creating a paradigm shift. Vet Comp Oncol. 2016; 14 Suppl 1: 1–7, doi: 10.1111/vco.12253, indexed in Pubmed: 27505685.

Submitted: 28 November, 2019
Accepted after reviews: 26 February, 2020
Available as AoP: 16 March, 2020

FOLIA HISTOCHEMICA ET CYTOBIOLOGICA
Vol. 58, No. 1, 2020
pp. 54–60

ORIGINAL PAPER

VIA MEDICA

Cholinergic and adrenergic innervation of the pancreas in chinchilla (*Chinchilla Laniger Molina*)

Malgorzata Radzimirska, Jacek Kuchinka, Elzbieta Nowak, Wojciech Trybus, Aleksander Szczurkowski

Department of Medical Biology, Institute of Biology, Jan Kochanowski University in Kielce, Poland

Abstract

Introduction. Cholinergic and adrenergic innervation of the pancreas in chinchilla (*Chinchilla Laniger Molina*) was examined in this study. The pancreas is both an exocrine and endocrine gland with autonomic and sensory innervation presented by the numerous nerve fibers and small agglomerations of nerve cells.

Material and methods. Investigations were performed on 16 adult chinchillas of both sexes. The material was collected immediately after death of the animals. Histochemical methods: AChE and SPG were used, in addition to routine technique of single and double immunohistochemical (IHC) staining using whole mount specimens and freezing sections with a thickness of 8 to 12 μm. In the immunofluorescence staining, primary antibodies directed against markers used to identify cholinergic — ChAT and VAChT, and adrenergic — DβH and TH neurons. Secondary antibodies were coupled to Alexa Fluor 488 and Alexa Fluor 555 fluorophores.

Results. Histochemical studies (AChE) revealed that chinchilla pancreatic cholinergic innervation consisted of ganglionic neurocytes and numerous nerve fibers. These structures are located in the parenchyma of the exocrine part of the organ in close proximity to blood vessels and are present within the walls of the pancreatic ducts and interstitial connective tissue. A delicate fiber network around the Langerhans islets was also observed. The most numerous cholinergic structures were found in the head and tail, and the least numbers were found in the body of the pancreas. The SPG method revealed that adrenergic fibers form a network in the adventitia of blood vessels, and individual fibers run throughout the pancreatic parenchyma. Moreover, adrenergic nerve fibers were observed around the ganglionic neurocytes. This innervation was similar in all parts of the investigated organ. IHC investigations allowed observations of both the cholinergic and adrenergic activities of autonomic nerve structures. Additionally, using ChAT/DβH double staining, colocalization of these substances was observed in the fibers of the pancreatic parenchyma that passed through the cholinergic ganglia. Colocalization of VAChT and TH was found in nerve fibers of the exocrine part, in the walls of blood vessels, and in individual nerve cells. Colocalization of ChAT/DβH and VAChT/TH was observed in the single nerve cells and in the small (2–3 cell) ganglia. ChAT- and DβH-immunopositive nerve fibers were found in the area of the islets of Langerhans.

Conclusions. The results indicate a more intense cholinergic innervation of the chinchilla's pancreas, which is represented by both ganglia and nerve fibers, while adrenergic structures are mainly represented by fibers and only single neurocytes. This arrangement of the investigated structures in this species may imply a major role for hormonal control of exocrine secretion in rodents. *(Folia Histochemica et Cytobiologica 2020, Vol. 58, No. 1, 54–60)*

Key words: chinchilla laniger; pancreas; cholinergic innervation; adrenergic innervation; histochemistry; IHC

Correspondence address: Malgorzata Radzimirska, PhD
Department of Medical Biology, Institute of Biology,
Jan Kochanowski University in Kielce,
Uniwersytecka 7, 25–406 Kielce, Poland
e-mail: malgorzata.radzimirska@ujk.edu.pl

Introduction

Corresponding to its important functions, the pancreas is extensively innervated by autonomic and afferent nerve fibers [1–5]. Nerve fibers reach the pancreas in the form of neurovascular stalks that follow the blood vessels also within the pancreatic tissue and end or begin close to capillary walls and endocrine cells [6].

Parasympathetic preganglionic nerve fibers running as a component of the vagal nerve reach the pancreatic ganglia, and then, as postganglionic fibers, these parasympathetic fibers innervate the pancreatic acini. The myelinated axons of the preganglionic sympathetic neurons, located in the lateral horn of the thoracic and the upper lumbar segments of the spinal cord, project to ganglionic cells in the paravertebral sympathetic ganglia or to the celiac and mesenteric ganglia *via* the splanchnic nerves and then supply the pancreas as postganglionic fibers [7, 8].

Autonomic innervation of the pancreas has been investigated in numerous vertebrate species, both in domestic animals, such as pigeon [9, 10], hen [11], cat [12], rabbit [12, 13], sheep [14, 15], pig [16], and the representatives of other species, such as the African silverbill [9, 10], and mainly rodents, such as rat [12, 17], mouse [5, 6, 18], or Egyptian spiny mouse [19].

The pancreatic autonomic structures in the investigated species consist of numerous nerve fibers and ganglia, located mainly in the exocrine part of the pancreas. Thin bundles of fibers around the islets of Langerhans and a few individual fibers between endocrine cells have been observed. In many animal species including humans [20], cholinergic innervation structures seem to be more intensively developed than the adrenergic structures and consist of both nerve fibers and an agglomeration of ganglionic cells, while the adrenergic fibers mainly form the delicate networks [11, 13, 15, 19].

Chinchillas were previously reared for their valuable fur, but in recent years this animal has more frequently served as a model species for research into human diseases, especially hearing dysfunction in addition to research related to digestive system and pneumonia [21]. They are also used as laboratory animals for studies of cerebral vascularization [22], innervation of the gastrointestinal system [23–25], and previously unreported morphology of the extrahepatic biliary tract [26].

The aim of this study was to describe cholinergic and adrenergic innervation in the chinchilla pancreas (*Chinchilla Laniger Molina*). Histochemical methods have often been used in studies of autonomic pancreatic innervation. We consider it justified to use immunohistochemistry for the study of innervation in this rodent, which will undoubtedly allow a more detailed analysis of the delicate nerve structures supplying the pancreas. Our results will provide valuable macromorphological comparative data for investigation of pancreatic innervation in different species of small mammals.

Material and methods

Investigations were carried out on sixteen adult (10 months) individuals of chinchilla (*Chinchilla Laniger Molina*) both sexes. Material was collected immediately after industrial slaughter in Chinchillas Fur Farm. These studies were approved in accordance with the law of Act of 15 January 2015: „The protection of animals used for scientific or educational purpose" (studies on tissues obtained post-mortem do not require an approval of the Ethics Committee). Tissue were collected from the head, body and tail of pancreas and stained by the histochemical and immunohistochemical (IHC) methods. Histochemical investigations were performed on pancreases of eight individuals according to acetylcholinesterase (AChE) method [19, 27, 28] and SPG method [29], and pancreases of eight animals were used for routine immunofluorescence staining.

Histochemical methods

Two types of specimens were prepared: macromorphological specimens (whole mount), and frozen specimens (Cryomatrix, Thermo Shandon, Waltham, MA, USA) and cut for 12 μm sections. Next specimens were stained for cholinergic structures using the AChE method. After incubation in the staining solution (acetyl thiocholine iodide, acetate buffer, sodium citrate, copper sulfate, distilled water, potassium ferricyanide) at 37°C, and pH 6.4–6.8, slides were rinsed in distilled water, dehydrated and mounted in DPX. Activity of non-specific cholinesterase was blocked with iso-OMPA ($C_{12}H_{32}N_4O_3P_2$ tetraisopropylpyrophosphoramide). For the detection of adrenergic nerve fibers the sucrose–phosphate–glyoxylic acid method was used (SPG solution: sucrose, potassium phosphate monobasic and glyoxylic acid monohydrate). The unfixed whole mount specimens and frozen section were dipped immediately in SPG solution for 5 sec, and dried under a strong stream of air for 10 min. Subsequently, sections were covered with a drop of light mineral oil and heated to 95°C for 3 min and cover-slipped. The histochemically stained specimens were observed using fluorescence microscope Nikon Eclipse 90i (Nikon, Tokyo, Japan) and digital pictures were taken with Nikon Digital Sight SD-L1 system, and Nis –Elements 3.22 software and 60 sections were used for the measurement.

Table 1. Primary antisera used in the research

Antigen	Host	Type	Dilution	Catalog No.	Supplier
ChAT	Goat	Polyclonal	1:100	NBP1-30052	Novus Biologicals
VAChT	Rabbit	Polyclonal	1:1000	EUD261	Acris Antibodies
DβH	Rabbit	Polyclonal	1:500	NBP1-78349	Novus Biologicals
TH	Mouse	Monoclonal	1:500	MAB318	Millipore

Table 2. Secondary antisera used in the research

Host	Fluorophore	Dilution	Catalog No.	Supplier
Donkey anti-rabbit	Alexa Fluor 488	1:500	A21206	Invitrogen
Donkey anti-goat	Alexa Fluor 555	1:500	A21432	Invitrogen
Donkey anti-mouse	Alexa Fluor 555	1:500	A31570	Invitrogen

Immunohistochemistry

Animals were transcardially perfused with 0.4 l of 4% ice-cold buffered paraformaldehyde (pH 7.4) and pancreas was collected. The tissues were postfixed by immersion in the same fixative for 15 min, rinsed with phosphate buffer (pH 7.4; 0.1M), transferred to and stored in 30% buffered sucrose solution (pH 7.4) until further processing. The pancreas was cut into 8 μm-thick cryostat sections (Shandon Cryotome E; Thermo Scientific). Next, slides and whole mount specimens were stained with single and double immunohistochemical method. Tissues were incubated for 16–20 h at room temperature (RT) with primary antibodies against choline acetyltransferase (ChAT), vesicular acetylcholine transporter (VAChT), dopamine β-hydroxylase (DβH), and tyrosine hydroxylase (TH) (Table 1). Thereafter, slides were incubated with secondary fluorophore (fluorochrome)-conjugated antibodies Alexa Fluor 555 and Alexa Fluor 488 for one hour (Table 2). Finally, specimens were coversliped with buffered glycerol and analyzed under a Nikon A1R confocal microscope based on a Nikon Eclipse T*i* inverted microscope (Nikon Instruments Inc., New York, NY, USA).

Control of specificity of staining was performed by preabsorption of a diluted antiserum with 20 μg/ml of an appropriate antigen, which abolished the specific immunoreactivity completely. In addition, experiments were carried out in which the primary antiserum was replaced by non-immune serum, or by PBS, in order to verify the specificity of particular immunoreactions.

Results

Histochemical investigation using the AChE method revealed that cholinergic innervation of the pancreas in the chinchilla consisted of numerous ganglia and nerve fibers (Fig. 1A–B). These ganglia were different in sizes and had oval or elongated shapes. Their dimensions ranged from 20.40 to 85.47 (49.77 ± 17.98 μm, mean ± SD) and 14.22 to 40.87 (28.06 ± 10.59 μm) micrometers in length and width, respectively. A few clearly larger ganglia with about 15 cells in the cross-section were seen to have dimensions of up to 60.07 and 113.64 μm for width and length, respectively. These ganglia were located in the interstitial connective tissue, in the parenchyma of the exocrine part, and in the immediate vicinity of blood vessels and intralobular and interlobular ducts. Additionally, individual nerve cells were observed in the parenchyma of the organ. Both individual fibers and fiber bundles of different thickness were found in the parenchyma, along the pancreatic ducts, and in the wall of pancreatic ducts and along of the blood vessels. The bundles of nerve fibers varied from 39.03 to 83.84 μm in thickness. Moreover, a delicate network of nerve fibers was visible around the islets of Langerhans and between endocrine cells. Most of the cholinergic structures were present in the head and tail of the pancreas with the least numerous in its body.

Using the SPG method, it was found that adrenergic fibers form a network in the adventitia wall of blood vessels (Fig. 1C–D). Additionally, this type of nerve fiber with its characteristic varicosities was visible around the ganglionic neurocytes and was observed as individual fibers in the parenchyma (Fig. 1D). The distribution of adrenergic fibers was similar in all parts of the pancreas.

Immunohistochemical investigations confirmed the results obtained with AChE and SPG methods. ChAT (Fig. 1E–G) and VAChT (Fig. 1H) were found as cholinergic markers in the nerve fibers, as well as in

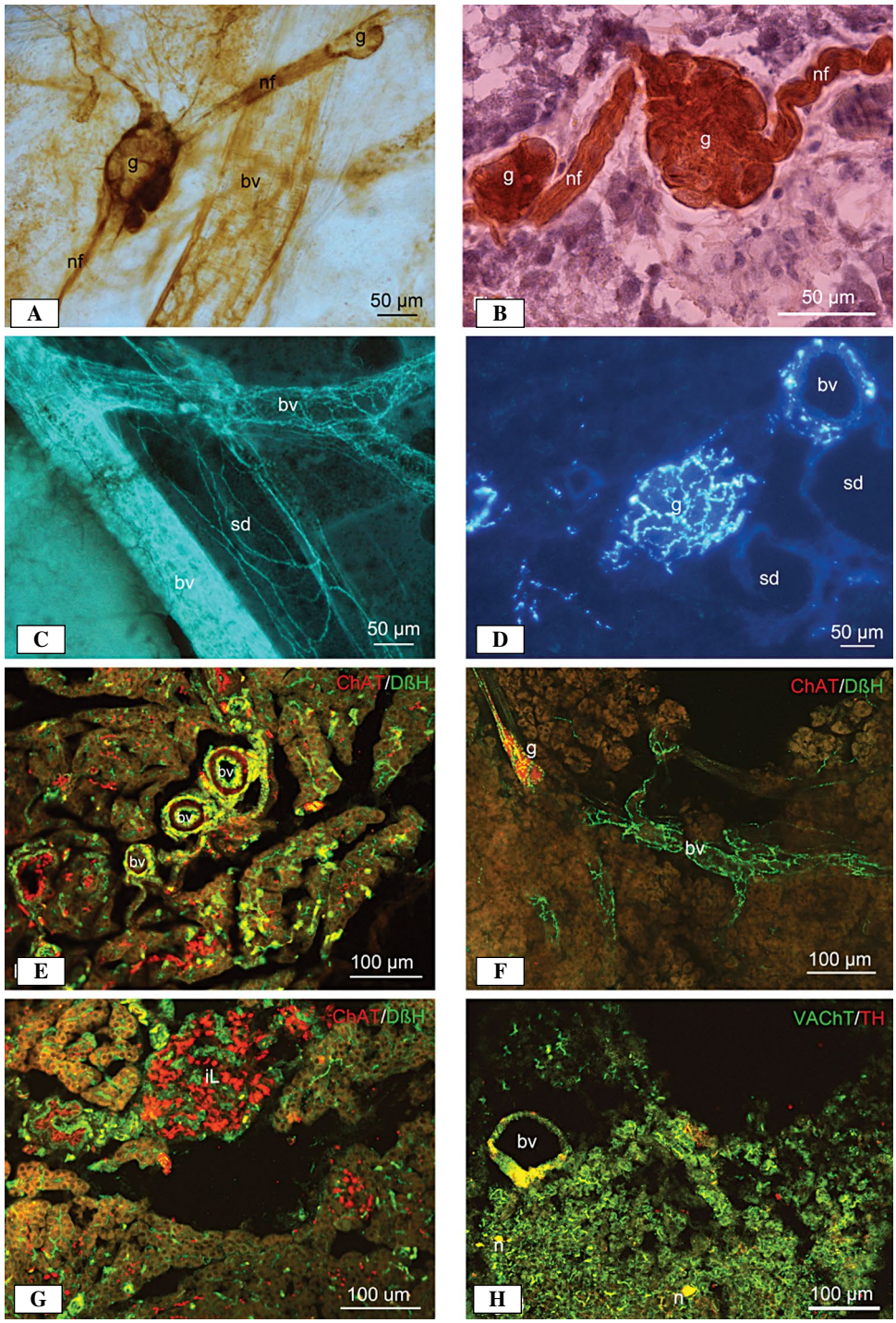

Figure 1. A. The cholinergic ganglia and nerve fibers in the parenchyma of the head of chinchilla's pancreas. The histochemical staining demonstrating AChE activity was performed as described in methods. Whole mount specimens; **B.** The cholinergic ganglia and nerve fibers in the parenchyma of the tail of pancreas. AChE, frozen section; **C.** The network of the adrenergic fibers in the blood vessels in the parenchyma of the head of pancreas (SPG, whole mount specimens); **D.** The adrenergic fibers in the blood vessels, in the parenchyma, and between cells in the ganglion of the corpus of pancreas (SPG, frozen section); **E.** The cholinergic and adrenergic nerve fibers in parenchyma, in the wall of blood vessels of the head of pancreas (ChAT — red, DβH — green, colocalization — gold/yellow, frozen section); **F.** The cholinergic ganglion in parenchyma and network of the adrenergic fibers in the wall of blood vessel of the head pancreas (ChAT — red, DβH — green, colocalization — gold/yellow, whole mount specimens); **G.** The cholinergic and adrenergic nerve fibers on the islet of Langerhans of the corpus of pancreas (ChAT — red, DβH — green, colocalization — gold/yellow, frozen section); **H.** The cholinergic and adrenergic nerve fibers in parenchyma, and in the wall of blood vessel of the tail in pancreas (VAChT — green, TH — red, colocalization — gold/yellow, whole mount specimens). Abbreviations: bv — blood vessel; g — ganglion; iL — islet of Langerhans; n — neurocytes; nf — nerve fibers; sd — secretory duct

the ganglionic neurocytes. They were located in the parenchyma of the exocrine part, around and in the wall of blood vessels, in the interlobular connective tissue, and in close vicinity to the pancreatic ducts. Moreover, delicate VAChT-immunoreactive (-Ir) nerve fibers were observed on the periphery of the pancreatic islets. DβH-positive and TH-positive nerve fibers between pancreatic parenchyma acini and in the wall of blood vessels were visible (Fig. 1E–H). The walls of the blood vessels were dominated by DβH-positive fibers that formed a distinct network (Fig. 1F). Immunoreactive ChAT and DβH fibers were found in the area of the Langerhans islets (Fig. 1G). Double labeling with ChAT/ /DβH revealed colocalization of these markers in the parenchymal fibers and in the fibers passing through the cholinergic ganglia (Fig. 1E–F). Individual nerve cells and very small ganglia consisting of 2 to 3 cells were also immunoreactive for both ChAT and DβH. Colocalization of VAChT and TH was found in the nerve fibers of the exocrine part, in the blood vessel walls, and in individual nerve cells (Fig. 1H). The activity of ChAT and VAChT was observed mainly in pancreas head and tail, and DβH+ and TH-positive structures were evenly distributed in each part of the investigated organ.

No sex-related differences were observed in the innervation of chinchilla's pancreas.

Discussion

According to various classical investigations, intrapancreatic nerve fibers generally form some plexuses: peri-ductal, peri-vascular, peri-acinar, and peri-insular. Similar, but not identical, distribution of the pancreatic innervation was observed in different groups of vertebrates.

In cold-blood animals, cholinergic innervation of the pancreas has been observed in a few amphibian and reptile species. In amphibians, AChE-positive nerve fibers have been found in the pancreatic parenchyma running along the blood vessels and in the interlobular connective tissue, but only a few reach the pancreatic acini and islets of Langerhans. The cholinergic fibers formed a delicate network as the intra- and peri-insular plexuses in frogs [9]. Cholinergic innervation of the exocrine part of the pancreas has been observed in lizards in which nerve fibers were found in the wall of blood vessels and pancreatic duct and wrapped pancreatic acini. In snakes, the density of cholinergic innervation of the pancreas is low and has mainly been observed in the interlobular connective tissue, along the blood vessels, and rarely between the acinar cells. In reptiles, sporadic cholinergic fibers have been found in the islets of Langerhans [9]. Compared to the studied species, which had numerous fibers and ganglionic cells within the exocrine part of the pancreas, only AChE-positive nerve fibers were found in amphibians and reptiles. In general, cholinergic innervation in lower vertebrates is definitely less developed compared to higher vertebrates. Results of the investigations on the adrenergic innervation of pancreas in amphibian and reptiles are not accessible in scientific databases [30].

A review of the literature indicates that cholinergic structures of birds and mammals consist of numerous nerve fibers and ganglia while the adrenergic innervation consists mainly of nerve fibers as found in most investigated species. Investigations carried out in hen revealed that cholinergic and adrenergic nerve fibers and bundles of differing thickness supply the pancreas along with blood vessels that form the perivascular plexus [11]. Some of these accompany the pancreatic ducts. Moreover, numerous cholinergic fibers have been observed under the connective tissue capsule of the pancreas. Both types of nerve fiber accompany the interlobar and interlobular arteries as the perivascular plexuses run in the connective tissue, and their numerous branches reached the pancreatic acini and islets. Individual ChAT- and TH-positive neurocytes were found in the pancreatic parenchyma [11].

Similar results regarding pancreatic cholinergic innervation were reported in the investigation of other species of birds, such as the domestic pigeon and African silverbill [9, 10]. The nerve fibers observed in the parenchyma form a perivascular plexus that supplies the exocrine parts of the pancreas. Moreover, small agglomerations of neurocytes were found mainly on the gland surface and in its immediate vicinity with less inside the gland. Only individual neurons were observed near the blood vessels, nerve fibers, and pancreatic ducts. Islet innervation is relatively weak, which suggests the presence of delicate fibers that wrap themselves around the periphery [10].

Cholinergic innervation of the chinchilla pancreas is better developed compared to investigated bird species. Agglomerations of neurocytes in this species form several-cell ganglia and are distributed throughout the entire organ. In contrast, adrenergic structures, as in birds, are single neurocytes and numerous nerve fibers.

Investigations involving rat, cat and rabbit have shown cholinergic fibers running in the interlobular connective tissue forming perivascular plexuses, the branches of which reach the pancreatic parenchyma. Numerous delicate nerve fibers were dispersed among the pancreatic acini forming peri-acinar and -insular plexuses that supply the islets of Langerhans [12]. Additionally, investigations conducted in rabbit revealed the presence of AChE-positive ganglionic cells except

cholinergic nerve fibers. Individual neurocytes and small ganglia were visible in the interlobular connective tissue. Characteristic DβH-positive networks were seen in the wall of the blood vessels, and individual fibers were observed around neurons [13].

The examination of adrenergic innervation in rat has revealed small TH-immunoreactive nerve cells in close contact with large TH-immuno-negative ganglionic neurocytes in the exocrine part of the pancreas and occasionally in the islets. Some of these TH- immunoreactive cells were also DβH-immuno-positive. All intrapancreatic ganglion cells were immunoreactive for DβH but not for TH. TH-immunoreactive nerve fibers were found in both the exocrine and endocrine parts of the pancreas [17].

Investigations performed on the mouse pancreas revealed thick AChE-positive nerve fibers in the interlobular connective tissue in which they formed perivascular plexuses. At the end of the vascular segment, fibers left vessels and formed a loosely organized network between the acini, which also sent off delicate branches toward the islets of Langerhans [6]. Moreover, immunohistochemical staining showed TH-positive nerve fibers in the exocrine part forming delicate network around blood vessels and adrenergic nerve fibers in the area of Langerhans islets [5]. Similar distribution of the cholinergic fibers was found in the pancreas of the Egyptian spiny mouse in which fibers along the pancreatic ducts and branches of pancreaticoduodenal arteries reached the Langerhans islets. AChE-positive ganglia were observed throughout the exocrine part and fine adrenergic fibers accompanied the blood vessels [19].

Studies of sheep pancreas revealed a moderate number of VAChT-positive nerve endings among the pancreatic acini, while only a few cholinergic fibers were found in the interlobular connective tissue. Similarly, a small number of VAChT-immunoreactive fibers supplied the endocrine part of the pancreas. VAChT and TH were shown to be colocalized in distinct populations of nerve fibers among the acini. TH was present in the vast majority of VAChT-positive intrapancreatic perikarya [14]. Studies of adrenergic pancreatic innervation in sheep revealed that most DβH-positive nerve fibers occur in the parenchyma between the acini, around blood vessels, and in the connective tissue, but only a small amount of adrenergic intrapancreatic neurons were found. Moreover, delicate DβH-immunoreactive nerve fibers were seen around the islets of Langerhans, of which only a few penetrated between DβH-negative endocrine cells [15].

Investigations of the pancreas of sow showed cholinergic structures as perivascular plexuses, inter-lobular nerve fibers, peri-lobular and -insular plexuses throughout the organ and as individual cholinergic neurons in the parenchyma [16].

Studies of the pancreas of newborn guinea pig revealed ChAT-immunoreactive ganglia in the interlobular connective tissue, between the acini, and in close proximity to the islets of Langerhans, blood vessels, and pancreatic ducts. Moreover, double staining showed the presence of ChAT and TH in the same ganglionic cells. ChAT-immunopositive nerve fibers were distributed as thick bundles running adjacent to blood vessels in the interlobular connective tissue, fine fibers in the adventitia of blood vessels, individual fiber bundles running between the acini throughout the whole organ or occasionally as small bundles near the periphery of the islets of Langerhans [31].

Similar results were obtained for pancreatic innervation in the Dromedary camel. Cholinergic fibers were observed in the parenchyma, around the pancreatic acini forming peri-acinar, -ductal, and -insular plexuses. Nerve cells were sporadically noted in close proximity or within islands. Adrenergic nerve fibers with characteristic varicosities were also observed to accompany blood vessels and interlobular ducts. Delicate adrenergic fiber ends were found in close proximity to the islets [32].

The results of our investigations on the autonomic innervation of chinchilla's pancreas indicate similar findings as seen in laboratory rodents, including the presence of distinctive nerve plexuses surrounding blood vessels and pancreatic ducts and acini. Forming the ganglia, agglomerations of the neurocytes mainly had cholinergic properties, whereas the adrenergic structures consisted of only fine nerve fibers and individual neurocytes. Moreover, our investigation indicates that the nerve plexuses in the chinchilla's pancreas are distinctly dense around the blood vessels but are loosely organized around pancreatic ducts and acini. This type of distribution of the pancreatic innervation in the studied species indicates a clear domination of cholinergic over adrenergic structures.

References

1. Löve JA, Yi E, Smith TG. Autonomic pathways regulating pancreatic exocrine secretion. Auton Neurosci. 2007; 133(1): 19–34, doi: 10.1016/j.autneu.2006.10.001, indexed in Pubmed: 17113358.
2. Ahrén B. Autonomic regulation of islet hormone secretion — implications for health and disease. Diabetologia. 2000; 43(4): 393–410, doi: 10.1007/s001250051322, indexed in Pubmed: 10819232.
3. Gilon P, Henquin JC. Mechanisms and physiological significance of the cholinergic control of pancreatic beta-cell function. Endocr Rev. 2001; 22(5): 565–604, doi: 10.1210/edrv.22.5.0440, indexed in Pubmed: 11588141.
4. Rodriguez-Diaz R, Abdulreda MH, Formoso AL, et al. Innervation patterns of autonomic axons in the human endo-

crine pancreas. Cell Metab. 2011; 14(1): 45–54, doi: 10.1016/j.cmet.2011.05.008, indexed in Pubmed: 21723503.
5. Lindsay TH, Halvorson KG, Peters CM, et al. A quantitative analysis of the sensory and sympathetic innervation of the mouse pancreas. Neuroscience. 2006; 137(4): 1417–1426, doi: 10.1016/j.neuroscience.2005.10.055, indexed in Pubmed: 16388907.
6. Ushiki T, Watanabe S. Distribution and ultrastructure of the autonomic nerves in the mouse pancreas. Microscopy Research and Technique. 1997; 37(5-6): 399–406, doi: 10.1002/(sici)1097-0029(19970601)37:5/6<399::aid-jemt4>3.0.co;2-9.
7. Babic T, Travagli RA. 2016. Neuronal control of the pancreas. Pancreapedia. Exocrine pancreas knowledge base. Version 1; 0: September, doi: 10.3998/panc.2016.27.
8. Li W, Yu G, Liu Y, et al. Intrapancreatic ganglia and neural regulation of pancreatic endocrine secretion. Front Neurosci. 2019; 13: 21, doi: 10.3389/fnins.2019.00021, indexed in Pubmed: 30842720.
9. Trandaburu T. Comparative observations on AChE distribution in pancreas of some amphibians, repitiles and birds, with special reference to the islets of langerhans. Histochemie. 1972; 32(3): 271–279, doi: 10.1007/bf00306034, indexed in Pubmed: 4562919.
10. Trandaburu T. Ultrastructural and acetylcholinesterase investigations on the pancreas intrinsic innervation of two bird species (Columba livia domestica Gm. and Euodice cantans Gm.). Gegenbaurs Morphol Jahrb. 1974; 120(6): 888–904, indexed in Pubmed: 4618821.
11. Ulas M, Penkowski A, Lakomy M. Adrenergic and cholinergic innervation of the chicken pancreas. Folia Morphol (Warsz). 2003; 62(3): 243–246, indexed in Pubmed: 14507057.
12. COUPLAND RE. The innervation of pan creas of the rat, cat and rabbit as revealed by the cholinesterase technique. J Anat. 1958; 92(1): 143–149, indexed in Pubmed: 13513506.
13. Löve JA, Szebeni K. Morphology and histochemistry of the rabbit pancreatic innervation. Pancreas. 1999; 18(1): 53–64, doi: 10.1097/00006676-199901000-00008, indexed in Pubmed: 9888661.
14. Arciszewski MB, Zacharko-Siembida A. Cholinergic innervation of the pancreas in the sheep. Acta Biol Hung. 2007; 58(2): 151–161, doi: 10.1556/ABiol.58.2007.2.2, indexed in Pubmed: 17585505.
15. Arciszewski MB, Zacharko-Siembida A. A co-localization study on the ovine pancreas innervation. Ann Anat. 2007; 189(2): 157–167, doi: 10.1016/j.aanat.2006.09.002, indexed in Pubmed: 17419548.
16. Lakomy M, Chodkowska D. Cholinergic innervation of pig pancreas. Acta Histochem. 1984; 75(1): 63–68, doi: 10.1016/S0065-1281(84)80072-0, indexed in Pubmed: 6209910.
17. Oomori Y, Iuchi H, Ishikawa K, et al. Immunocytochemical study of tyrosine hydroxylase and dopamine beta-hydroxylase immunoreactivities in the rat pancreas. Histochemistry. 1994; 101(5): 313–323, doi: 10.1007/bf00268992, indexed in Pubmed: 7523336.
18. Gienc J, Kosierkiewicz D, Kuder T. Ganglionic cells and their localization within the secretory system of pancreas in vertebrates. Zool Pol. 1993; 38: 27–38.
19. Szczurkowski A, Kuchinka J, Nowak E, et al. Autonomic innervation of pancreas in egyptian spiny mouse (acomys cahirinus, desmarest). Acta Veterinaria Brno. 2009; 78(4): 557–561, doi: 10.2754/avb200978040557.
20. Fabris SE, Thorburn A, Litchfield A, et al. Effect of parasympathetic denervation of liver and pancreas on glucose kinetics in man. Metabolism. 1996; 45(8): 987–991, doi: 10.1016/s0026-0495(96)90268-1, indexed in Pubmed: 8769357.
21. Suckow M A, Stevens K A, Wilson R P. The laboratory rabbit, guinea pig, hamster, and other rodents. 1st ed. Saunders: Elsevier 2012.
22. Kuchinka J. Morphometry and variability of the brain arterial circle in chinchilla (Chinchilla laniger, Molina). Anat Rec (Hoboken). 2017; 300(8): 1472–1480, doi: 10.1002/ar.23566, indexed in Pubmed: 28181413.
23. Nowak E. Organization of the innervation of the oesophagus and stomach in chinchilla (Chinchilla laniger, Molina). Folia Histochem Cytobiol. 2013; 51(2): 115–120, doi: 10.5603/fhc.2013.0018.
24. Nowak E. Organisation of autonomic nervous structures in the large intestine of chinchilla (Chinchilla laniger Molina). Folia Biol (Krakow). 2013; 61(3-4): 135–141, doi: 10.3409/fb61_3-4.135, indexed in Pubmed: 24279160.
25. Nowak E. Organisation of autonomic nervous structures in the small intestine of chinchilla (Chinchilla laniger, Molina). Anat Histol Embryol. 2014; 43(4): 301–309, doi: 10.1111/ahe.12077, indexed in Pubmed: 23848953.
26. Nowak E, Kuchinka J, Szczurkowski A, et al. Extrahepatic biliary tract in chinchilla (Chinchilla laniger, Molina). Anat Histol Embryol. 2015; 44(3): 236–240, doi: 10.1111/ahe.12137, indexed in Pubmed: 25091180.
27. Karnovsky MJ, Roots L. A "direct-coloring" thiocholine method for cholinesterases. J Histochem Cytochem. 1964; 12: 219–221, doi: 10.1177/12.3.219, indexed in Pubmed: 14187330.
28. Tsuji S, Larabi Y. A modification of thiocholine-ferricyanide method of Karnovsky and Roots for localization of acetylcholinesterase activity without interference by Koelle's copper thiocholine iodide precipitate. Histochemistry. 1983; 78(3): 317–323, doi: 10.1007/bf00496619, indexed in Pubmed: 6193086.
29. De la Torre JC. An improved approach to histofluorescence using the SPG method for tissue monoamines. J Neurosci Methods. 1980; 3(1): 1–5, doi: 10.1016/0165-0270(80)90029-1, indexed in Pubmed: 6164878.
30. Trandaburu T. Comparative observations on adrenergic innervation and monoamine content in endocrine pancreas of some amphibians, reptiles and birds. Endokrinologie. 1972; 59(2): 260–264, indexed in Pubmed: 4556423.
31. Liu HP, Tay SS, Leong S, et al. Colocalization of ChAT, DbetaH and NADPH-d in the pancreatic neurons of the newborn guinea pig. Cell Tissue Res. 1998; 294(2): 227–231, doi: 10.1007/s004410051172, indexed in Pubmed: 9799438.
32. Qayyum MA, Fatani JA, Shaad FU, et al. A histochemical study on the innervation of the pancreas of the one-humped camel (Camelus dromedarius). J Anat. 1987; 151: 117–123, indexed in Pubmed: 3654346.

Submitted: 6 November, 2019
Accepted after reviews: 16 March, 2020
Available as AoP: 23 March, 2020

INSTRUCTIONS FOR AUTHORS

MANUSCRPIT SUBMISSION

Folia Histochemica et Cytobiologica accepts manuscripts (original articles, short communications, review articles) from the field of histochemistry, as well as cell and tissue biology. Each manuscript is reviewed by independent referees. Book reviews and information concerning congresses, symposia, meetings etc., are also published.

All articles should be submitted to FHC electronically online at www.fhc.viamedica.pl where detailed instruction regarding submission process will be provided.

AUTHOR'S STATEMENT

The manuscript must be accompanied by the author's statement that it has not been published (or submitted to publication) elsewhere.

GHOSTWRITTING

Ghostwriting and guest-authorship are forbidden. In case of detecting ghost written manuscripts, their actions will be taking involving both the submitting authors and the participants involved.

The corresponding author must have obtained permission from all authors for the submission of each version of the paper and for any change in authorship. Submission of a paper that has not been approved by all authors may result in immediate rejection.

COST OF PUBLICATION

The cost of publication of accepted manuscript is 800 Euro.

OFFPRINTS

PDF file of each printed paper is supplied for the author free of charge. Orders for additional offprints should be sent to the Editorial Office together with galley proofs.

ORGANIZATION OF MANUSCRIPT

The first page must include: the title, name(s) of author(s), affiliation(s), short running head (no more than 60 characters incl. spaces) and detailed address for correspondence including e-mail. Organization of the manuscript: 1. Abstract (not exceeding one typed page — should consist of the following sections: Introduction, Material and methods, Results, Conclusions); 2. Key words (max. 10); Introduction; Material and methods; Results; Discussion; Acknowledgements (if any); References; Tables (with legends); Figures; Legends to figures.

In a short communication, Results and Discussion should be written jointly. Organization of a review article is free.

TECHNICAL REQUIREMENTS

Illustrations (line drawings and halftones) — either single or mounted in the form of plates, can be 85 mm, 125 mm, or 175 mm wide and cannot exceed the size of 175 × 250 mm. The authors are requested to plan their illustrations in such a way that the printed area is eco-nomically used. Numbers, inscriptions and abbreviations on the figures must be about 3 mm high. In case of micrographs, magnification (*e.g.* × 65 000) should be given in the legend. Calibration bars can also be used. For the best quality of illustrations please provide images in one of commonly used formats e.g. *.tiff, *.png, *pdf (preferred resolution 300 dpi). Color illustrations can be published only at author's cost and the cost estimate will be sent to the author after submission of the manuscript. Tables should be numbered consecutively in Arabic numerals and each table must be typed on a separate page. The authors are requested to mark the places in the text, where a given table or figure should appear in print. Legends must begin on a new page and should be as concise as necessary for a self-sufficient explanation of the illustrations. PDF file of each paper is supplied free of charge.

CITATIONS

In References section of article please use following American Medical Association 9th Ed. citation style. Note, that items are listed numerically in the order they are cited in the text, not alphabetically. If you are using a typewriter and cannot use italics, then use underlining.

Authors: use initials of first and second names with no spaces. Include up to six authors. If there are more than six, include the first three, followed by et al. If no author is given, start with the title. **Books:** include the edition statement (ex: 3rd ed. or Rev ed.) between the title and place if it is not the first edition. **Place:** use abbreviations of states, not postal codes. **Journals:** abbreviate titles as shown in *Index Medicus*. If the journal does not paginate continuously through the volume, include the month (and day). **Websites:** include the name of the webpage, the name of the entire website, the full date of the page (if available), and the date you looked at it. The rules concerning a title within a title are *not* displayed here for purposes of clarity. See the printed version of the manual for details. For documents and situations not listed here, see the printed version of the manual.

EXAMPLES

Book:

1. Okuda M, Okuda D. *Star Trek Chronology: The History of the Future.* New York: Pocket Books; 1993.

Journal or Magazine Article (with volume numbers):

2. Redon J, Cifkova R, Laurent S et al. Mechanisms of hypertension in the cardiometabolic syndrome. *J Hypertens.* 2009; 27(3):441–451. doi: 10.1097/HJH.0b013e32831e13e5.

Book Article or Chapter:

3. James NE. Two sides of paradise: the Eden myth according to Kirk and Spock. In: Palumbo D, ed. *Spectrum of the Fantastic*. Westport, Conn: Greenwood; 1988:219–223.

When the manufacturers of the reagents etc. are mentioned for the first time, town, (state in the US) and country must be provided wheras for next referral only the name of the firm should be given.

Website:

4. Lynch T. DSN trials and tribble-ations review. Psi Phi: Bradley's Science Fiction Club Web site. 1996. Available at: http://www.bradley.edu/campusorg/psiphi/DS9/ep/503r.htm. Accessed October 8, 1997.

Journal Article on the Internet:

5. McCoy LH. Respiratory changes in Vulcans during pon farr. *J Extr Med* [serial online]. 1999;47:237–247. Available at: http:// //infotrac.galegroup.com/itweb/nysl_li_liu. Accessed April 7, 1999.